Polyhedron 198 (2021) 115068

Contents lists available at ScienceDirect

Polyhedron

journal homepage: www.elsevier.com/locate/poly

The versatile coordination chemistry of 1,3-benzenedicarboxylate in the last 20 years: An investigation from the coordination modes to spectroscopic insights

Isabelle K.V. Gonçalves [a], Willian X.C. Oliveira [b], Filipe B. de Almeida [c], Maria Vanda Marinho [d], Walace D. do Pim [a,e,*], Priscila P. Silva-Caldeira [a,*]

[a] Departamento de Química, Centro Federal de Educação Tecnológica de Minas Gerais, Avenida Amazonas, 5253, 30421-169 Belo Horizonte, MG, Brazil
[b] Departamento de Química, Universidade Federal de Minas Gerais, Avenida Antônio Carlos, 6627, 31270-901 Belo Horizonte, MG, Brazil
[c] Instituto de Química, Universidade Federal Fluminense, Outeiro de São João Batista s/n, 24020-141 Niterói, RJ, Brazil
[d] Instituto de Química, Universidade Federal de Alfenas, Campus Santa Clara, 37133-840 Alfenas MG, Brazil
[e] Department of Chemistry and Biomolecular Sciences and Centre for Catalysis Research and Innovation, University of Ottawa, K1N 6N5 Ottawa, ON, Canada

ARTICLE INFO

Article history:
Received 15 November 2020
Accepted 23 January 2021
Available online 1 February 2021

Keywords:
1,3-Benzenedicarboxylic acid
Isophtalic acid
Coordination polymer
Coordination modes
Structural diversity
Infrared spectroscopy

ABSTRACT

Aromatic carboxylates have been vastly applied as building blocks for the assembly of robust molecular-based materials owing to their potential application in various fields. In this family, 1,3-benzenedicarboxylate (1,3-bdc), which possesses a "V"-type configuration, has been distinguished. Over the past 20 years, the number of compounds based on 1,3-bdc rapidly expanded due to its multifaceted coordination chemistry and the possibility to generate materials with diversified applications. Therefore, the main purpose of this study is to explore the structural aspects, diversity, and the factors that influence coordination modes of 1,3-bdc by comparison of a series of structurally related compounds. In this sense, we highlight some aspects that can assist in a more rational design of coordination networks based on 1,3-bdc. We also discuss the structural-spectroscopic correlation of the metal-carboxylate bonds aimed at providing support for further investigation on multifunctional materials based on 1,3-bdc, including the amorphous solids. As a direct application of this knowledge, we produced two new Cu^{II}-based compounds by the combination of 1,3-bdc and 1,10-phenanthroline (phen). We obtained a discrete complex formed by two cocrystallized mononuclear complexes, $\{[Cu(1,3\text{-Hbdc})(phen)(H_2O)_2]ClO_4\cdot[Cu(1,3\text{-bdc})(phen)(H_2O)_2]\cdot 2(H_2O)\}$ (**1**), and a coordination polymer, $\{[Cu(1,3\text{-bdc})(phen)(H_2O)]\cdot DMF\}_n$ (**2**), and we provided a further investigation of the nature and features of these compounds based on the discussion raised in this systematic study.

© 2021 Elsevier Ltd. All rights reserved.

1. Introduction

Benzenedicarboxylic acid (H_2bdc) is a group of three isomeric compounds named phthalic acid (1,2-benzenedicarboxylic acid, 1,2-H_2bdc), isophthalic acid (1,3-benzenedicarboxylic acid, 1,3-H_2bdc), and terephthalic acid (1,4-benzenedicarboxylic acid, 1,4-H_2bdc) (Fig. 1). These and several other aromatic carboxylic acids are widely explored in the fields of *Coordination Chemistry*, *Supramolecular Chemistry*, and *Materials Chemistry* due to their ability to form stable bonds with different metal ions [1], including but not limited to Zn^{II}, Cu^{II}, Co^{II}, Cd^{II}, and Ln^{III} ions. This combination leads to highly stable coordination networks showing a great variety of coordination modes [2]. Moreover, carboxylic acids/carboxylates are excellent candidates to act as hydrogen donors/acceptors establishing strong hydrogen bonds with different families of molecules and leading to the formation of a plethora of fascinating supramolecular architectures [3–5].

As the benzenedicarboxylates are divergent polydentate ligands, they show versality in assembling metal–organic polynuclear systems by bridging a large number of metal ions. Especially the divergent 1,3-H_2bdc and 1,4-H_2bdc ligands are useful building blocks for the design of coordination polymers (CPs) and metal–organic frameworks (MOFs). The self-assembly of metal–organic structures is a fascinating field of research considering the infinite variety of building blocks that can be combined to form highly crystalline and amorphous multifunctional materials, being the

---

* Corresponding authors at: Departamento de Química, Centro Federal de Educação Tecnológica de Minas Gerais, Avenida Amazonas, 5253, 30421-169 Belo Horizonte, MG, Brazil.

E-mail addresses: walacedopim@cefetmg.br (W.D. do Pim), priscila@cefetmg.br (P.P. Silva-Caldeira).

https://doi.org/10.1016/j.poly.2021.115068
0277-5387/© 2021 Elsevier Ltd. All rights reserved.

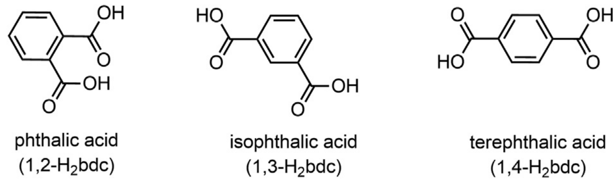

Fig. 1. The structural formulae of benzenedicarboxylic acids.

latter more challenging to characterize but also relevant in several fields [6–8]. 1,4-bdc is the linker employed in the assembly of the prototypical $[Zn_4O(1,4\text{-}bdc)_3]$ (MOF-5) described by Yaghi and coworkers [9], and other largely employed MOFs including $[Zr_6O_4(OH)_4(1,4\text{-}bdc)_6]$ (UiO-66), [Fe(OH)(1,4-bdc)] (MIL-53), and $[Cr_3(OH)(H_2O)_2O(1,4\text{-}bdc)_3]$ (MIL-101) (Fig. 2). Although MOFs based on 1,3-H_2bdc are less described, we present in Fig. 3 some examples highlighting the fascinating architectures of MOFs $[In_2O(1,3\text{-}bdc)_2]$, $[Eu_2(1,3\text{-}bdc)_3(DMF)_2]$, $[NH_2(CH_3)_2][ZnNa(1,3\text{-}bdc)_2]$ (MOF CJ2), and $[Fe_3(OH)(H_2O)_2(1,3\text{-}bdc)_3]$ (PCN-234) [10–12].

Based on the aforementioned, we selected one benzenedicarboxylic acid, the 1,3-benzenedicarboxylic acid (1,3-H_2bdc), to summarize and highlight the recent advancements in its coordination compounds.

Benzenedicarboxylic acids and their derivatives are commonly used as building blocks for constructing CPs and MOFs with or without the utilization of auxiliary ligands. Among a multitude of options, neutral *N*-donor ligands have been the most employed as auxiliary ligands of compounds containing carboxylates [13,14]. Although the impressive number of mixed ligand coordination compounds described so far containing both benzenedicarboxylates and *N*-donor ligands, the first works describing their crystal structures started only in the 2000s [15].

Fig. 4 presents the number of articles published each year describing the synthesis, structure, and characterization of CPs based on benzenedicarboxylates and their derivatives from 2000 to 2020. The fast growth in the number of publications shows the relevance of these linkers to the field. Also, assets including robustness, cost and low toxicity of these organic platforms make them suitable to be employed in the fabrication of metal–organic polymeric structures in larger scales with an enormous potential for diverse industries [16]. In the graph (Fig. 4), the peak in the number of publications in 2013 signaled a slowdown in the use of this type of ligands, however the number of publications based on the 1,3-H_2bdc ligand – the focus of this systematic study – in 2020 (21 papers so far) is already greater than those published in 2017 (15 papers), 2018 (14 papers) and 2019 (12 papers), showing that a lot more is yet to be discovered. In this study, for example, we present the structure of a new discrete complex, $\{[Cu(1,3\text{-}Hbdc)(phen)(H_2O)_2]ClO_4\cdot[Cu(1,3\text{-}bdc)(phen)(H_2O)_2]\cdot 2(H_2O)\}$ (**1**), and with the same building blocks, we were able to obtain the CP $\{[Cu(1,3\text{-}bdc)(phen)(H_2O)]\cdot DMF\}_n$ (**2**). There are other two different coordination polymers previously described [17,18] whose building blocks are the same, highlighting the richness and the need for more research in this fascinating research field.

The present work provides an overview of the complexes bearing 1,3-benzenedicarboxylate reported in the last twenty years including the description of two novel crystal structures containing this ligand and 1,10-phenanthroline (phen) as co-ligand. The compounds consist of a discrete complex with formula $\{[Cu(1,3\text{-}Hbdc)(phen)(H_2O)_2]ClO_4\cdot[Cu(1,3\text{-}bdc)(phen)(H_2O)_2]\cdot 2(H_2O)\}$(**1**) and a coordination polymer $\{[Cu(1,3\text{-}bdc)(phen)(H_2O)]\cdot DMF\}_n$ (**2**).

2. 1,3-Benzenedicarboxylic acid and its derivatives as ligands

In the last two decades, remarkable progress has been made in the synthesis of CPs with 1,3-H_2bdc and its derivatives as ligands. This kind of ligand offers almost unlimited possibilities to design a metal framework with customized properties. 1,3-benzenedicarboxylic acid has a rigid 120° angle between the benzene ring and the two carboxylate groups. Angular dicarboxylate groups, also known as "V"-type O-donor ligands, including the 1,3-H_2bdc motif, are often adopted as organic spacers for the building of CPs and MOFs due to the possibility of assembling a gigantic number of diverse structural topologies [15]. Fig. 5 presents some of the most

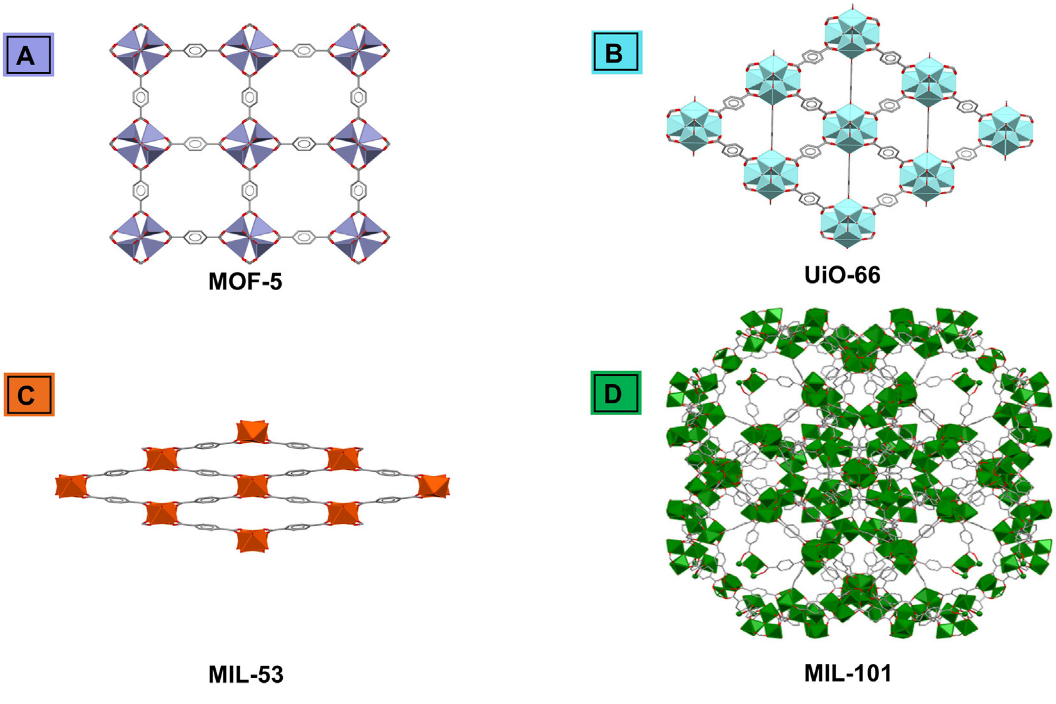

Fig. 2. Representation of the structures of MOF-5, UiO-66, MIL-53 and MIL-101.

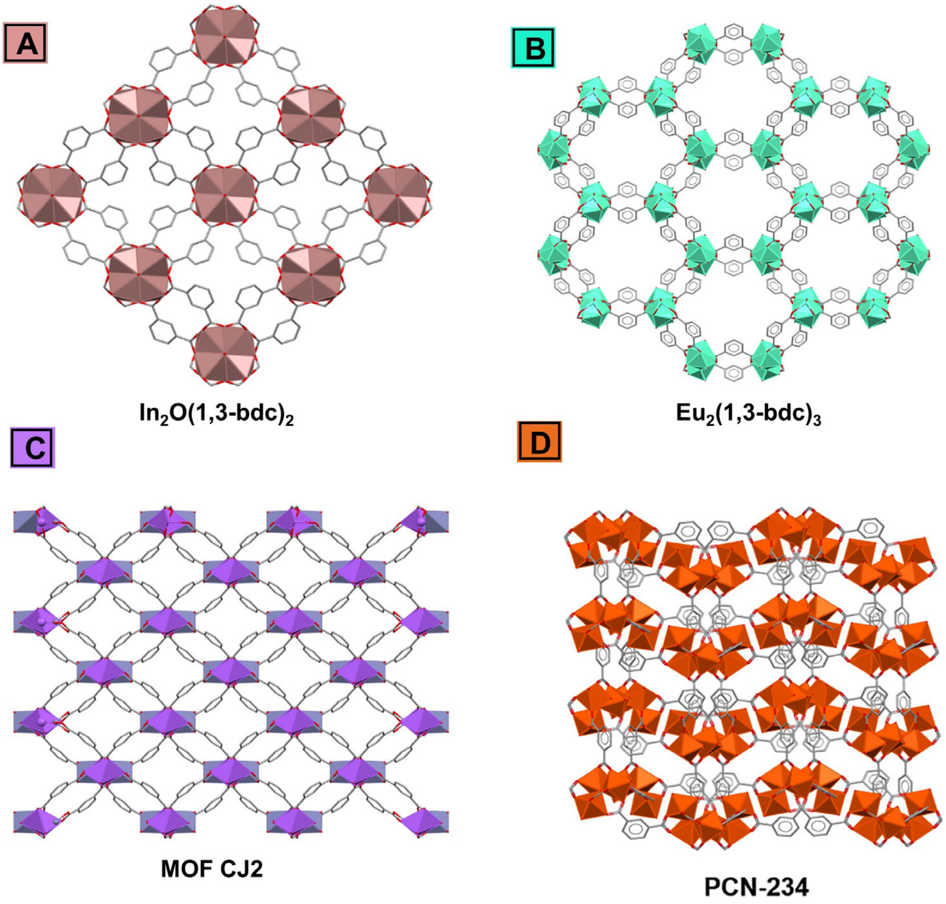

Fig. 3. Representation of the structures of [$In_2O(1,3\text{-bdc})_2$], [$Eu_2(1,3\text{-bdc})_3$], MOF CJ2, and PCN-234.

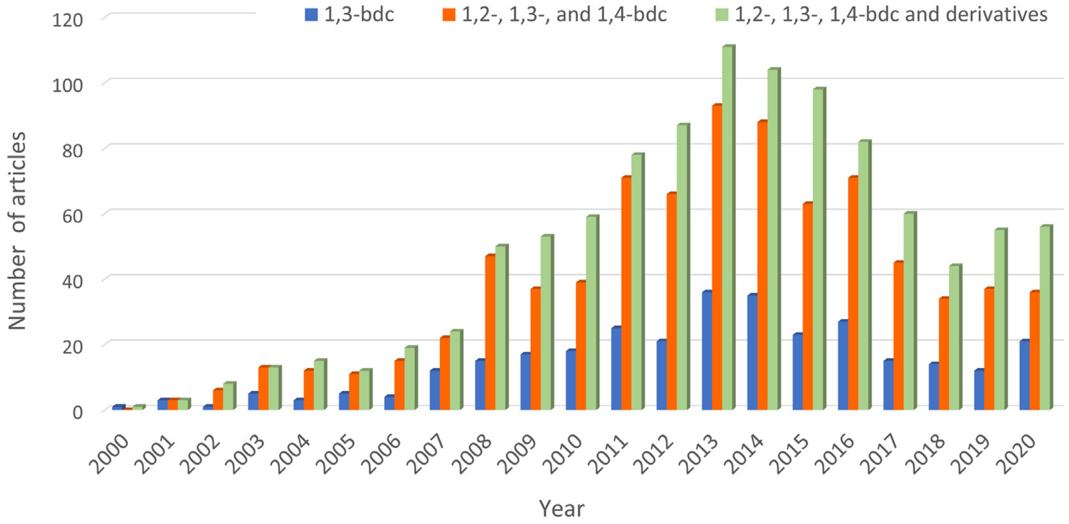

Fig. 4. Evolution of the number of reported articles published per year containing the terms "benzenedicarboxylic coordination polymer". This graph was constructed based on the data searched on *SciFinder* and only research articles were considered. Blue: number of articles containing only CPs bearing 1,3-benzenedicarboxylate. Orange: number of articles containing CPs with benzenedicarboxylates as ligands. Green: number of articles containing CPs with benzenedicarboxylates and their derivatives.

used 1,3-H_2bdc derivatives, including those exhibiting additional functional groups which enables wider options for structure modulation [19–22].

1,3-H_2bdc ligand and its derivatives can also be highlighted as versatile molecular building blocks for the preparation of helical coordination compounds [13,18,23–35]. In general, helical compounds have intriguing molecular structures and are widely present in biological systems [23,36]. Synthetic helical polymers have been attracting special attention in fields including *Coordination Chemistry* and *Crystal Engineering* [37]. Furthermore, owing to its rigid V-shape, 1,3-H_2bdc coordinated to metal ions can commonly generate zigzag [11,14,17,18,38–54] or wave-like chains [33,41,55–69]. An additional possibility is the coordination of 1,3-bdc to metal ions to produce a fishbone-like chain [70,71].

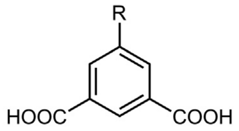

R = CH_3, CN, NH_2, NO_2, OH, OCH_2Ph, Cl, I, SO_3H

Fig. 5. Structural formulae of some 1,3-benzenedicarboxylic acid derivatives.

In this study, we restricted our survey to coordination networks bearing 1,3-H_2bdc and its partially or fully deprotonated forms, excluding the 1,3-H_2bdc derivatives, and we found more than 350 coordination networks containing this compound as a ligand. In the literature, 1,3-H_2bdc and its deprotonated forms have received an assortment of abbreviations (Table 1).

The 1,3-H_2bdc may be fully (1,3-bdc^{2-}) or partially deprotonated (1,3-$Hbdc^{-}$) in solution and in the solid-state. To simplify, we will use the form 1,3-bdc to refer to the fully deprotonated and 1,3-Hbdc to the partially deprotonated form throughout this systematic study. The ability to be stabilized within crystal structures as a neutral molecule, mono- or dianion (coordinated or not) has been yielding a huge variety of crystal structures with fascinating topologies built by both covalent bonds and non-covalent interactions [175].

3. The versatility of the coordination modes of 1,3-bdc and its partially protonated species toward metal centers

Carboxylate groups adopt several coordination modes from simple bis-monodentate observed, for example, in paddlewheel-like dinuclear clusters of Zn and Cu, to combinations of monodentate and chelate, monodentate and bidentate-bridge, among others [165]. Furthermore, the ligand 1,3-bdc can connect metal ions through diverse bridging modes including monodentate and chelating bridging, monoatomic bridging or even a combination of them. As depicted in Table 2 and in Fig. 6, we found in our survey nineteen distinct coordination modes for 1,3-bdc acting as a bridge between two (μ) [24,52], three (μ_3) [63,109], four (μ_4) [49,162], five (μ_5) [104,187], or even six (μ_6) [30,206] metal centers, resulting in a richness of geometries/topologies.

Table 1
Set of abbreviations used to designate 1,3-benzenedicarboxylic acid in research articles.

Abbreviations for 1,3-benzenedicarboxylic acid	Number of reports	References
1,3-H_2BDC	38	[2,21,24,25,29,40,61,63,66,67,72–99]
1,3-H_2bdc	17	[59,100–117]
H_2BDC	16	[11,26,66,76,118–129]
m-H_2BDC	14	[23,52,60,68,130–139]
m-H_2bdc	14	[13,14,42,140–150]
H_2ip	14	[33,151–163]
H_2bdc	10	[34,51,71,164–170]
H_2ipa	7	[18,27,30,171–174]
1,3-bdc	6	[54,175–179]
H_2IPA	3	[180–182]
1,3-bdcH_2	3	[183–185]
H_2mbdc	3	[186–188]
1,3-BDCH_2	3	[189–191]
1,3-BDC	2	[192,193]
H_2*m*BDC	2	[187,194]
H_2iso	2	[49,69]
BDC	1	[10]
H_2(1,3-bdc)	1	[195]
H_2(m-BDC)	1	[196]
mH_2BDC	1	[197]
H_2IP	1	[56]
ipH_2	1	[198]
H_2iph	1	[199]
H_2ipt	1	[44]
m-H_2bdic	1	[200]
H_2bdic	1	[38]
H_2phth	1	[17]
H_2-1,3-bdc	1	[201]
m-BDC	1	[202]
H_2MBDA	1	[203]
H_2bba	1	[204]
bdcH_2	1	[205]

Nevertheless, it is worth noting that considering the orientations of the carboxylate groups (*syn-syn*, *anti-syn*, or *anti-anti*), 1,3-bdc will exhibit much more than 19 coordination fashions. Unfortunately, it was difficult to expand our survey in this field since just few papers describe the carboxylate orientations in the coordination networks based on 1,3-bdc, even though it is remarkable the influence of the carboxylate orientation on the magnetic properties of carboxylate complexes, for instance [207].

Among the nineteen 1,3-bdc bridge coordination possibilities, there are three distinct coordination modes for μ (**I–III**), six for μ_3 (**IV–IX**), four for μ_4 (**X–XIII**) and μ_5 (**XIV–XVII**), and two for μ_6 (**XVIII** and **XIX**), as shown in Fig. 6. One should note that 1,3-bdc is in its fully deprotonated form in almost all cases, acting as bridging ligand between the metal centers, although we have found one example of the partially deprotonated form, 1,3-Hbdc, performing as a bridging ligand in the μ-bis-monodentate fashion (**81**, Table 2) [208].

Interestingly, despite the ligand 1,3-bdc being divergent, some reports describe it acting as a one-end coordinated ligand [94,98,121,136,138,177,180,205]. Fig. 7 presents the possibilities of coordination modes for 1,3-bdc and its partially protonated acid acting as terminal ligands. Moreover, in few cases, we found 1,3-Hbdc and 1,3-bdc playing the role of free counterions within the structure of coordination compounds [103,199,209,210]. Another possibility is the presence of 1,3-bdc inserted in the network structure as a noncoordinated molecule [49].

Table 3 describes the coordination modes of 1,3-bdc, represented in Figs. 6 and 7, employing the kappa (κ) convention, according to IUPAC recommendations [211], and the Harris notation [212,213], which is more intuitive to use for polydentate ligands such as carboxylates.

Even though 1,3-bdc can also perform as μ_5- and μ_6-bridging linker (see Fig. 6), the most common coordination modes adopted by this ligand range from μ- to μ_4-bridge, as illustrated in Fig. 8. Transition metals including Zn^{II}, Cu^{II}, and Co^{II} (3*d*-block) and Cd^{II} (4*d*-block) as well as an assortment of lanthanide ions (Ln^{III}, 4*f*-block), are the most common metal centers employed for building coordination networks with 1,3-bdc (Fig. 8).

The coordination mode of 1,3-bdc with the highest number of occurrences is the μ_3-chelate-bidentate (**IV**) followed by the μ-bis-monodentate (**I**). Comparing the coordination compounds that employ one of the three μ-bridging coordination modes, the results seem to indicate that while metal ions with small ionic radius are preferably surrounded by 1,3-bdc in the mono/bi-coordinated modes, the larger metal ions would rather choose the chelating ones. As depicted in Fig. 8, the coordination mode μ-bis-monodentate (**I**) is preferably adopted by 3*d*-block transition metals, such as Zn^{II}, Cu^{II}, and Co^{II} (ionic radii varying from 58 to 60 pm for CN = 4 and from 65 to 74 pm for CN = 6) [214], over other bigger metal centers like Cd^{II} (ionic radius: 95 pm for CN = 6) [214] and Ln^{III} (average ionic radius: 90 pm for CN = 6) [214]. Moreover, in the mode **I**, the 3*d*-metal ions exhibit mostly CN = 4 and 5. In contrast, μ-chelate-monodentate (**II**) and μ_3-chelate-bidentate (**IV**) perform an intermediary behavior being usually found coordinated to 3*d*-metal ions (mostly CN = 5 and 6) as well as to Cd^{II} and Ln^{III}. Differently from what is observed for mode **I**, μ-bis-chelating (**III**)

Table 2
Some characteristics of coordination networks based on 1,3-bdc published in the last 20 years.

Coordination mode	Formulae	Metal ion (CN)		Experimental approach	IR ν(COO$^-$) [cm^{-1}] Δν	Distinct coordination mode for 1,3-bdc in the compound	Ref.
μ-κO:κO" 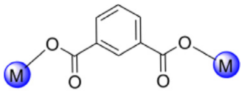	$[Cu(1,3\text{-}bdc)(phen)]_n$ (**3**) (phen = 1,10-phenanthroline)	Cu^{II} (4)		Hydrothermal (140 °C/120 h)	Not assigned		[18]
	$\{[Cu(1,3\text{-}bdc)(phen)(H_2O)]\cdot DMF\cdot(H_2O)\}_n$ (**4**) (phen = 1,10-phenanthroline)	Cu^{II} (5)	1D	Slow evaporation DMF	–		[17]
	$\{[Cu(1,3\text{-}bdc)(bpy)]\cdot 2(H_2O)\}_n$ (**5**) (bpy = 2,2′-bipyridine)	Cu^{II} (4)		Hydrothermal (150 °C/144 h)	Not assigned		[18]
	$[Cu(1,3\text{-}bdc)(dap)(H_2O)]_n$ (**6**) (dap = 1,3-diaminopropane)	Cu^{II} (5)	1D	Slow evaporation H_2O	1565_{as}; 1385_s		[44]
	$\{[Cu(1,3\text{-}bdc)(tacn)]\cdot 0.5(MeOH)\cdot 0.5(H_2O)\}_n$ (**7**) (tacn = 1,4,7-triazaciclononane)	Cu^{II} (5)		H_2O: EtOH: CH_3CN (1:1)	–		[47]
	$[Cu(1,3\text{-}bdc)(bpa)_{0.5}(H_2O)(DMF)]_n$ (**8**) (bpa = 1,2-bis(4-pyridyl)ethane)	Cu^{II} (5)	1D	Slow evaporation DMF	Not assigned		[221]
	$[[Cu_6(1,3\text{-}bdc)_6(bpa)_6(DMF)_3]\cdot 8DMF\}_n$ (**9**) (bpa = 1,2-bis(4-pyridyl)ethane)	Cu^{II} (4/5)	2D	Microwave DMF (140 °C/1 h)	Not assigned	1-μ-κO:κO” 2-μ-κO:κ^2O”,O’”	[221]
	$[[Cu_2(1,3\text{-}bdc)_2(bip)_2(H_2O)_3]\cdot 2(H_2O)]_n$ (**10**) (bip = 2-(4-bromophe-nyl)-1H-imidazo[4,5-f][1,10] phenanthroline)	Cu^{II} (5)	2D	Hydrothermal (170 °C/72 h)	Not assigned		[202]
	$\{[Cu(1,3\text{-}bdc)(dimb)]\cdot(DMA)\}_n$ (**11**) (dimb = 1,4-di(imidazolidin-1-yl)benzene)	Cu^{II} (4)	2D	Solvothermal DMA: EtOH: H_2O (1:1:2) (130 °C/72 h)	1611_{as}; 1396_s Δν = 215		[164]
	$[Cu(1,3\text{-}bdc)(1,4\text{-}bib)]_n$ (**12**) (1,4-bib = 1,4-bis(imidazole)butane)	Cu^{II} (4)	2D	Solvothermal H_2O:MeOH (4:1) (140 °C/72 h)	1623_{as}; 1329_s Δν = 294		[248]
	$[Cu(1,3\text{-}bdc)(4\text{-}dpyh)(H_2O)]_n$ (**13**) (4-dpyh = N,N′-bis(4-pyridinecarboxamide)-1,6-hexane)	Cu^{II} (5)	2D	Hydrothermal (120 °C/96 h)	1616_{as}; 1226_s		[85]
	$\{[Cu(1,3\text{-}bdc)(d3po)(H_2O)_2]\cdot 3(H_2O)\}_n$ (**14**) (d3po = N,N′-di(3-pyridyl)octanediamide)	Cu^{II} (5)	3D	Hydrothermal (120 °C/96 h)	Not assigned		[92]
	$\{[Cu(1,3\text{-}bdc)(py)_3]\cdot 5.5(H_2O)\}_n$ (**15**) (py = pyridine)	Cu^{II} (5)	1D	Slow evaporation DMSO:py (7:2)	–		[179]
	$\{[Cu(1,3\text{-}bdc)(py)_3]\cdot(H_2O)\cdot MeOH\}_n$ (**16**) (py = pyridine)	Cu^{II} (5)	1D	Slow evaporation MeOH:py (10:1)	–		[179]
	$[Zn_2(1,3\text{-}bdc)_2(d3pa)(H_2O)_2]_n$ (**17**) (d3pa = N,N′-di(3-pyridyl)adipoamide)	Zn^{II} (4)	2D	Hydrothermal (120 °C/48 h)	Not assigned		[2]
	$\{[Zn(1,3\text{-}bdc)(bix)](solv)_x\}_n$ (**18**) (bix = 1,4-bis(imidazol-l-yl-methyl)-benzene) Solv = guest solvent molecules not refined	Zn^{II} (4)	2D	Solvothermal DMF (95 °C/72 h)	Not assigned		[14]
	$\{[Zn_2(1,3\text{-}bdc)_2(bix)_2](solv)_x\}_n$ (**19**) (bix = 1,4-bis(imidazol-l-yl-methyl)-benzene) Solv = guest solvent molecules not refined	Zn^{II} (4)	3D	Solvothermal DMF:EtOH (12:1) (95 °C/72 h)	Not assigned		[14]
	$\{[Zn(1,3\text{-}bdc)(bix)](solv)_x\}_n$ (**20**) (bix = 1,4-bis(imidazol-l-yl-methyl)-benzene) Solv = guest solvent molecules not refined	Zn^{II} (4)	2D	Solvothermal DMF:EtOH (6:1) (9 °C/72 h)	Not assigned		[14]
	$\{[Zn(1,3\text{-}bdc)(bbip)]\cdot(H_2O)\}_n$ (**21**) (bbip = 1,1′-(1,4-butanediyl)bis(imidazole-2-phenyl))	Zn^{II} (4)	2D	Hydrothermal (160 °C/72 h)	Not assigned		[42]
	$\{[Zn(1,3\text{-}bdc)(bmt)(H_2O)]\cdot 0.5(H_2O)\}_n$ (**22**) (bmt = 1-((benzo-triazol-1-yl)methyl)-1-H-1,2,4-triazole))	Zn^{II} (4)	1D	Solvothermal H_2O:DMF (5:2) (120 °C/96 h)	1616_{as}; 1424_s Δν = 192		[38]
	$\{[Zn_2(1,3\text{-}bdc)(tiym)_2]\cdot 4.75(H_2O)\}_n$ (**23**) (tiym = tetrakis(imidazol-1-ylmethyl)methane)	Zn^{II} (4)	3D	Hydrothermal (150 °C/72 h)	Not assigned		[41]
	$\{[Zn(1,3\text{-}bdc)(4,4'\text{-}bipy)(H_2O)]\cdot 1.5(H_2O)\}_n$ (**24**) (4,4′-bipy = 4,4′-bipyridine)	Zn (5)	2D	Slow evaporation H_2O:EtOH	–		[71]
	$\{[Zn_2(1,3\text{-}bdc)_2(4,4'\text{-}bipy)(EtOH)(H_2O)_2]$ $EtOH\ 0.5(H_2O)\}_n$ (**25**) (4,4′-bipy = 4,4′-bipyridine)	Zn (4/6)	2D	Slow evaporation H_2O:EtOH	–	1-μ-κO:κO” 2-μ_3-κO:κO’:κO”	[71]
	$\{[Zn(1,3\text{-}bdc)(3\text{-}dpyh)]\cdot 3(H_2O)\}_n$ (**26**) (3-dpyh = N,N′-bis(3-pyridinecarboxamide)-1,6-hexane)	Zn^{II} (4)	1D	Hydrothermal (120 °C/96 h)	1615_{as}; 1224_s		[85]
	$[Zn(1,3\text{-}bdc)(bmimx)]_n$ (**27**) (bmimx = 1,4-bis(2-methylimidazol-1-yl-methyl)-2,3,5,6-tetramethylbenzene)	Zn^{II} (4)	2D	Hydrothermal (140 °C/70 h)	Not assigned		[88]
	$[Zn(1,3\text{-}bdc)(bb3pb)]_n$ (**28**) (bb3pb = 1,1′-(1,4-butanediyl)-bis[2-(3-pyridyl) benzimidazole])	Zn^{II} (4)	2D	Solvothermal H_2O:MeOH (1:1) (140 °C/72 h)	Not assigned		[148]
	$\{[Zn(1,3\text{-}bdc)(bpmd)(H_2O)]\cdot(H_2O)\}_n$ (**29**) (bpmd = N,N′-bis(pyridine-3-yl)-5-methylisophthalicdicarboxamide)	Zn^{II} (5)	1D	Hydrothermal (120 °C/96 h)	Not assigned		[115]
	$\{[Zn(1,3\text{-}bdc)(bbp)\cdot(H_2O)]_8\}_n$ (**30**) (bbp = 1,3-bis(benzimidazol-1-yl)-2-propanol)	Zn^{II} (4)	3D	Hydrothermal (140 °C/72 h)	1614_{as}; 1352_s Δν = 262		[151]
	$\{[Zn(1,3\text{-}bdc)(pobd)]\cdot(H_2O)\}_n$ (**31**) pobd = N,N′-bis(pyridine-3-yl)-4,4′-oxybis(benzoic) dicarboxamide	Zn^{II} (4)	2D	Solvothermal DMF:H_2O (1:1) (85 °C/96 h)	1545_{as}; 1395_s		[77]
	$[Zn(1,3\text{-}bdc)(bmb)]_n$ (**32**) (bmb = 1,4-bis(2-methylbenzimidazol-1-ylmethyl) benzene)	Zn^{II} (4)	2D	Hydrothermal (160 °C/96 h)	Not assigned		[142]
	$\{[Zn_2(1,3\text{-}bdc)_2(pyim)_2]\cdot 4DMF\}_n$ (**33**) pyim = 2,6-bis(imidazol-1-yl)pyridine	Zn^{II} (4)	1D	Slow evaporation DMF: MeOH (7:4)	1622_{as}; 1385_s Δν = 237		[249]
	$\{[Zn(1,3\text{-}bdc)(bpbd)]\cdot(H_2O)\}_n$ (**34**) (bpbd = N,N′-bis(pyridine-3-yl)-4,4′-oxybis(benzoic) dicarboxamide)	Zn^{II} (4)	2D	Solvothermal DMA: H_2O (1:1) (85 °C/96 h)	1616_{as}; 1354_s		[110]
	$\{[Zn(1,3\text{-}bdc)(pmdb)]\cdot(MeCN)\cdot 0.5(H_2O)\}_n$ (**35**) (pmdb = (pyridin-3-yl)methyl 4-(2-(4-((pyridin-3-yl) methoxy)phenyl)diazenyl)benzoate	Zn^{II} (4)	1D	Solvothermal MeCN: H_2O (1:1) (170 °C/96 h)	Not assigned		[78]
	$\{[Zn(1,3\text{-}bdc)(btx)]\cdot 2(H_2O)\cdot(DMF)\}_n$ (**36**) (btx = 1,4-bis(1,2,4-triazol-4-yl) benzene)	Zn^{II} (4)	2D	Slow evaporation DMF: H_2O (1:2)	Not assigned		[250]
	$\{[Zn(1,3\text{-}bdc)(bte)]\cdot 0.5(H_2O)\}_n$ (**37**) (bte = 1,2-bis(1,2,4-triazol-1-yl)ethane)	Zn^{II} (4)	2D	Slow evaporation H_2O:MeOH	Not assigned		[19]
	$[Zn_2(1,3\text{-}bdc)_2(titmb)(H_2O)]_n$ (**38**) titmb = 1,3,5-tris(imidazol-1-ylmethyl)-2,4,6-trimethylbenzene)	Zn^{II} (4)	2D	Hydrothermal (150 °C/24 h)	Not assigned	1-μ-κO:κO” 2-μ-κO:κ^2O”,O’”	[90]
	$[Zn_2(1,3\text{-}bdc)_2(ttyt)(H_2O)]_n$ (**39**) (ttyt = 1,3,5-tris(1H-1,2,4-triazol-1-ylmethyl)-2,4,6-trimethylbenzene)	Zn^{II} (4)	2D	Solvothermal MeOH:H_2O (1:1) (150 °C/72 h)	Not assigned		[150]
	$\{[Zn_8(1,3\text{-}bdc)_8(tib)_5(H_2O)]\cdot 7DMF\cdot 18(H_2O)\}_n$ (**40**) (tib = 1,3,5-tris(1-imidazolyl)-benzene)	Zn^{II} (4)	3D	Solvothermal DMF:H_2O (1:1) (120 °C/84 h)	1616_{as}; 1390_s Δν = 220		[167]
	$[Zn(1,3\text{-}bdc)(btmx)]_n$ (**41**) (btmx = 1,4-bis(1,2,4-triazol-1-ylmethyl)-2,3,5,6tetramethyl-benzene)	Zn^{II} (4)	2D	Hydrothermal (160 °C/70 h)	Not assigned		[251]
	$[Zn(1,3\text{-}bdc)(dHyn)]_n$ (**42**) (dHyn = 1,3-di(1H-imidazol-4-yl) benzene)	Zn^{II} (4)	1D	Hydrothermal (180 °C/72 h)	Not assigned		[188]
	$[Zn(1,3\text{-}bdc)(2,3'\text{-}tmbpt)]_n$ (**43**)	Zn^{II}	3D	Hydrothermal	Not assigned		[141]

(continued on next page)

Table 2 (*continued*)

Coordination mode	Formulae	Metal ion (CN)		Experimental approach	IR ν(COO$^-$) [cm^{-1}] Δν	Distinct coordination mode for 1,3-bdc in the compound	Ref.
	(2,3′-tmbpt = 1-((1H-1,2,4-triazol-1-yl)methyl)-3-(3-pyridyl)-5-(2-pyridyl)-1,2,4-triazole)	(4)		(130 °C/72 h)			
	{[Zn(1,3-bdc)(3,3′-tmbpt)(H_2O)]·(H_2O)}$_n$ (**44**) (3,3′-tmbpt = 1- ((1H-1,2,4-triazol-1-yl)methyl)-3,5-bis (3-pyridyl)-1,2,4-triazole)	Zn^{II} (4)	3D	Hydrothermal (130 °C/72 h)	Not assigned		[141]
	{[Zn_2(1,3-bdc)$_2$(4,4′-bpt)(H_2O)$_3$]·(H_2O)}$_n$ (**45**) (4,4′-bpt = 1H-3,5-bis(4-pyridyl)-1,2,4-triazole)	Zn^{II} (5)	1D	Solvothermal H_2O:EtOH (2:1) (140 °C/72 h)	Not assigned		[196]
	{[Zn_2(1,3-bdc)$_2$(hbpb)]·2.25(H_2O)}$_n$ (**46**) (hbpb = 1,1′-(1,6-hexanediyl)bis[2-(2-pyridyl) benzimidazole)	Zn^{II} (4)	2D	Solvothermal H_2O:MeOH (1:1) (140 °C/72 h)	Not assigned		[68]
	[Zn_2(1,3-bdc)$_2$(dHib)(H_2O)]$_n$ (**47**) (dHib = 1,4-di(1H-imidazol-4-yl)benzene)	Zn^{II} (4/5)	2D	Hydrothermal (160 °C/72 h)	Not assigned	1-μ-κO:κO'' 2-μ_3-κ^2O,O':κO:κO''	[95]
	{[Zn(1,3-bdc)(tib)]·(H_2O)}$_n$ (**48**) (tib = 1,3,5-tris(1-imidazolyl)benzene)	Zn^{II} (4)	2D	Hydrothermal (180 °C/72 h)	Not assigned		[97]
	{[Zn_2(1,3-bdc)$_2$(tib)(H_2O)]·2(H_2O)}$_n$ (**49**) (tib = 1,3,5-tris(1-imidazolyl)benzene)	Zn^{II} (5)	3D	Hydrothermal (180 °C/72 h)	Not assigned	1-μ-κO:κO'' 2-μ-κO:κ^2O'',O'''	[97]
	{[Zn(1,3-bdc)(3-bpp)]·2(H_2O)·MeOH}$_n$ (**50**) (3-bpp = 2,2′-bis(3-pyridylmethyleneoxy)-1,1′-biphenylene)	Zn^{II} (4)	1D	Slow evaporation MeOH:H_2O (1:1)	Not assigned		[252]
	{[Zn(1,3-bdc)(en)]·3(H_2O)}$_n$ (**51**) (en = ethylenediamine)	Zn^{II} (4)	2D	Reflux 4 h EtOH	–		[253]
	{[Ni(1,3-bdc)(dbyp)(H_2O)$_2$]·0.5(H_2O)}$_n$ (**52**) (dbyp = 3,5-di(1H-benzimidazol-1-yl)pyridine)	Ni^{II} (6)	1D	Solvothermal DMF:H_2O (1:3) (120 °C/72 h)	Not assigned		[52]
	[Ni_2(1,3-bdc)$_2$(3pyp)$_2$(H_2O)]$_n$ (**53**) (3pyp = 3-pyridin-3-ylimidazo[1,2-*a*]pyridine)	Ni^{II} (6)	3D	Solvothermal DMF:H_2O (1:4) (140 °C/48 h)	Not assigned		[183]
	{[Ni(1,3-bdc)(3-dpyp)(H_2O)]·(H_2O)}$_n$ (**54**) (3-dpyp = N,N′-bis(3-pyridinecarboxamide)-1,3-propane)	Ni^{II} (6)	1D	Hidrothermal (120 °C/96 h)	1604_{as}; 1419_{s}		[91]
	[Ni(1,3-bdc)(dap)$_2$]$_n$ (**55**) (dap = 1,3-diaminopropane)	Ni^{II} (6)	1D	Slow evaporation MeOH	1545_{as}; 1371_{s}		[44]
	[Ni(1,3-bdc)(MeOH)$_4$]$_n$ (**56**)	Ni^{II} (6)	1D	Slow diffusion MeOH	–		[179]
	[M(1,3-bdc)(pbmb)]$_n$ (pbmb = 1,10-(1,3-propane)bis-(2-methylbenzimidazole)) M = Zn (**57**) or Co (**58**)	Zn^{II} Co^{II} (4)	2D	Hydrothermal (130 °C/72 h)	Not assigned		[54]
	{[M(1,3-bdc)(4-bpah)(H_2O)]}$_n$ (4-bpah = N,N′-bis(4-pyridinecarboxamide)-1,2-cyclohexane) M = Cu (**59**), Co (**60**), Ni (**61**), or Zn (**62**)	Cu^{II} Co^{II} Ni^{II} Zn^{II} (5)	2D	Hydrothermal (120 °C/144 h)	$(1608–1610)_{as}$; $(1419–1438)_{s}$		[24]
	[Co(1,3-bdc)(ampy)$_2$]$_n$ (**63**) (ampy = 4-aminopyridine)	Co^{II} (4)	1D	Solvothermal EtOH (120 °C/48 h)	Not assigned		[29]
	[$Co_{1.5}$(1,3-bdc)$_{1.5}$(tib)(H_2O)]$_n$ (**64**) (tib = 1,3,5-tris(1-imidazolyl)benzene)	Co^{II} (5)	2D	Hydrothermal (170 °C/72 h)	Not assigned	1-μ-κO:κO'' 2-μ-κO:κ^2O'',O'''	[114]
	{[Co(1,3-bdc)(d3po)(H_2O)$_2$]·(H_2O)}$_n$ (**65**) (d3po = N,N′-di(3-pyridyl)octanediamide)	Co^{II} (6)	2D	Hydrothermal (120 °C/96 h)	Not assigned		[92]
	{[Co(1,3-bdc)(BCbpe)]·3(H_2O)}$_n$ (**66**) (BCbpe = 1-(4-carboxy-benzyl)4-[2-(4-pyridyl)-vinyl])	Co^{II} (4)	2D	Solvothermal EtOH:H_2O (1:1) (95 °C/72 h)	–		[172]
	[Co(1,3-bdc)(b3pm)(H_2O)$_2$]$_n$ (**67**) (b3pm = N,N′-bis(3-pyridyl)malonamide)	Co^{II} (6)	1D	Hydrothermal (120 °C/96 h)	Not assigned		[61]
	{[Co(1,3-bdc)(biim-5)]·(H_2O)}$_n$ (**68**) (biim-5 = 1,1′-(1,5-pentanedidyl)bis-(imidazole))	Co^{II} (4)	2D	Hydrothermal (140 °C/72 h)	Not assigned		[254]
	{[Co(1,3-bdc)(py)$_3$(H_2O)]$_n$ (**69**) (py = pyridine)	Co^{II} (6)	1D	MeOH;py (5:1) Reflux 30 min	–		[179]
	{[Co(1,3-bdc)(py)$_3$(MeOH)]·(H_2O)}$_n$ (**70**) (py = pyridine)	Co^{II} (6)	1D	MeOH:py (10:1)	–		[179]
	[Co(1,3-bdc)(MeOH)$_4$]$_n$ (**71**)	Co^{II} (6)	1D	Slow diffusion MeOH	–		[179]
	{[$NH_2(CH_3)_2$][MNa(1,3-bdc)$_2$]}$_n$ M = Co (**72**) or Cd (**73**)	Co^{II} Cd^{II} (4) Na^{I} (6)	3D	Solvothermal DMF (140 °C/72 h)	1580_{as}; 1450_{s}		[133]
	{[Cd(1,3-bdc)(bpmd)(H_2O)]·(H_2O)}$_n$ (**74**) (bpmd = N,N′-bis(pyridine-3-yl)-5-methylisophthalicdicarboxamide)	Cd^{II} (6)	2D	Hydrothermal (120 °C/96 h)	Not assigned		[115]
	[Cd(1,3-Hbdc)$_2$(bmb)]$_n$ (**75**) (bmb = 1,4-bis(2-methylbenzimidazol-1-ylmethyl) benzene)	Cd^{II} (6)	3D	Hydrothermal (160 °C/72 h)	Not assigned		[163]
	[Ag(1,3-bdc)$_{0.5}$(bpe)]$_n$ (**76**) (bpe = *trans*-1-(2-pyridyl)-2-(4-pyridyl)ethylene)	Ag^{I} (3)	3D	Slow evaporation MeOH	Not assigned		[152]
	{[Ag_2(1,3-bdc)(dmapym)$_2$)]·2(H_2O)}$_n$ (**77**) (dmapym = 2-amino-4,6-dimethylpyrimidine)	Ag^{I} (2/4)	3D	Ultrasonic conditions 50 °C MeOH:H_2O (2:1)	1661_{as}, 1562_{as}; 1481_{s}, 1381_{s}		[169]
	{[Ag_2(1,3-bdc)(dtb)]·2(H_2O)}$_n$ (**78**) (dtb = 1,3-di-(1,2,4-triazole-4-yl)benzene)	Ag^{I} (3)	2D	Hydrothermal (140 °C/72 h)	Not assigned		[113]
	{[Gd_2(1,3-bdc)$_3$(H_2O)$_8$]•2DMF•6(H_2O)}$_n$ (**79**)	Gd^{III} (9)	1D	Slow evaporation DMF	Not assigned	1-μ-κO:κO'' 2-μ-κ^2O,O':κ^2O'',O'''	[69]
	{[Y_2Ni_2(1,3-bdc)$_5$(tpa)(H_2O)$_3$]·7(H_2O)}$_n$ (**80**) (tpa = tris(2-benzimidazolylmethyl)amine)	Y^{III} (8/9) Ni^{II} (5)	1D	Hydrothermal (140 °C/72 h)	Not assigned	1-μ-κO:κO'' 2-μ-κO:κ^2O'',O''' 3-μ_3-κ^2O,O':κO'':κO''' 4-μ-κ^2O,O':κ^2O'',O'''	[168]
μ-κO:κO'' 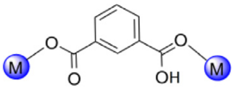 	[Ag(1,3-Hbdc)(PyBIm)]$_n$ (**81**) (PyBIm = 2-(4-pyridyl)benzimidazole)	Ag^{I} (4)	2D	Hydrothermal (150 °C/120 h)			[208]

Table 2 (*continued*)

Coordination mode	Formulae	Metal ion (CN)		Experimental approach	IR ν(COO$^-$) [cm^{-1}] Δν	Distinct coordination mode for 1,3-bdc in the compound	Ref.
μ-κO:κ^{2}O",O''' 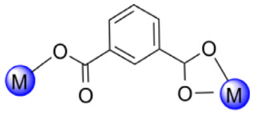 	{[Cu(1,3-bdc)(phen)(H$_2$O)]·DMF}$_n$ (**2**) (phen = 1,10-phenanthroline)	Cu^{II} (6)	1D	Slow evaporation DMF:H$_2$O	1554$_{as}$; 1382$_s$; 1360$_s$ Δν = 194; 172		The present work
	{[Cu$_2$(1,3-bdc)$_2$(3-bpah)]·(H$_2$O)}$_n$ (**82**) (3-bpah = N,N′-bis(3-pyridinecarboxamide)-1,2-cyclohexane)	Cu^{II} (5)	3D	Hydrothermal (120 °C/144 h)	1608$_{as}$; 1454$_s$	1-μ-κ^{2}O,O':κ^{2}O",O''' 2-μ$_3$-κO:κO':κO"	[24]
	{[Cu$_3$(1,3-bdc)(OH)(pz)$_3$(Hpz)(H$_2$O)]·4(H$_2$O)}$_n$ (**83**) (Hpz = pyrazol)	Cu^{II} (4/5)	1D	Solvothermal H$_2$O:MeOH (1:1) (120 °C/48 h)	–		[35]
	{[Cu(1,3-bdc)(9Meade)(H$_2$O)$_2$]$_n$ (**84**) (9Meade = 9-methyladenine)	Cu^{II} (6)	1D	Slow diffusion MeOH:H$_2$O	–		[49]
	[Cu(1,3-bdc)(d3ps)(H$_2$O)] $_n$ (**85**) (d3ps = N,N'-di(3-pyridyl)succinimide)	Cu^{II} (6)	2D	Hydrothermal (120 °C/96 h)	Not assigned		[66]
	{[Cu$_6$(1,3-bdc)$_6$(bpa)$_6$(DMF)$_3$]·8DMF}$_n$ (**9**) (bpa = 1,2-bis(4-pyridyl)ethane)	Cu^{II} (4/5)	2D	Microwave DMF (140 °C/1 h)	Not assigned	1-μ-κO:κO" 2-μ-κO:κ^{2}O",O'''	[221]
	{[Cu(1,3-bdc)(3-bpmp)(H$_2$O)]·2(H$_2$O)}$_n$ (**86**) (3-bpmp = N,N′-bis(3-pyridyl-methyl)piperazine)	Cu^{II} (6)	2D	Hydrothermal (80 °C/240 h)	1553$_{as}$; 1383$_s$		[255]
	[Zn(1,3-bdc)(dpq)(H$_2$O)]$_n$ (**87**) (dqp = 2,3-di-2-pyridylquinoxaline)	Zn^{II} (6)		Hydrothermal (160 °C/144 h)	–		[43]
	[Zn$_2$(1,3-bdc)$_2$(titmb)(H$_2$O)]$_n$ (**38**) (titmb = 1,3,5-tris(imidazol-1-ylmethyl)-2,4,6-trimethylbenzene)	Zn^{II} (4)	2D	Hydrothermal (150 °C/24 h)	Not assigned	1-μ-κO:κO" 2-μ-κO:κ^{2}O",O'''	[90]
	{[Zn$_2$(1,3-bdc)$_2$(tib)(H$_2$O)]·2(H$_2$O)}$_n$ (**49**) (tib = 1,3,5-tris(1-imidazolyl)benzene)	Zn^{II} (5)	3D	Hydrothermal (180 °C/72 h)	Not assigned	1-μ-κO:κO" 2-μ-κO:κ^{2}O",O'''	[97]
	[Zn(1,3-bdc)(H$_3$tris)(MeOH)]$_n$ (**88**) (H$_3$tris = tris(hydroxymethyl)aminomethane)	Zn^{II} (6)	3D	Solvothermal MeOH (110 °C/20 h)	Not assigned		[116]
	{[Zn(1,3-bdc)(1,3-bip)]·2(H$_2$O)}$_n$ (**89**) (1,3-bip = 1,3-bis(imidazole)propane)	Zn^{II} (5)	2D	Hydrothermal (110 °C/72 h)	Not assigned		[178]
	{[Zn$_2$(1,3-bdc)$_2$(ttbt)$_2$]·2(H$_2$O)}$_n$ (**90**) (ttbt = 10,11,12,13-tetrahydro-4,5,9,14-tetraaza-benzo[*b*]triphenylene)	Zn^{II} (6)	2D	Hydrothermal (140 °C/120 h)	–	1-μ-κO:κ^{2}O",O''' 2-μ$_4$-κO,O':κO''',O'''	[96]
	{[Zn(1,3-bdc)(3-pp)(H$_2$O)]·3(H$_2$O)}$_n$ (**91**) (3-pp = 3-(2-pyridyl)pyrazole)	Zn^{II} (6)	1D	Hydrothermal (140 °C/48 h)	1615$_{as}$; 1551$_{as}$; 1355$_s$ Δν = 260; 196		[256]
	{[Zn(1,3-bdc)(Hdpp)]·DMF]}$_n$ (**92**) (Hdpp = di(4-pyridyl)-1H-pyrazole)	Zn^{II} (6)	2D	Solvothermal DMF (120 °C/48 h)	–		[186]
	{[Zn(1,3-bdc)(tmbpt)(H$_2$O)]·(H$_2$O)}$_n$ (**93**) (tmbpt = 1-((1H-1,2,4-triazol-1-yl)methyl)-3-(4-pyridyl)-5-(3-pyridyl)-1,2,4-triazole (3,4′-tmbpt))	Zn^{II} (5)	2D	Hydrothermal (130 °C/70 h)	1608$_{as}$, 1558a$_{ss}$; 1380$_s$.		[144]
	[Ni(1,3-bdc)(bdh)·(H$_2$O)]$_n$ (**94**) (bdh = 1,6-bis(5,6-dimethylbenzimidazol-1-yl)hexane)	Ni^{II} (6)	2D	Hydrothermal (140 °C/72 h)	1604$_{as}$, 1545$_s$; 1373$_s$.		[181]
	{[Ni(1,3-bdc)(bibp)(H$_2$O)]·0.5(H$_2$O)}$_n$ (**95**) (bibp = 1,4-bis(4-(imidazole-1-yl)benzyl)piperazine)	Ni^{II} (6)	3D	Hydrothermal (160 °C/48 h)	Not assigned		[177]
	[Ni(1,3-bdc)(bix)$_2$(H$_2$O)]$_n$ (**96**) (bix = 1,4-bis((1H-imidazol-1-yl) methyl)-benzene)	Ni^{II} (6)	2D	Hydrothermal (160 °C/72 h)	Not assigned		[125]
	{[Ni(1,3-bdc)(didp)(H$_2$O)]·5(H$_2$O)}$_n$ (**97**) (didp = 2,8-di(1H-imidazol-1-yl)-dibenzothiophene)	Ni^{II} (6)	1D	Solvothermal DMF: H$_2$O (1:1) (105 °C/72 h)	Not assigned		[147]
	[Ni(1,3-bdc)(3-dpye)(H$_2$O)$_2$]$_n$ (**98**) (3-dpye = N,N′-bis(3-pyridinecarboxamide)-1,2-ethane)	Ni^{II} (6)	2D	Hidrothermal (120 °C/96 h)	1602$_{as}$; 1419$_s$		[91]
	{[Ni(1,3-bdc)(3-dpyb)(H$_2$O)$_2$]·(H$_2$O)}$_n$ (**99**) (3-dpyb = N,N′-bis(3-pyridinecarboxamide)-1,4-butane)	Ni^{II} (6)	2D	Hidrothermal (120 °C/96 h)	1604$_{as}$; 1432$_s$		[91]
	{[Ni(1,3-bdc)(3-dpyh)(H$_2$O)$_2$]·(H$_2$O)}$_n$ (**100**) (3-dpyh = N,N′-bis(3-pyridinecarbox amide)-1,6-hexane)	Ni^{II} (6)	2D	Hidrothermal (120 °C/96 h)	1604$_{as}$; 1427$_s$		[91]
	{[Ni(1,3-bdc)(tmtz)$_{1.5}$]·0.5(H$_2$O)}$_n$ (**101**) (tmtz = 1,4-bis(1,2,4-triazol-1-ylmethyl)-2,3,5,6-tetramethyl-benzene)	Ni^{II} (5)	2D	Slow evaporation H$_2$O	Not assigned		[257]
	[Mn(1,3-bdc)(tmtz)$_{1.5}$]$_n$ (**102**) (tmtz = 1,4-bis(1,2,4-triazol-1-ylmethyl)-2,3,5,6-tetramethyl-benzene)	Mn^{II} (6)	2D	Solvothermal H$_2$O:MeOH (2:1) (110 °C/24 h)	Not assigned		[257]
	{[Mn(1,3-bdc)(btp)(H$_2$O)]·2.5(H$_2$O)}$_n$ (**103**) (btp = 1,3-bis(1,2,4-triazol-1-yl)propane)	Mn^{II} (6)	2D	Slow diffusion MeOH:H$_2$O	Not assigned		[258]
	[Co$_{1.5}$(1,3-bdc)$_{1.5}$(tib)(H$_2$O)]$_n$ (**64**) (tib = 1,3,5-tris(1-imidazolyl)benzene)	Co^{II} (5)	2D	Hydrothermal (170 °C/72 h)	Not assigned	1-μ-κO:κO" 2-μ-κO:κ^{2}O",O'''	[114]
	[Co(1,3-bdc)(bim)]$_n$ (**104**) (bim = bis(imidazol-1-yl)methane)	Co^{II} (5)	2D	Hydrothermal (140 °C/72 h)	1620$_{as}$, 1564$_{as}$; 1359$_s$ Δν = 261; 205		[159]
	{[Co(1,3-bdc)(4-bpmh)]·2(H$_2$O)}$_n$ (**105**) (4-bpmh = N,*N*-bis-pyridin-4-ylmethylene-hydrazine)	Co^{II} (6)	3D	Solvothermal MeOH:DMF:H$_2$O (6:1:1) (120 °C/48 h)	–		[100]
	{[Co$_2$(1,3-bdc)$_2$(dpyi)$_2$]·DMF·0.2(H$_2$O)}$_n$ (**106**) (dpyi = N,*N*-di(pyridin-4-yl)isophthalamide)	Co^{II} (5)	2D	Solvothermal DMF (120 °C/48 h)	Not assigned		[259]
	[CoCu(1,3-bdc)(bipy)$_{1.5}$(m-nbz)]$_n$ (**107**) (bipy = 4,4′-bipyridine) (m-Hnbz = m-nitrobenzoic acid)	Co^{II} (5) Cu^{I} (3)	2D	Solvothermal CH$_3$CN (140 °C/72 h)	Not assigned		[130]
	{[Co(1,3-bdc)(bbyb)(H$_2$O)]·1.5(H$_2$O)}$_n$ (**108**) (bbyb = 4,4′-bis(benzimidazol-1-ylmethyl)biphenyl)	Co^{II} (6)	2D	Hydrothermal (130 °C/72 h)	1610$_{as}$; 1553$_s$, 1362$_s$ Δν = 57; 248		[112]
	{[Co(1,3-bdc)(bpmd)(H$_2$O)]·(H$_2$O)}$_n$ (**109**) (bpmd = N,N′-bis(pyridine-3-yl)-5-methylisophthalic dicarboxamide)	Co^{II} (6)	2D	Hydrothermal (120 °C/96 h)	1612$_{as}$; 1425$_s$		[111]
	{[In(1,3-bdc)(1,3-Hbdc)]·2DMF}$_n$ (**110**)	In^{III} (6)	2D	Solvothermal DMF (120 °C/96 h)	1619$_{as}$; 1405$_s$		[129]
	{[Cd(1,3-bdc)(bix)(H$_2$O)](DMF)}$_n$ (**111**) (bix = 1,4-bis(imidazol-l-yl-methyl)-benzene)	Cd^{II} (6)	2D	Solvothermal DMF (90 °C/60 h)	Not assigned		[14]
	[Cd(1,3-bdc)(bip)(H$_2$O)]$_n$ (**112**) (bip = 3,5-bis(imidazole-1-yl)pyridine)	Cd^{II} (7/6)	2D	Hydrothermal (160 °C/96 h)	Not assigned	1-μ-κ^{2}O,O':κ^{2}O",O''' 2-μ-κO:κ^{2}O",O'''	[27]
	[Cd$_2$(1,3-bdc)$_2$(d3pa)(H$_2$O)$_4$]$_n$ (**113**) (d3pa = N,N′-di(3-pyridyl)adipoamide)	Cd^{II} (6)	–	Hydrothermal (120 °C/48 h)	Not assigned		[2]
	[Cd(1,3-bdc)(bb3pb)]$_n$ (**114**) (bb3pb = 1,1′-(1,4-butanediyl)-bis[2-(3-pyridyl) benzimidazole])	Cd^{II} (6)	3D	Solvothermal H$_2$O:MeOH (1:1) (160 °C/72 h)	Not assigned		[148]
	[Cd(1,3-bdc)(bmb)(EtOH)(H$_2$O)]$_n$ (**115**) (bmb = 1,4-bis(2-methylbenzimidazol-1-ylmethyl) benzene)	Cd^{II} (6)	1D	Solvothermal H$_2$O:EtOH (4:1) (100 °C/72 h)	Not assigned		[163]
	[Cd$_2$(1,3-bdc)(3-pp)$_2$(H$_2$O)]$_n$ (**116**) (3-pp = 3-(2-pyridyl)pyrazole)	Cd^{II} (6)		Hydrothermal (140 °C/48 h)	1606$_{as}$, 1537$_{as}$; 1378$_s$ Δν = 228; 159	1-μ-κ^{2}O,O':κ^{2}O",O''' 2-μ$_3$-κ^{2}O,O':κO:κO"	[256]

(*continued on next page*)

Table 2 (*continued*)

Coordination mode	Formulae	Metal ion (CN)		Experimental approach	IR ν(COO$^-$) [cm^{-1}] Δν	Distinct coordination mode for 1,3-bdc in the compound	Ref.
	{[Cd(1,3-bdc)(H$_2$ceim)(H$_2$O)](H$_2$O)$_2$}$_n$ (**117**) (H$_2$ceim = 2,2′-(1,2-ethanediyl)bis(1H-benzimidazole)	Cd^{II} (6)	1D	Hydrothermal (160 °C/72 h)	–		[260]
	{[Cd(1,3-bdc)Bpyen)$_{0.5}$(H$_2$O)Br]·4(H$_2$O)}$_n$ (**118**) (Bpyen = 1,2-bis(4,4′-bipyridinium)ethane)	Cd^{II} (6)	2D	Solvothermal DMF:MeOH: H$_2$O (2:2:3) (75 °C/48 h)	Not assigned		[135]
	{[Cd(1,3-bdc)(3,3′-tmbpt)]·2(H$_2$O)}$_n$ (**119**) (3,3′-tmbpt = 1-((1H-1,2,4-triazol-1-yl)methyl)-3,5-bis (3-pyridyl)-1,2,4-triazole)	Cd^{II} (6)	2D	Hydrothermal (130 °C/72 h)	1602$_{as}$; 1380$_s$		[146]
	{[Cd(1,3-bdc)(ttr4a)]·2DMF·2(H$_2$O)}$_n$ (**120**) (ttr4a = tetrakis(1,2,4-triazol-ylmethylresorcin[4]arene)	Cd^{II} (6)		Solvothermal DMF:H$_2$O (1:1) (90 °C/96 h)	Not assigned		[261]
	[Cd(1,3-bdc)(bmyb)$_{1.5}$]$_n$ (**121**) (bmyb = 1,4-bis(2-methylimidazol-3-ium-1-yl) biphenyl)	Cd^{II} (6)	3D	Hydrothermal (160 °C/96 h)	1621$_{as}$, 1532$_{as}$; 1366$_s$ Δν = 155; 244		[89]
	[Cd$_2$(1,3-bdc)$_2$(2-mBIM)$_2$]$_n$ (**122**) (2-mBIM = bis(2-methylimidazol-1-yl)methane)	Cd^{II} (5/6)	2D	Hydrothermal (160 °C/48 h)	Not assigned		[39]
	[Cd$_2$Cl$_2$(1,3-bdc)(ttbt)(H$_2$O)]$_n$ (**123**) (ttbt = 10,11,12,13–tetrahydro-4,5,9,14-tetraaza-benzo [*b*]triphenylene)	Cd^{II} (6)	–	Hydrothermal (180 °C/72 h)	1414; 1395		[262]
	[Cd(1,3-bdc)(imd)$_2$(H$_2$O)]$_n$ (**124**) (imd = imidazole)	Cd^{II} (6)	–	Hydrothermal (160 °C/96 h)	–		[263]
	[Cd(1,3-bdc)(phen)]$_n$ (**125**)	Cd^{II} (6)	1D	Solvothermal DMF:H$_2$O:EtOH (4:3:2) (140 °C/72 h)	Not assigned		[99]
	{[Cd(1,3-bdc)(imb)(H$_2$O)]·2(H$_2$O)}$_n$ (**126**) (imb = 2-[(1H-imidazol-1-yl)methyl]-1H-benzimidazole)	Cd^{II} (6)	2D	Hydrothermal (120 °C/72 h)	Not assigned		[200]
	{[Cd(m-bdc)(MQ)(H$_2$O)Br]·3(H$_2$O)}$_n$ (**127**) (MQ = 1-methyl-4,4′-bipyridinium)	Cd^{II} (6)	1D	Slow evaporation DMF: H$_2$O	Not assigned		[134]
	{[Ln$_2$(1,3-bdc)$_3$(mpip)$_2$]·2(H$_2$O)}$_n$ (mpip = 2-(3-methylphenyl)imidazo(4,5-f)(1,10)-phenanthroline) Ln = Dy (**128**), Ho (**129**), or Er (**130**)	Dy^{III} Ho^{III} Er^{III} (8)	2D	Solvothermal CH$_3$CN: H$_2$O (3:2) (120 °C/72 h)	Not assigned	1-μ-κO:κ^{2}O”,O’” 2-μ$_3$-κ^{2}O,O’:κO”:κO’” 3-μ$_4$-κO,O’:κO’”,O’”	[195]
	{[Y$_2$Ni$_2$(1,3-bdc)$_5$(tpa)(H$_2$O)$_3$]·7(H$_2$O)}$_n$ (**80**) (tpa = tris(2-benzimidazolylmethyl)amine)	Y^{III} (8/9) Ni^{II} (5)	1D	Hydrothermal (140 °C/72 h)	Not assigned	1-μ-κO:κO” 2-μ-κO:κ^{2}O”,O’” 3-μ$_3$-κ^{2}O,O’:κO”:κO’” 4-μ-κ^{2}O,O’:κ^{2}O”,O’”	[168]
μ-κ^{2}O,O':κ^{2}O'',O''' 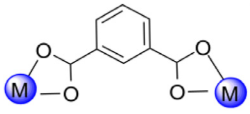	{[Cu$_2$(1,3-bdc)$_2$(3-bpah)]·H$_2$O}$_n$ (**82**) (3-bpah = N,N′-bis(3-pyridinecarboxamide)-1,2-cyclohexane)	Cu^{II} (5)	3D	Hydrothermal (120 °C/144 h)	1608$_{as}$; 1454$_s$	1-μ-κ^{2}O,O’:κ^{2}O”,O’” 2-μ$_3$-κO:κO’:κO”	[24]
	{[Cu(1,3-bdc)(4-bpcb)]$_2$·0.5(4-bpcb)}$_n$ (**131**) (4-bpcb = N,N′-bis(4-pyridinecarboxamide)-1,4-benzene)	Cu^{II} (6)	2D	Hydrothermal (120 °C/96 h)	1665$_{as}$, 1614$_{as}$; 1368$_s$		[40]
	[Cu(1,3-bdc)(9Meade)]$_n$ (**132**) (9Meade = 9-methyladenine)	Cu^{II} (6)	2D	Slow diffusion MeOH:H$_2$O	–		[49]
	[Cu$_2$(1,3-bdc)(bptzp)$_2$Cl$_2$]$_n$ (**133**) (bptzp = 1,4-bis(5-(4-pyridyl)tetrazolyl)propane	Cu^{II} (6)	1D	Solvothermal CH$_3$CN:H$_2$O (3:2) (120 °C/96 h)	1620$_{as}$; 1207$_s$		[124]
	[Zn$_2$(1,3-bdc)$_2$(bpy)$_2$]$_n$ (**134**) (bpy = 2,2′-bipyridine)	Zn^{II} (6)		Hydrothermal (160 °C/120 h)	1562$_{as}$, 1552$_{as}$; 1431$_s$ Δν = 131; 101	1-μ-κ^{2}O,O’:κ^{2}O”,O’” 2-μ$_3$-κ^{2}O,O’:κO”:κO’”	[31]
	[Zn(1,3-bdc)(bmb)]$_n$ (**135**) (bmb = 1,3-bis(2-methylbenzimidazol-1-ylmethyl) benzene)	Zn^{II} (6)	1D	Hydrothermal (140 °C/72 h)	Not assigned		[105]
	[Zn(1,3-bdc)(4,4′-tmbpt)]$_n$ (**136**) (4,4′-tmbpt = 1-((1H-1,2,4-triazol-1-yl)methyl)-3,5-bis (4-pyridyl)-1,2,4-triazole)	Zn^{II} (5)	3D	Hydrothermal (130 °C/72 h)	Not assigned		[140]
	[Co(1,3-bdc)(bpy)]$_n$ (**137**) (bpy = 2,2′-bipyridine)	Co^{II} (6)	2D	Hydrothermal (140 °C/72 h)	–	1-μ-κ^{2}O,O’:κ^{2}O”,O’” 2-μ$_3$-κ^{2}O,O’:κO”:κO’”	[264]
	{[Co(1,3-bdc)(bbyb)]·(H$_2$O)}$_n$ (**138**) (bbyb = 1,3-bis(benzimidazol-1-ylmethyl) benzene)	Co^{II} (6)	1D	Hydrothermal (140 °C/72 h)	1605as; 1430s Δν = 175		[51]
	[Co(1,3-bdc)(Hdap)]$_n$ (**139**) (Hdap = 2,6-diaminopurine)	Co^{II} (6)	2D	Solvothermal H$_2$O:DMF (3:2) (100 °C/72 h)	Not assigned		[193]
	[M$_4$(μ4-O)(1,3-bdc)$_3$(bipy)]$_n$ (**140**) (M$_4$ = Zn$_{2.36}$ Co$_{1.64}$) bipy = 4,4′-bipyridine	Zn^{II} Co^{II} (4/5)	2D	Hydrothermal (180 °C/60 h)		1-μ$_4$-κO,O’:κO’”,O’” 2-μ-κ^{2}O,O’:κ^{2}O”,O’”	[132]
	{[Mn(1,3-bdc)$_{0.5}$(3-tptp)]·5(H$_2$O)}$_n$ (**141**) (3-tptp = 4′-(3-tetrazolylphenyl)-2,2′:6′2′′-terpyridine)	Mn^{II} (6)	1D	Solvothermal EtOH: H$_2$O (1:1) (170 °C/72 h)	Not assigned		[197]
	[Mn$_2$(1,3-bdc)$_2$(ttbt)]$_n$ (**310**) (ttbt = 10,11,12,13-tetrahydro-4,5,9,14-tetraaza-benzo [*b*]triphenylene)	Mn^{II} (6)	2D	Hydrothermal (140 °C/120 h)	–	1-μ-κ^{2}O,O’:κ^{2}O”,O’” 2-μ$_4$-κO,O’:κO’”,O’”	[96]
	[Ni(1,3-bdc)(bbh)]$_n$ (**142**) (bbh = 1,6-bis(benzimidazol-1-yl)hexane)	Ni^{II} (6)	3D	Hydrothermal (140 °C/72 h)	1638$_{as}$; 1544$_s$		[181]
	{[Ni$_2$(1,3-bdc)$_2$(ampy)$_4$]·(H$_2$O)·EtOH}$_n$ (**143**) (ampy = 4-aminopyridine, EtOH = ethanol)	Ni^{II} (6)	1D	Solvothermal EtOH (120 °C/48 h)	Not assigned		[29]
	[Cd(1,3-bdc)(bip)(H$_2$O)]$_n$ (**112**) (bip = 3,5-bis(imidazole-1-yl)pyridine)	Cd^{II} (7/6)	2D	Hydrothermal (160 °C/96 h)	Not assigned	1-μ-κ^{2}O,O’:κ^{2}O”,O’” 2-μ-κO:κ^{2}O”,O’”	[27]
	[Cd(1,3-bdc)(bbip)]$_n$ (**144**) (bbip = 1,1′-(1,4-butanediyl)bis(imidazole-2-phenyl))	Cd^{II} (6)	3D	Hydrothermal (160 °C/72 h)	Not assigned		[42]
	[Cd(1,3-bdc)(tpcb)$_{0.5}$]$_n$ (**145**) (tpcb = tetrakis(4-pyridyl)cyclobutene)	Cd^{II} (6)	3D	Hydrothermal (170 °C/24 h)	Not assigned		[53]
	{[Cd(1,3-bdc)(bmt)(H$_2$O)$_2$]·2(H$_2$O)}$_n$ (**146**) (bmt = 1-((benzo-triazol-1-yl)methyl)-1-H-1,2,4-triazole))	Cd^{II} (7)	1D	Solvothermal H$_2$O:DMF (5:2) (120 °C/96 h)	1544$_{as}$; 1486$_s$ Δν = 58		[38]
	{[Cd(1,3-bdc)(tipe)$_{0.5}$(H$_2$O)]·MeOH·(H$_2$O)}$_n$ (**147**) (tipe = tetra(3-imidazoylphenyl)ethylene)	Cd^{II} (7)	2D	Solvothermal MeOH:H$_2$O (2:1) (160 °C/96 h)	Not assigned		[149]
	[Cd$_2$(1,3-bdc)$_2$(LevofH)(H$_2$O)$_2$]$_n$ (**148**) (LevofH = levofloxacin)	Cd^{II} (7/6)	1D	Hydrothermal (150 °C/48 h)	Not assigned	1-μ-κ^{2}O,O’:κ^{2}O”,O’” 2-μ$_3$-κ^{2}O,O’:κO”:κO’”	[265]

Table 2 (*continued*)

Coordination mode	Formulae	Metal ion (CN)		Experimental approach	IR $\nu(COO^-)$ [cm^{-1}] $\Delta\nu$	Distinct coordination mode for 1,3-bdc in the compound	Ref.
	$\{[Cd_2(1,3\text{-}bdc)_2(btbb)(H_2O)]\cdot 2(H_2O)\}_n$ (**149**) (btbb = 1,4-bis(2-(4-thiazolyl)benzimida-zol-1-ylmethyl)benzene)	Cd^{II} (7/6)	3D	Hydrothermal (120 °C/72 h)	Not assigned	1-μ-κ^2O,O':κ^2O", O''' 2-μ_3-κ^2O,O':κO":κO'''	[13]
	$\{[Cd(1,3\text{-}bdc)(imb)(H_2O)]\cdot MeOH\}_n$ (**150**) (imb = 2-(1H-imidazol-1-methyl)-1H-benzimidazole)	Cd^{II} (7)	2D	Slow diffusion MeOH:H_2O	Not assigned		[166]
	$\{[Cd(1,3\text{-}bdc)(3\text{-}dpyh)_{0.5}(H_2O)_2]\cdot(H_2O)\}_n$ (**151**) (3-dpyh = N,N′-bis(3-pyridinecarboxamide)-1,6-hexane)	Cd^{II} (7)	1D	Hydrothermal (120 °C/96 h)	1604$_{as}$; 1227$_{s}$		[85]
	$[Cd(1,3\text{-}bdc)(bib)]_n$ (**152**) (bib = 1,4-bis(2-methyl-imidazole-yl)-butane)	Cd^{II} (6)	3D	Solvothermal DMF:H_2O (3:1) (120 °C/72 h)	Not assigned		[173]
	$[Cd(1,3\text{-}bdc)(bbmb)]_n$ (**153**) (bbmb = 1,1′-(1,4-butanediyl)bis-(2-methylbenzimidazole)	Cd^{II} (6)	2D	Hydrothermal –	1604$_{as}$; 1412$_{s}$		[34]
	$\{[Cd(1,3\text{-}bdc)(bbtz)(H_2O)]\cdot(H_2O)\}_n$ (**154**) (bbtz = 1,4-bis(1,2,4-triazol-1-ylmethyl)benzene)	Cd^{II} (7)	2D	Slow evaporation MeOH:H_2O	–		[266]
	$\{[Cd(1,3\text{-}bdc)(bmimx)]\cdot 1.5(H_2O)\}_n$ (**155**) (bmimx = 1,4-bis(2-methylimidazol-1-ylmethyl)-2,3,5,6-tetramethylbenzene)	Cd^{II} (6)	2D	Solvothermal H_2O:EtOH (1:1) (150 °C/70 h)	Not assigned		[84]
	$\{[Cd(1,3\text{-}bdc)(bpbd)]\cdot 2(H_2O)\}_n$ (**156**) (bpbd = N,N′-bis(pyridine-3-yl)-4,4′-oxybis(benzoic) dicarboxamide)	Cd^{II} (7)	2D	Solvothermal DMA:H_2O (2:1) (85 °C/96 h)	1604$_{as}$; 1334$_{s}$		[110]
	$\{[Cd_2(1,3\text{-}bdc)_2(bip)_2(H_2O)_2]\cdot 3(H_2O)\}_n$ (**157**) (bip = 3,5-bis(imidazole-1-yl)pyridine)	Cd^{II} (7)	2D	Solvothermal H_2O: DMF (5:2) (80 °C/48 h)	Not assigned		[145]
	$\{[Cd_2(1,3\text{-}bdc)_2\ (CBbpy)(H_2O)_4]\cdot(H_2O)\}_n$ (**158**) (CBbpy = 1-(2-carboxyethyl)-4,4′-bipyridinium)	Cd^{II} (7)	2D	Slow evaporation H_2O:DMF (3:1)	Not assigned		[60]
	$[Cd(1,3\text{-}bdc)(bmb)]\cdot(H_2O)\}_n$ (**159**) (bmb = 1,4-bis(2-methylbenzimidazol-1-ylmethyl) benzene)	Cd^{II} (6)	2D	Hydrothermal (130 °C/72 h)	Not assigned		[163]
	$\{[Cd(1,3\text{-}bdc)(cmb)(H_2O)_2][Cd(1,3\text{-}bdc)(1,3\text{-}Hbdc)(H_2O)]\}_n$ (**160**) (cmb = 1-(1-cyclohexylmethane)-4,4′-bipyridinium bromide)	Cd^{II} (7)		Slow evaporation H_2O:DMF: EtOH (5:1:1)	Not assigned	1-μ-κ^2O,O':κ^2O", O''' 2-κ^2O,O'	[136]
	$[Cd(1,3\text{-}bdc)(bpbp)]_n$ (**161**) (bpbp = 1,4-bis [1-(2-pyridylmeth yl)benzimidazol-2yl] butane)	Cd^{II} (6)		Hydrothermal (170 °C/72 h)	–		[267]
	$[Cd_2(1,3\text{-}bdc)(pHimb)_2]_n$ (**162**) (pHimb = (4-((2-(pyridine-2-yl)-1H-imidazol-1-yl) methyl)benzoic acid)	Cd^{II} (6)	3D	Hydrothermal (150 °C/72 h)	Not assigned		[170]
	$[Pb(1,3\text{-}bdc)(b3pb)]_n$ (**163**) (b3pb = 1,4-bis(3-pyridylaminomethyl)benzene)	Pb^{II} (6)	–	Hydrothermal (120 °C/72 h)	Not assigned		[106]
	$\{[(UO_2)_{1.5}(1,3\text{-}bdc)_2(H_2O)]\cdot 0.5(H_2bipy)\}_n$ (**164**) (bipy = 4,4′-bipyridine)	U^{VI} (8)	1D	Hydrothermal (160 °C/72 h)	Not assigned		[171]
	$\{(UO_2)_{1.5}(H_2O)(1,3\text{-}bdc)_2]\cdot 0.5(H_2dap)\cdot 1.5(H_2O)\}_n$ (**165**) (dap = 1,3-diaminopropane)	U^{VI} (8)	2D	Hydrothermal (200 °C/24 h)	–		[101]
	$\{[UO_2(1,3\text{-}bdc)_{1.5}]\cdot 0.5H_2dap\cdot 2(H_2O)\}_n$ (**166**) (dap = 1,3-diaminopropane)	U^{VI} (8)	2D	Hydrothermal (200 °C/24 h)	–		[101]
	$\{[Gd_2(1,3\text{-}bdc)_3(H_2O)_8]\bullet 2DMF\bullet 6(H_2O)\}_n$ (**79**)	Gd^{III} (9)	1D	Slow evaporation DMF	Not assigned	1-μ-κO:κO" 2-μ-κ^2O,O':κ^2O", O'''	[69]
	$\{[Y_2Ni_2(1,3\text{-}bdc)_5(tpa)(H_2O)_3]\cdot 7(H_2O)\}_n$ (**80**) (tpa = tris(2-benzimidazolylmethyl)amine)	Y^{III} (8/9) Ni^{II} (5)	1D	Hydrothermal (140 °C/72 h)	Not assigned	1-μ-κO:κO" 2-μ_3-κO:κO':κO" 3-μ_3-κ^2O,O':κO":κO''' 4-μ-κ^2O,O':κ^2O", O'''	[168]
	$\{[Ln_2(1,3\text{-}bdc)_3(ptcp)_2]\cdot(H_2O)\}_n$ (ptcp = 2-phenyl-1H-1,3,7,8-tetraazacyclopenta[*l*] phenanthrene) Ln = Pr (**167**), Sn (**168**), Eu (**169**), Tb (**170**), or Dy (**171**)	Pr^{III} Sn^{III} Eu^{III} Tb^{III} Dy^{III} (8)	1D	Hydrothermal (160 °C/72 h)	Pr = 1608; 1479 Sm = 1603; 1456 Eu = 1637; 1451 Tb = 1629; 1449 Dy = 1646; 1408	1-μ_4-κO,O':κO''', O''' 2-μ-κ^2O,O':κ^2O", O'''	[55]
	$\{[Eu(1,3\text{-}bdc)_{1.5}(mopip)]\cdot 0.5(H_2O)\}_n$ (**172**) (mopip = 2-(4-methoxyphenyl)-1H-imidazo[4,5-f][1,10] phenanthroline).	Eu^{III} (8)	1D	Hydrothermal (165 °C/120 h)	1640$_{as}$; 1485$_{s}$ $\Delta\nu$ = 155	1-μ-κ^2O,O':κ^2O", O''' 2-μ_4-κO,O':κO''', O'''	[138]
	$\{[Ln_2(1,3\text{-}bdc)_3(mopip)_2]\cdot(H_2O)\}_n$ (**173**) (mopip = 2-(4-methoxyphenyl)-1H-imidazo[4,5-f][1,10] phenanthroline). Ln = Sm or Nd	Sm^{III} Nd^{III} (8)	1D	Hydrothermal (160 °C/120 h)	Sm = 1615$_{as}$; 1451$_{s}$ Nd = 1614$_{as}$; 1450$_{s}$	1-μ-κ^2O,O':κ^2O", O''' 2-μ_4-κO,O':κO''', O'''	[137]
	$\{[Gd_2(1,3\text{-}bdc)_3(mopip)_2]\cdot(H_2O)\}_n$ (**174**) (mopip = 2-(4-methoxyphenyl)-1H-imidazo[4,5-f][1,10] phenanthroline)	Gd^{III} (8)	1D	Hydrothermal (165 °C/120 h)	Not assigned	1-μ-κ^2O,O':κ^2O", O''' 2-μ_4-κO,O':κO''', O'''	[79]
	$\{[Y_2Co(1,3\text{-}bdc)_4(tpa)(H_2O)]\cdot 2(H_2O)\}_n$ (**175**) $\{[Y_2Zn(1,3\text{-}bdc)_4(tpa)(H_2O)]\cdot 2(H_2O)\}_n$ (**176**) $\{[Er_2Co(1,3\text{-}bdc)_4(tpa)(H_2O)]\cdot 2(H_2O)\}_n$ (**177**) $\{[Er_2Zn(1,3\text{-}bdc)_4(tpa)(H_2O)]\cdot 2(H_2O)\}_n$ (**178**) $\{[Sm_2Co(1,3\text{-}bdc)_4(tpa)(H_2O)]\cdot 0.5(H_2O)\}_n$ (**179**) (tpa = tris(2-pyridylmethyl)amine)	Y^{III} Er^{III} Sm^{III} (8) Zn^{II} Co^{II} (5)	2D	Hydrothermal (140 °C/96 h)	Not assigned	1-μ-κ^2O,O':κ^2O", O''' 2-μ_3-κO:κO':κO" 3-μ_3-κ^2O,O':κO":κO''' 4-μ_4-κO:κO:κO":κO'''	[168]
μ_3- κ^2O,O':κO":κO''' 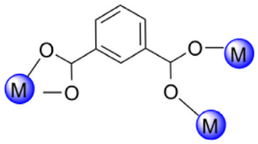	$\{[Cu(1,3\text{-}bdc)(4\text{-}bpcb)]\cdot(H_2O)\}_n$ (**180**) (4-bpcb = N,N′-bis(4-pyridinecarboxamide)-1,4-benzene)	Cu^{II} (6)	2D	Hydrothermal (120 °C/96 h)	1646$_{as}$, 1613$_{as}$; 1393$_{s}$		[40]
	$\{[Cu_2(1,3\text{-}bdc)_2(9Meade)(H_2O)]\cdot(H_2O)\}_n$ (**181**) (9Meade = 9-methyladenine)	Cu^{II} (5)	3D	Slow diffusion MeOH:H_2O	–	1-μ_3-κ^2O,O':κO":κO''' 2-μ_3-κO:κO':κO"	[49]
	$\{[Cu_2(1,3\text{-}bdc)_2(9Meade)(H_2O)_2]\cdot 1.5(H_2O)\}_n$ (**182**) (9Meade = 9-methyladenine)	Cu^{II} (5)	3D	Slow diffusion MeOH:H_2O	–	1-μ_3-κ^2O,O':κO":κO''' 2-μ_3-κO:κO':κO"	[49]
	$[Cu(1,3\text{-}bdc)(b3ph)]\cdot(H_2O)\}_n$ (**183**) (b3ph = N,N′-bis(3-pyridylamide)-1,6-hexane)	Cu^{II} (6)	2D	Hydrothermal (120 °C/144 h)	1615; 1385		[119]
	$[Cu(1,3\text{-}bdc)(bptzp)]_n$ (**184**) (bptzp = 1,4-bis(5-(4-pyridyl)tetrazolyl)propane	Cu^{II} (6)	1D	Solvothermal CH_3CN:H_2O (1:1) (120 °C/96 h)	1627$_{as}$; 1211$_{s}$		[124]
	$\{[Cu_4(1,3\text{-}bdc)_4(bpa)_2(DMF)]\cdot DMF\}_n$ (**185**) (bpa = 1,2-bis(4-pyridyl)ethane)	Cu^{II} (5/6)	3D	Microwave DMF (140 °C/1 h)	Not assigned	1-μ_3-κ^2O,O':κO":κO''' 2-μ_4-κO,O':κO''', O'''	[221]

(*continued on next page*)

Table 2 (*continued*)

Coordination mode	Formulae	Metal ion (CN)		Experimental approach	IR ν(COO$^-$) [cm^{-1}] Δν	Distinct coordination mode for 1,3-bdc in the compound	Ref.
	{[Cu$_2$(1,3-bdc)$_2$(py2ttz)$_2$](DMF)$_3$(H$_2$O)$_3$}$_n$ (**186**) (py2ttz = 2,5-bis(4-pyridyl)thiazolo[5,4-*d*]thiazole)	Cu^{II} (6)	2D	Solvothermal DMF:H$_2$O (4:1) (100 °C/48 h)	–	3-μ$_4$-κ^{2}O,O':κO: κO'':κO'''	[75]
	[Zn$_2$(1,3-bdc)$_2$(bpy)$_2$]$_n$ (**134**) (bpy = 2,2′-bipyridine)	Zn^{II} (6)		Hydrothermal (160 °C/120 h)	1562$_{as}$, 1532$_{as}$; 1431$_s$ Δν = 131; 101	1-μ-κ^{2}O,O':κ^{2}O'', O''' 2-μ$_3$-κ^{2}O,O':κO'': κO'''	[31]
	{[Zn(1,3-bdc)(pba)]·DMF}$_n$ (**187**) (pba = pyridine-3,5-bis(5-azabenzimidazole))	Zn^{II} (4)	1D	DMF:H$_2$O (1:2) in a sealed glas tube at 100 °C.	–		[268]
	[Zn(1,3-bdc)(3-bptzh)]$_n$ (**188**) (3-bptzh = 1,4-bis(5-(3-pyridyl)tetrazolyl)hexane)	Zn^{II} (6)	2D	Hydrothermal (120 °C/96 h)	1616$_{as}$; 1184$_s$		[76]
	[Zn(1,3-bdc)(4-bptzh)]$_n$ (**189**) (4-bptzh = 1,4-bis(5- (4-pyridyl)tetrazolyl)hexane)	Zn^{II} (6)	2D	Hydrothermal (120 °C/96 h)	1593$_{as}$; 1211$_s$		[76]
	[Zn(1,3-bdc)(1,4-bpetmb)]$_n$ (**190**) (1,4-bpetmb = 1,4-bis[2-(4-*pyridyl*)*ethenyl*]-2,3,5,6-tetramethylbenzene)	Zn^{II} (6)	2D	Hydrothermal (170 °C/72 h)	Not assigned		[22]
	[Zn(1,3-bdc)(3-bpdb)]$_n$ (**191**) (3-bpdb = 1,4-bis(3-pyridyl)-2,3-diaza-1,3-butadiene)	Zn^{II} (6)	2D	Solvothermal H$_2$O:DMF: MeOH (1:1:6) (120 °C/48 h)	Not assigned		[102]
	{[Zn(1,3-bdc)(4-bpdb)]·2(H$_2$O)}$_n$ (**192**) (4-bpdb = 1,4-bis(4-pyridyl)-2,3-diaza-1,3-butadiene)	Zn^{II} (6)	2D	Solvothermal H$_2$O:DMF: MeOH (1:1:6) (120 °C/48 h)	Not assigned		[102]
	[Zn(1,3-bdc)(d3ps)$_{0.5}$]$_n$ (**193**) (d3ps = N,N′-di(3-pyridyl)succinimide)	Zn^{II} (5)	3D	Hydrothermal (120 °C/96 h)	Not assigned		[87]
	[Zn(1,3-bdc)(3,4′-bpt)]$_n$ (**194**) (3,4′-bpt = 1H-3-(3-pyridyl)-5-(4-pyridyl)-1,2,4-triazole))	Zn^{II} (6)	1D	Solvothermal H$_2$O:EtOH (2:1) (140 °C/72 h)	Not assigned		[196]
	[Zn(1,3-bdc)(3,3′-bpt)]·(H$_2$O)}$_n$ (**195**) (3,3′-bpt = 1H-3,5-bis(3-pyridyl)-1,2,4-triazole)	Zn^{II} (6)	1D	Solvothermal H$_2$O:EtOH (2:1) (140 °C/72 h)	Not assigned		[196]
	{[Zn$_2$(1,3-bdc)$_2$(bbpb)]·2(H$_2$O)}$_n$ (**196**) (bbpb = 1,1′-(1,4-butanediyl)bis[2-(2-pyridyl) benzimidazole)	Zn^{II} (6)	1D	Solvothermal H$_2$O:MeOH (4:1) (140 °C/72 h)	Not assigned		[68]
	{[Zn$_3$(1,3-bdc)$_3$(py)$_2$](MeOH)}$_n$ (**197**) (py = pyridine)	Zn^{II} (6)		Slow evaporation MeOH:MeNO$_2$:py (10:5:6)	–	1-μ$_3$-κ^{2}O,O':κO'': κO''' 2-μ$_4$-κO,O':κO''', O'''	[189]
	[Mn(1,3-bdc)(3-pip)]$_n$ (**198**) (3-pip = 2-(3-pyridyl)-imidazo[4,5-*f*]1,10-phenanthroline)	Mn^{II} (6)	1D	Hydrothermal (170 °C/96 h)	1568$_{as}$, 1458$_{as}$; 1386$_s$ Δν = 182; 72		[109]
	{[Mn(1,3-bdc)(bte)$_{0.5}$(H$_2$O)]·(H$_2$O)}$_n$ (**199**) (bte = 1,2-bis(1,2,4-triazol-1-yl)ethane)	Mn^{II} (6)	2D	Slow diffusion MeOH:H$_2$O	Not assigned		[258]
	[Mn(1,3-bdc)(fdp)]$_n$ (**200**) (fdp = 11-fluoro-dipyrido[3,2-*a*:2′,3′-*c*]phenazine)	Mn^{II} (5)	1D	Hydrothermal (153 °C/144 h)	Not assigned		[93]
	[[Mn(1,3-bdc)(4,4′-bipy)]·0.75(H$_2$O)·0.25(EtOH)]$_n$ (**201**) (4,4′-bipy = bipyridine)	Mn^{II} (6)	2D	Solvothermal H$_2$O: EtOH (1:1) (110 °C/96 h)	Not assigned		[225]
	[Fe(1,3-bdc)(phen)]$_n$ (**202**) (phen = 1,10-phenanthroline)	Fe^{II} (6)		Hydrothermal (180 °C/144 h)	Not assigned		[32]
	{[Co(1,3-bdc)(3-bpcb)]·(H$_2$O)}$_n$ (**203**) (3-bpcb = N,N′-bis(3-pyridinecarboxamide)-1,4-benzene)	Co^{II} (6)	2D	Hydrothermal (120 °C/96 h)	1677$_{as}$, 1617$_{as}$; 1384$_s$		[40]
	{[Co$_2$(1,3-bdc)2(d3ps)$_2$]·4(H$_2$O)}$_n$ (**204**) (d3ps = N,N′-di(3-pyridyl)succinamide)	Co^{II} (6)	3D	Hydrothermal (120 °C/96 h)	Not assigned		[61]
	[Co(1,3-bdc)(bptzh)]$_n$ (**205**) (bptzh = 1,4-bis(5-(3-pyridyl)tetrazolyl)propane)	Co^{II} (6)	2D	Hydrothermal (120 °C/96 h)	–		[67]
	[Co(13-bdc)(bipyen)]$_n$ (**206**) (bipyen = *trans*-1,2-bis(4-pyridyl)ethylene)	Co^{II} (6)	2D	Hydrothermal (180 °C/48 h)	1611 ad 1397		[191]
	[Co(1,3-bdc)(bpy)]$_n$ (**137**) (bpy = 2,2′-bipyridine)	Co^{II} (6)	2D	Hydrothermal (140 °C/72 h)	–	1-μ-κ^{2}O,O':κ^{2}O'', O''' 2-μ$_3$-κ^{2}O,O':κO'': κO'''	[264]
	{[Co(1,3-bdc)(L)]·(H$_2$O)}$_n$ (**207**) (b3pt = N,N′-bis(3-pyridyl)-terephthalamide)	Co^{II} (6)	3D	Hydrothermal (120 °C/72 h)	1605$_{as}$; (1229–1477)$_s$		[118]
	[Co(1,3-bdc)(bimb)]$_n$ (**208**) (bimb = 1,4-bis(1-imidazol-yl)-2,5-dimethylbenzene)	Co^{II} (6)	2D	Hydrothermal (140 °C/96 h)	–		[128]
	[{Co(1,3-bdc)(3-bpna)}·DMF·2(H$_2$O)]$_n$ (**209**) (3-bpna = N′,N′′-bis(3-pyridyl)naphthalene-2,6-dicarboxamide)	Co^{II} (6)	2D	Solvothermal DMF:MeOH: H$_2$O (3:1:1) (75 °C/60 h)	Not assigned		[269]
	[Co(1,3-bdc)(pxppa)]$_n$ (**210**) (pxppa = α,α′-p-xylylenebis(1-(4-pyridylmethy-lene)-piper-4-azine))	Co^{II} (6)	2D	Hydrothermal (160 °C/36 h)	–		[182]
	[Co(1,3-bdc)(bip)]$_n$ (**211**) (bip = 3,6-bis(1H-imidazol-1-yl)pyridazine)	Co^{II} (5)	2D	Solvothermal DMF (140 °C/12 h)	Not assigned		[73]
	{[Co(1,3-bdc)(3-bpna)]·DMF·2(H$_2$O)}$_n$ (**212**) (3-bpna = N′,N′′-di(pyridin-3-yl)naphthalene-2,6-dicarboxamide)	Co^{II} (6)	2D	Solvothermal DMF: MeOH: H$_2$O (3:1:1) (75 °C/60 h)	Not assigned		[269]
	{[Co(1,3-bdc)(bptpa)]·2(H$_2$O)}$_n$ (**213**) (bptpa = N,N′-bis(pyridine-3-yl)thiophene-2,5-dicarbox-amide)	Co^{II} (6)	2D	Hydrothermal (120 °C/96 h)	1612$_{as}$; 1274$_s$		[157]
	{[Co(1,3-bdc)(bptpa)]·2(H$_2$O)}$_n$ (**214**) (bptpa = N,N'-bis(pyridine-3-yl)thiophene-2,5-dicarbox-amide)	Co^{II} (6)	3D	Solvothermal DMA: H2O (1:2) (120 °C/96 h)	1609$_{as}$; 1298$_s$		[157]
	{[Co(1,3-bdc)(3-dpyb)]·(H$_2$O)}$_n$ (**215**) (3-dpyh = N,N'-bis(3-pyridinecarboxamide)-1,6-hexane)	Co^{II} (6)	2D	Hydrothermal (120 °C/96 h)	1600$_{as}$; 1422$_s$		[127]
	[Co(1,3-bdc)(py)$_2$]$_n$ (**216**) (py = pyridine)	Co^{II} (6)	–	Slow diffusion EtOH:H$_2$O (2:1)	–		[107]
	[Co(1,3-bdc)(3,4′-bpt)]$_n$ (**217**) (3,4′-bpt = 3,4′-(1H-1,2,4-triazole-3,5-diyl)dipyridine)	Co^{II} (6)	2D	Solvothermal H$_2$O:EtOH (2:1) (140 °C/72 h)	Not assigned		[270]
	{[Co(1,3-bdc)(3,3′-bpt)]·(H$_2$O)}$_n$ (**218**) (3,3′-bpt = 3,3′-(1H-1,2,4-triazole-3,5-diyl)dipyridine)	Co^{II} (6)	3D	Solvothermal H$_2$O:EtOH (2:1) (140 °C/72 h)	Not assigned		[270]
	{[Co(1,3-bdc)(dpa)]·3(H$_2$O)}$_n$ (**219**) (dpa = 4,4′-dipyridylamine)	Co^{II} (6)	3D	Solvothermal H$_2$O:MeOH (9:1) (120 °C/48 h)	Not assigned		[271]

Table 2 (*continued*)

Coordination mode	Formulae	Metal ion (CN)		Experimental approach	IR $\nu(COO^-)$ [cm^{-1}] $\Delta\nu$	Distinct coordination mode for 1,3-bdc in the compound	Ref.
	$\{[Co(1,3\text{-}bdc)(dpyi)]\cdot DMF\}_n$ (**220**) (dpyi = N,*N*-di(pyridin-4-yl)isophthalamide)	Co^{II} (6)	3D	Solvothermal DMF (120 °C/48 h)	Not assigned		[259]
	$[Co(1,3\text{-}bdc)(bpp)]_n$ (**221**) (bpp = 4,4′-trimethylene dipyridine)	Co^{II} (6)	1D	Slow diffusion H_2O:EtOH (1:1)	Not assigned		[123]
	$\{[Cd_2(1,3\text{-}bdc)_2(btbb)(H_2O)]\cdot 2(H_2O)\}_n$ (**149**) (btbb = 1,4-bis(2-(4-thiazolyl)benzimida-zol-1-ylmethyl)benzene)	Cd^{II} (7/6)	3D	Hydrothermal (120 °C/72 h)	Not assigned	1-μ-κ^2O,O':κ^2O'', O''' 2-μ_3-κ^2O,O':κO'':κO'''	[13]
	$\{[Cd(1,3\text{-}bdc)(4\text{-}bpah)]\}_n$ (**222**) (4-bpah = N,N′-bis(4-pyridinecarboxamide)-1,2-cyclohexane)	Cd^{II} (6)	2D	Hydrothermal (120 °C/144 h)	1605_{as}; 1446_{s}		[24]
	$\{[Cd(1,3\text{-}bdc)(3\text{-}bpah)]\cdot(H_2O)\}_n$ (**223**) (3-bpah = N,N′-bis(3-pyridinecarboxamide)-1,2-cyclohexane)	Cd^{II} (6)	2D	Hydrothermal (120 °C/144 h)	1601_{as}; 1439_{s}		[24]
	$[Cd(1,3\text{-}bdc)(bbyp)]_n$ (**224**) (bbyp = 3,5-bis(benzoimidazol-q-yl)pyridine)	Cd^{II} (6)	3D	Hydrothermal (160 °C/96 h)	Not assigned		[27]
	$\{[Cd_2(1,3\text{-}bdc)_2(ttyt)]\cdot 2(H_2O)\}_n$ (**225**) (ttyt = 1,3,5-tris(1H-1,2,4-triazol-1-ylmethyl)-2,4,6-trimethylbenzene)	Cd^{II} (6)	3D	Hydrothermal (100 °C/72 h)	Not assigned		[150]
	$[Cd_2(1,3\text{-}bdc)_2(LevofH)(H_2O)_2]_n$ (**148**) (LevofH = levofloxacin)	Cd^{II} (7/6)	1D	Hydrothermal (150 °C/48 h)	Not assigned	1-μ-κ^2O,O':κ^2O'', O''' 2-μ_3-κ^2O,O':κO'':κO'''	[265]
	$[Cd(1,3\text{-}bdc)(b3pb)]_n$ (**226**) (b3pb = 1,4-bis(3-pyridylaminomethyl)benzene)	Cd^{II} (6)	2D	Hydrothermal (120 °C/72 h)	Not assigned		[106]
	$[Cd(1,3\text{-}bdc)(bimb)]_n$ (**227**) (bimb = 4,4′-bis(1-imidazolyl)bibenzene)	Cd^{II} (6)		Hydrothermal (170 °C/24 h)	Not assigned		[21]
	$[Cd(1,3\text{-}bdc)(bim)]_n$ (**228**) (bim = bis(imidazol-1-yl)-methane)	Cd^{II} (6)	2D	Hydrothermal (160 °C/48 h)	Not assigned		[39]
	$[Cd_2(1,3\text{-}bdc)_2(bib)_{1.5}]_n$ (**229**) (bib = 1,4-bis(1-imidazol-yl)-2,5-dimethyl benzene)	Cd^{II} (6/7)	3D	Hydrothermal (160 °C/96 h)	Not assigned	1-μ_3-κ^2O,O':κO'':κO''' 2-μ_4-κ^2O,O':κO:κ^2O'',O''':κO''	[174]
	$[Cd_2(1,3\text{-}bdc)_2(3\text{-}dpyb)_2]_n$ (**230**) (3-dpyh = N,N′-bis(3-pyridinecarboxamide)-1,6-hexane)	Cd^{II} (6)	2D	Hydrothermal (120 °C/96 h)	1618_{as}; 1416_{s}		[127]
	$\{[Cd_4(1,3\text{-}bdc)_4(btd)_3]\cdot(H_2O)\}_n$ (**231**) (btd = 1,10-bis(1,2,4-triazol-1-yl)decane)	Cd^{II} (6/7)	2D	Hydrothermal (170 °C/72 h)	–		[272]
	$[Cd(1,3\text{-}bdc)(ttbt)]_n$ (**232**) (ttbt = 10,11,12,13-tetrahydro-4,5,9,14-tetraaza-benzo[*b*]triphenylene)	Cd^{II} (6)	1D	Hydrothermal (140 °C/120 h)	–		[96]
	$\{(Me_2NH_2)_2[Cd_3(1,3\text{-}bdc)_4]\cdot(H_2O)\cdot 2(EtOH)\}_n$ (**233**)	Cd^{II} (6)	2D	Solvothermal DMF:EtOH (1:1) (130 °C/48 h)	1576; 1385	1-μ_3-κ^2O,O':κO'':κO''' 2-μ_4-κ^2O,O':κO:κO'':κO'''	[184]
	$\{[Cd(1,3\text{-}bdc)(1,3\text{-}bip)]\cdot(H_2O)\}_n$ (**234**) (1,3-bip = 1,3-bis(imidazole)propane)	Cd^{II} (6)	2D	Hydrothermal (110 °C/72 h)	Not assigned		[178]
	$\{[Cd(1,3\text{-}bdc)(bpmb)]\cdot 0.125(H_2O)\}_n$ (**235**) (bpmb = 1,3-bis(pyridine-3-ylmethoxy)benzene)	Cd^{II} (6)	2D	Hydrothermal (150 °C/96 h)	Not assigned		[86]
	$[Cd(1,3\text{-}bdc)(phen)]_n$ (**236**) (phen = 1,10-phenanthroline)	Cd^{II} (6)	1D	Hydrothermal (160 °C/120 h)	Cd = 1564_{as}, 1515_{as}; 1400_{s} $\Delta\nu$ = 164; 115		[31]
	$[Cd_2(1,3\text{-}bdc)_2(bpy)_2]_n$ (**237**) (bpy = 2,2′-bipyridine)	Cd^{II} (6)	1D	Hydrothermal (160 °C/120 h)	1564_{as}, 1515_{as}; 1400_{s} $\Delta\nu$ = 164; 115		[31]
	$[Cd_2(1,3\text{-}bdc)_2(bdzp)(H_2O)_2]_n$ (**238**) (bdzp = 1,3-bis(5,6-dimethylbenzimida-zol-1-yl) propane)	Cd^{II} (6)	2D	Hydrothermal (140 °C/72 h)	Not assigned		[74]
	$[Cd(1,3\text{-}bdc)(mbbt)]_n$ (**239**) (mbbt = 1-(2-methylbenzimidazol-1-ylmethyl) benzotriazole)	Cd^{II} (6)	3D	Hydrothermal (120 °C/72 h)	Not assigned		[175]
	$\{[M(1,3\text{-}bdc)(4\text{-}bpdb)]\cdot(4\text{-}bpdb)_{0.5}\}_n$ (4-bpdb = N, N′-bis–pyridine-4-ylmethylene–hydrazine) M = Mn (**240**), Fe (**241**), Co (**242**)	Mn^{II} Fe^{II} Co^{II} (6)	2D	Slow evaporation MeOH:H_2O	Not assigned		[201]
	$\{[M(1,3\text{-}bdc)(4,4'\text{-}bipy)]\cdot(EtOH)\}_n$ (4,4′-bipy = 4,4′-bipyridine) M = Zn (**243**) or Cd (**244**)	Zn^{II} Cd^{II} (6)	2D	Solvothermal DMF:EtOH (1:1) (55 °C/72 h)	$(1610–1550)_{as}$; $(1420–1300)_{s}$		[273]
	$[M(1,3\text{-}bdc)(bptzp)]_n$ M = Co (**246**), Zn (**247**), or Cd (**248**) (bptzp = 1,4-bis(5-(3-pyridyl)tetrazolyl)propane)	Co^{II} Zn^{II} Cd^{II} (6)	1D	Hydrothermal (85 °C/72 h)	Co = 1614_{as}; 1184_{s} Zn = 1620_{as};1190_{s} Cd = 1604_{as}; 1180_{s}		[81]
	$[M(1,3\text{-}bdc)(bptp)]_n$ M = Co (**249**), Zn (**250**), or Cd (**251**) (bptp = 1,4-bis(5-(3-pyridyl)tetrazolyl)propane)	Co^{II} Zn^{II} Cd^{II} (6)	2D	Solvothermal H_2O:DMA (3:2) (120 °C/96 h)	Co = 1616;1211 Zn = 1612; 1211 Cd = 1601; 1213		[80]
	$[(UO_2)_2(OH)_2(H_2O)(1,3\text{-}bdc)(H_2O)]_n$ (**252**)	U^{VI} (8)	1D	Hydrothermal (200 °C/24 h)	–		[101]
	$\{[Pb_5(1,3\text{-}bdc)_4(tcpbc)_2]\cdot 3(H_2O)\}_n$ (**253**) (Htcpbc = 2′-(1H-1,3,7,8-tetraaza-cyclopenta [l] phenanthren-2-yl)biphenyl-2-carboxylic acid)	Pb^{II} (4/5/6)	2D	Hydrothermal (140 °C/72 h)	–	1-μ_3-κ^2O,O':κO'':κO''' 2-μ_4-κO:κO:κO'':κO'''	[70]
	$[Pb(1,3\text{-}bdc)(tip)]_n$ (**254**) (tip = 2-(2-thienyl)imidazo[4,5-*f*]1,10-phenanthroline)	Pb^{II} (6)	1D	Hydrothermal (180 °C/72 h)	Not assigned		[108]
	$\{[Dy_3(1,3\text{-}bdc)_4(NO_3)(phen)_3]\cdot 2(H_2O)\}_n$ (**255**)	Dy^{III} (9)	3D	Solvothermal DMF:H_2O:EtOH (10:3:2) (85 °C/48 h)	1641_{as}; 1393_{s}	1-μ_3-κ^2O,O':κO'':κO''' 2-μ_4-κO,O':κO''', O'''	[25]
	$[Dy_2(1,3\text{-}bdc)_3(H_2O)_2]\cdot(H_2O)\}_n$ (**256**)	Dy^{III} (7/8)	2D	Hydrothermal (160 °C/96 h)	1602_{as}; 1372_{s}	1-μ_3-κ^2O,O':κO'':κO''' 2-μ_4-κO,O':κO''', O''' 3-μ_4-κ^2O,O':κO:κO'':κO'''	[25]

(*continued on next page*)

Table 2 (*continued*)

Coordination mode	Formulae	Metal ion (CN)		Experimental approach	IR ν(COO$^-$) [cm^{-1}] Δν	Distinct coordination mode for 1,3-bdc in the compound	Ref.
	$\{[Ln_4(1,3\text{-}bdc)_6(DMF)(H_2O)_4]\cdot DMF\cdot 2(H_2O)\}_n$ Ln = Tb (**257**), Ho (**258**), or Er (**259**)	Tb^{III} Ho^{III} Er^{III} (7/9)	–	Solvothermal DMF:H_2O (5:2) (85 °C/72 h)	1612_{as}; 1534_s	1-μ_3-κ^2O,O’:κO”:κO’’’ 2-μ_4-κO,O’:κO’’’,O’’’	[25]
	$\{[Y_2(1,3\text{-}bdc)_3(H_2O)(DMF)]\cdot 3DMF\}_n$ (**260**)	Y^{III} (7)	2D	Solvothermal DMF:H_2O (2:1) (60 °C/96 h)	1612_{as}, 1544_{as}; 1453_s; 1389_s		[26]
	$\{[Eu_2(1,3\text{-}bdc)_3(phen)_2(H_2O)_2]\cdot 4(H_2O)\}_n$ (**261**) (phen = 1,10-phenanthroline)	Eu^{III} (8)	2D	Hydrothermal (150 °C/120 h)	Not assigned	1-μ_3-κ^2O,O’:κO”:κO’’’ 2-μ_3-κO:κO’:κO”	[63]
	$\{[Y_2Ni_2(1,3\text{-}bdc)_5(tpa)(H_2O)_3]\cdot 7(H_2O)\}_n$ (**80**) (tpa = tris(2-benzimidazolylmethyl)amine)	Y^{III} (8/9) Ni^{II} (5)	1D	Hydrothermal (140 °C/72 h)	Not assigned	1-μ-κO:κO” 2-μ-κO:κ^2O”,O’’’ 3-μ_3-κ^2O,O’:κO”:κO’’’ 4-μ-κ^2O,O’:κ^2O”,O’’’	[168]
	$\{[Y_2Co(1,3\text{-}bdc)_4(tpa)(H_2O)]\cdot 2(H_2O)\}_n$ (**175**) $\{[Y_2Zn(1,3\text{-}bdc)_4(tpa)(H_2O)]\cdot 2(H_2O)\}_n$ (**176**) $\{[Er_2Co(1,3\text{-}bdc)_4(tpa)(H_2O)]\cdot 2(H_2O)\}_n$ (**177**) $\{[Er_2Zn(1,3\text{-}bdc)_4(tpa)(H_2O)]\cdot 2(H_2O)\}_n$ (**178**) $\{[Sm_2Co(1,3\text{-}bdc)_4(tpa)(H_2O)]\cdot 0.5(H_2O)\}_n$ (**179**) (tpa = tris(2-pyridylmethyl)amine)	Y^{III} Er^{III} Sm^{III} (8) Zn^{II} Co^{II} (5)	2D	Hydrothermal (140 °C/96 h)	Not assigned	1-μ-κ^2O,O’:κ^2O”,O’’’ 2-μ_3-κO:κO’:κO” 3-μ_3-κ^2O,O’:κO”:κO’’’ 4-μ_4-κ^2O,O’:κO:κO”:κO’’’	[168]
	$\{[LnZn(1,3\text{-}bdc)(imdc)(H_2O)_2]\cdot 3(H_2O)\}_n$ (H_3imdc = imidazole-4,5-dicarboxylic acid) Ln = Nd (**262**), Eu (**263**), or Gd (**264**)	Nd^{III} Eu^{III} Gd^{III} (8) Zn^{II} (5)	3D	Hydrothermal (160 °C/72 h)	$(1615–1513)_{as}$; $(1381–1476)_s$		[218]
	$\{[LnAg(1,3\text{-}bdc)(dspt)(H_2O)_2]\cdot(H_2O)\}_n$ (dspt = 4′-(2,4-disulfophenyl)-2,2′:6′2″-terpyridine) Ln = Sm (**265**) or Er (**266**)	Sm^{III} Er^{III} (8) Ag^{I} (4)	2D	Hydrothermal (170 °C/70 h)	Not assigned		[194]
	$\{[Ln(1,3\text{-}bdc)(ac)(H_2O)_2]\cdot 0.5(H_2O)\}_n$ (ac = acetate) Ln = La (**267**) or Eu (**268**)	La^{III} Eu^{III} (9)		Hidrothermal La (200 °C/72 h) Eu (160 °C/72 h)	–		[57]
	$\{[Ln_2(1,3\text{-}bdc)_2(mpip)_2(NO_3)_2]\cdot 3(H_2O)\}_n$ Ln = Tb (**269**) or Gd (**270**) (mpip = 2-(3-methylphenyl)imidazo(4,5-f)(1,10)-phenanthroline)	Tb^{III} Gd^{III} (8)	2D	Solvothermal CH_3CN:H_2O (5:1) (120 °C/72 h)	Not assigned	1-μ_4-κO,O’:κO’’’,O’’’ 2-μ_3-κ^2O,O’:κO”:κO’’’	[195]
	$\{[Ln_2(1,3\text{-}bdc)_3(mpip)_2]\cdot 2(H_2O)\}_n$ Ln = Dy (**128**), Ho (**129**), or Er (**130**) (mpip = 2-(3-methylphenyl)imidazo(4,5-f)(1,10)-phenanthroline)	Dy^{III} Ho^{III} Er^{III} (8)	2D	Solvothermal CH_3CN:H_2O (3:2) (120 °C/72 h)	Not assigned	1-μ-κO:κ^2O”,O’’’ 2-μ_3-κ^2O,O’:κO”:κO’’’ 3-μ_4-κO,O’:κO’’’,O’’’	[195]
	$[Eu_2(1,3\text{-}bdc)_2(mpip)_2(CH_3COO)_2]_n$ (**271**) (mpip = 2-(3-methylphenyl)imidazo(4,5-f)(1,10)-phenanthroline)	Eu^{III} (9)	1D	Solvothermal CH_3CN:H_2O (3:1) (120 °C/72 h)	Not assigned		[195]
	$\{[La_2(1,3\text{-}bdc)_3(mpip)_2]\cdot 5(H_2O)\}_n$ (**272**) $\{[Nd_2(1,3\text{-}bdc)_3(mpip)_2]\cdot 7(H_2O)\}_n$ (**273**) (mpip = 2-(3-methylphenyl)imidazo(4,5-f)(1,10)-phenanthroline)	La^{III} Nd^{III} (9)	2D	Hydrothermal (180 °C/72 h)	Not assigned	1-μ_3-κ^2O,O’:κO”:κO’’’ 2-μ_4-κ^2O,O’:κO:κ^2O”,O’’’:κO”	[195]
μ_3-κO:κO':κO'' 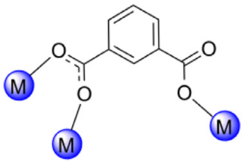 	$\{[Li_2(1,3\text{-}bdc)(DMF)_{0.5}]\cdot(H_2O)\}_n$ (**274**)	Li^{I} (2/4)	3D	Solvothermal DMF:THF (2:1) (180 °C/72 h)	–		[274]
	$\{[Cu_2(1,3\text{-}bdc)_2(9Meade)(H_2O)]\cdot(H_2O)\}_n$ (**181**) (9Meade = 9-methyladenine)	Cu^{II} (5)	3D	Slow diffusion MeOH:H_2O	–	1-μ_3-κ^2O,O’:κO”:κO’’’ 2-μ_3-κO:κO’:κO”	[49]
	$\{[Cu_2(1,3\text{-}bdc)_2(9Meade)(H_2O)_2]\cdot 1.5(H_2O)\}_n$ (**182**) (9Meade = 9-methyladenine)	Cu^{II} (5)	3D	Slow diffusion MeOH:H_2O	–	1-μ_3-κ^2O,O’:κO”:κO’’’ 2-μ_3-κO:κO’:κO”	[49]
	$[Cu_3(1,3\text{-}bdc)_4(dpq)_2]_n$ (**275**) (dpq = dipyrido[3,2-*d*:2′,3′-*f*]quinoxaline)	Cu^{II} (4/5)	1D	Hydrothermal (120 °C/96 h)	1624_{as}, 1570_s; 1380_s	1-μ_3-κO:κO’:κO” 2-κO:O’	[98]
	$[Cu(1,3\text{-}bdc)(py)_2]_n$ (**276**) (py = pyridine)	Cu^{II} (6)	2D	Slow evaporation DMF:py (7:2)	–		[179]
	$\{[Cu_4(1,3\text{-}bdc)_3(dimb)_4](O_2)(H_2O)_8(OH)_2\}_n$ (**277**) (dimb = 1,4-di(imidazolidin-1-yl)benzene)	Cu^{II} (6)	2D	Hydrothermal (130 °C/72 h)	1608_{as}, 1560_{as}; 1435_s, 1360_s Δν = 173; 200	1-μ_4-κO,O’:κO’’’,O’’’ 2-μ_3-κ^2O,O’:κO:κ^2O”,O’’’.	[164]
	$[Zn(1,3\text{-}bdc)(phen)]_n$ (**278**) Phen = 1,10-phenanthroline	Zn^{II} (5)	1D	Hydrothermal (160 °C/120 h)	1614_{as}, 1558_{as}; 1397_s. Δν = 217; 161		[31]
	$\{[Zn(1,3\text{-}bdc)(phen)]_2\}_n$ (**279**) (phen = 1,10-phenathroline)	Zn^{II} (5)	1D	Solvothermal MeOH (150 °C/12 h)	Not assigned		[275]
	$\{[Zn_2(1,3\text{-}bdc)_2(4,4'\text{-}bipy)(EtOH)(H_2O)_2]\cdot(EtOH)\cdot 0.5(H_2O)\}_n$ (**25**) (4,4′-bipy = 4,4′-bipyridine)	Zn (4/6)	2D	Slow evaporation H_2O:EtOH	–	1-μ-κO:κO” 2-μ_3-κO:κO’:κO”	[71]
	$\{[Zn_5(1,3\text{-}bdc)_3(Htea)_2(H_2O)]\cdot 2.6(H_2O)\}_n$ (**280**) (H_3tea = triethanolamine)	Zn^{II} (4/5/6)	–	Solvothermal MeOH (110 °C/20 h)	Not assigned	1-μ_3-κO:κO’:κO” 2-μ_4-κO,O’:κO’’’,O’’’	[116]
	$\{[Zn_2(1,3\text{-}bdc)_2(bpda)_2]\cdot 3DMF\cdot 0.5(H_2O)\}_n$ (**281**) (bpda = N,N′-bis(pyridine-4-yl)-1,4-benzenedicarboxamide)	Zn^{II} (5)	–	Solvothermal DMF:H_2O (14:1) (100 °C/72 h)	Not assigned		[276]
	$[Zn_2(1,3\text{-}bdc)(\mu_3\text{-}OH)(4\text{-}pimb)]_n$ (**282**) (4-pimb = 4-((2-(pyridine-2-yl)-1H-imidazol-1-yl) methyl)benzoic acid)	Zn^{II} (6)	3D	Hydrothermal (150 °C/72 h)	1614_{as}; 1416_s		[139]
	$[Zn_2(1,3\text{-}bdc)_2(dbi)]_n$ (**283**) (dbi = 1,1′-(1,10-decanediyl)bis(imidazole))	Zn^{II} (4)	3D	Hydrothermal (160 °C/60 h)	–		[131]
	$\{[Zn_2(1,3\text{-}bdc)_2(btre)(H_2O)_2]\cdot 2(H_2O)\}_n$ (**284**) (btre = 1,2-bis(1,2,4-triazol-4-yl)ethane)	Zn^{II} (5)	3D	Hydrothermal (180 °C/72 h)	1609_{as}, 1562_{as}; 1429_s, 1371_s		[153]
	$\{[Zn_2(1,3\text{-}bdc)_4(DMSO)_2(H_2O)]\cdot 3DMSO\}_n$ (**285**)	Z^{II} (6/4)	3D	Reaction (H_2O); Recryst. (DMF)		1-μ_3-κO:κO’:κO” 2-μ_4-κO,O’:κO’’’,O’’’	[198]
	$[Zn_2(1,3\text{-}bdc)_2(bcbpy)]_n$ (**286**) (bcbpy = 1,1′-bis(3-carboxyphenyl)-4,4′-bipyridinium)	Zn^{II} (4)	2D	Hydrothermal (160 °C/48 h)	Not assigned		[192]
	$\{[Zn_2(1,3\text{-}bdc)_2(dbpb)]\cdot 2(H_2O)\}_n$ (**287**) (dbpb = 1,1′-(1,10-decanediyl)bis[2-(2-pyridyl) benzimidazole)	Zn^{II} (5)	3D	Solvothermal MeOH:H_2O (4:1) (140 °C/72 h)	Not assigned		[68]
	$\{[Cd_2(1,3\text{-}bdc)_2(ppaH)_2]\cdot 4.25(H_2O)\}_n$ (**288**) (ppaH = pipemidic acid)	Cd^{II} (6)	2D	Hydrothermal (120 °C/96 h)	Not assigned		[265]
	$\{[Eu_2(1,3\text{-}bdc)_3(phen)_2(H_2O)_2]\cdot 4(H_2O)\}_n$ (**261**) (phen = 1,10-phenanthroline)	Eu^{III} (8)	2D	Hydrothermal (150 °C/120 h)	Not assigned	1-μ_3-κ^2O,O’:κO”:κO’’’ 2-μ_3-κO:κO’:κO”	[63]

Table 2 (*continued*)

Coordination mode	Formulae	Metal ion (CN)		Experimental approach	IR ν(COO$^-$) [cm^{-1}] Δν	Distinct coordination mode for 1,3-bdc in the compound	Ref.
	[Yb$_2$(1,3-bdc)$_3$(mpip)]$_n$ (**289**) (mpip = 2-(3-methylphenyl)imidazo(4,5-f)(1,10)-phenanthroline)	Yb^{III} (6)	2D	Hydrothermal (180 °C/72 h)	Not assigned	1-μ_4-κO,O':κO''', O''' 2-μ_3-κO:κO':κO''	[195]
	{[Y$_2$Co(1,3-bdc)$_4$(tpa)(H$_2$O)]·2(H$_2$O)}$_n$ (**175**) {[Y$_2$Zn(1,3-bdc)$_4$(tpa)(H$_2$O)]·2(H$_2$O)}$_n$ (**176**) {[Er$_2$Co(1,3-bdc)$_4$(tpa)(H$_2$O)]·2(H$_2$O)}$_n$ (**177**) {[Er$_2$Zn(1,3-bdc)$_4$(tpa)(H$_2$O)]·2(H$_2$O)}$_n$ (**178**) {[Sm$_2$Co(1,3-bdc)$_4$(tpa)(H$_2$O)]·0.5(H$_2$O)}$_n$ (**179**) (tpa = tris(2-pyridylmethyl)amine)	Y^{III} Er^{III} Sm^{III} (8) Zn^{II} Co^{II} (5)	2D	Hydrothermal (140 °C/96 h)	Not assigned	1-μ-κ^{2}O,O':κ^{2}O'', O''' 2-μ_3-κO:κO':κO'' 3-μ_3-κ^{2}O,O':κO'': κO''' 4-μ_3-κ^{2}O,O':κO: κ^{2}O'',O'''	[168]
	{Na$_2$[Nd$_4$(1,3-bdc)$_6$(ox)(H$_2$O)$_6$]}$_n$ (**290**) (ox = oxalate)	Nd^{III} (8/9)	3D	Hydrothermal (190 °C/72 h)	1642$_{as}$, 1582$_{as}$; 1360$_s$		[120]
μ_3-κ^{2}O,O':κO:κO'' 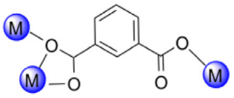	[Zn$_2$(1,3-bdc)$_2$(dHib)(H$_2$O)]$_n$ (**87**) (dHib = 1,4-di(1H-imidazol-4-yl)benzene)	Zn^{II} (4/5)	2D	Hydrothermal (160 °C/72 h)	Not assigned	1-μ-κO:κO'' 2-μ_3-κ^{2}O,O':κO: κO''	[95]
	[Cd$_2$(1,3-bdc)(3-pp)$_2$(H$_2$O)]$_n$ (**116**) (3-pp = 3-(2-pyridyl)pyrazole)	Cd^{II} (6)		Hydrothermal (140 °C/48 h)	1606$_{as}$, 1537$_{as}$; 1378$_s$ Δν = 228; 159	1-μ-κ^{2}O,O':κ^{2}O'', O''' 2-μ_3-κ^{2}O,O':κO: κO''	[256]
	[Pb(1,3-bdc)(phen)]$_n$ (**354**) (phen = 1,10-phenanthroline)	Pb^{II} (7)		Hydrothermal (160 °C/48 h)			[223]
μ_3-κ^{2}O:κO'' 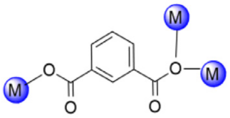	{[Cu$_5$(1,3-bdc)$_2$(μ3-OH)$_2$(ta)$_4$]·2(H$_2$O)}$_n$ (**29**) (ta = 1,2,3-triazolate)	Cd^{II} (4)	3D	Hydrothermal (160 °C/96 h)	Not assigned	1-μ_4-κ^{2}O,O':κO: κO'':κO''' 2-μ_3-κ^{2}O:κO''	[158]
μ_3-κO:κO:κO'',O''' 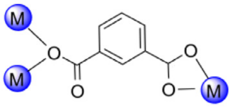	[Cd(1,3-bdc)(4,4′-tmbpt)]$_n$ (**292**) (4,4′-tmbpt = 1-((1H-1,2,4-triazol-1-yl)methyl)-3,5-bis(4-pyridyl)-1,2,4-triazole)	Cd^{II} (6)	3D	Hydrothermal (130 °C/72 h)	Not assigned		[140]
	{[Cd$_2$(1,3-bdc)$_2$(bpyed)]·2(H$_2$O)}$_n$ (**293**) (bpyed = N,N′-bis(pyridin-3-ylmethyl)ethane-1,2-diamine)	Cd^{II} (7/6)	3D	Hydrothermal (130 °C/72 h)	Not assigned	1-μ_3-κO:κO:κO'', O''' 2-μ_3-κ^{2}O,O':κO: κ^{2}O'',O'''	[277]
μ_3-κ^{2}O,O':κO:κ^{2}O'',O''' 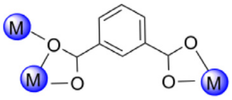	{[Cd$_2$(1,3-bdc)$_2$(bpyed)]·2(H$_2$O)}$_n$ (**293**) (bpyed = N,N′-bis(pyridin-3-ylmethyl)ethane-1,2-diamine)	Cd^{II} (6/7)	3D	Hydrothermal (130 °C/72 h)	Not assigned	1-μ_3-κO:κO:κO'', O''' 2-μ_3-κ^{2}O,O':κO: κ^{2}O'',O'''	[277]
	{[Cd(1,3-bdc)(bpp)$_{0.5}$(H$_2$O)]·(H$_2$O)}$_n$ (**294**) (bpp = 1,4-bis(3-pyridylmethyl) piperazine)	Cd^{II} (6)	2D	Hydrothermal (160 °C/96 h)	Not assigned		[82]
	{[Cd(1,3-bdc)(bppt)]·MeOH}$_n$ (**295**) (bppt = 2,5-bis(3-(pyridine-4-yl)phenyl)thiazolo[5,4-*d*] thiazole)	Cd^{II} (7)	3D	Solvothermal H$_2$O:MeOH (1:1) (160 °C/72 h)	1600; 1423		[56]
	{[Cd(1,3-bdc)(bte)$_{0.5}$(H$_2$O)]·(H$_2$O)}$_n$ (**296**) (bte = bis(triazol)ethane))	Cd^{II} (7)	2D	Hydrothermal (160 °C/72 h)	Not assigned		[278]
	[Cd(1,3-bdc)(dHyn)]$_n$ (**297**) (dHyn = 1,3-di(1H-imidazol-4-yl) benzene)	Cd^{II} (6)	2D	Hydrothermal (180 °C/72 h)	Not assigned		[188]
	{[Cd$_3$(1,3-bdc)$_2$(dHib)$_2$(H$_2$O)$_2$]·2(H$_2$O)}$_n$ (**298**) (dHib = 3,5-di(1H-imidazol-1-yl)benzoic acid)	Cd^{II} (6/7)	3D	Hydrothermal (180 °C/72 h)	Not assigned		[203]
	[Cd(1,3-bdc)(tym)$_{0.5}$]$_n$ (**299**) (tym = tetrakis(imidazol-1-ylmethyl)methane)	Cd^{II} (6)	3D	Hydrothermal (170 °C/72 h)	Not assigned		[279]
	{[CeAg(1,3-bdc)(dspt)(H$_2$O)$_2$]·(H$_2$O)}$_n$ (**300**) (dspt = 4′-(2,4-disulfophenyl)-2,2′:6′2″-terpyridine)	Ce^{III} (9)	3D	Hydrothermal (170 °C/70 h)	Not assigned		[194]
μ_4-κO,O':κO''',O''' 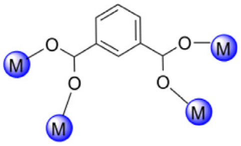	{[Cu(1,3-bdc)(H$_2$O)] (H$_2$O)}$_n$ (**301**)	Cu^{II} (6)		Solvothermal H$_2$O: iPrOH (3:2) (160 °C/120 h)	Not assigned		[48]
	{[Cu$_2$(1,3-bdc)$_2$(9Meade)$_2$(H$_2$O)]·2(1,3-H$_2$bdc)}$_n$ (**356**) (9Meade = 9-methyladenine)	Cu^{II} (5)	2D	Slow diffusion MeOH:H$_2$O	–		[49]
	{[Cu$_4$(1,3-bdc)$_3$(dimb)$_4$](O$_2$)(H$_2$O)$_8$(OH)$_2$}$_n$ (**277**) (dimb = 1,4-di(imidazolidin-1-yl)benzene)	Cu^{II} (6)	2D	Hydrothermal (130 °C/72 h)	1608$_{as}$, 1560$_{as}$, 1435$_s$, 1360$_s$ Δν = 173; 200	1-μ_4-κO,O':κO''', O''' 2-μ_3-κ^{2}O,O':κO: κ^{2}O'',O'''	[164]
	{[Cu(1,3-bdc)(H$_2$O)]·2(H$_2$O)}$_n$ (**302**)	Cu^{II} (6)	2D	Solvothermal H$_2$O:benzene (3:5)	–		[190]
	{[Cu$_4$(1,3-bdc)$_4$(bpa)$_2$(DMF)]·DMF}$_n$ (**185**) (bpa = 1,2-bis(4-pyridyl)ethane)	Cu^{II} (5/6)	3D	Microwave DMF (140 °C/1 h)	Not assigned	1-μ_3-κ^{2}O,O':κO'': κO''' 2-μ_4-κO,O':κO''', O''' 3-μ_4-κ^{2}O,O':κO: κO'':κO'''.	[221]
	[Cu$_2$(1,3-bdc)(fhop)]$_n$ (**303**) (fhop = 2-(2-fluorophenyl)-1H-imidazo[4,5-f][1,10] phenanthroline)	Cu^{II} (5) Cu^{I} (3)	3D	Hydrothermal (185 °C/144 h)	Not assigned		[83]
	{[Cu$_2$(1,3-bdc)$_2$(DMF)]·(H$_2$O)·DMF·0.5(EtOH)}$_n$ (**304**)	Cu^{II} (5)	2D	Slow evaporation DMF:EtOH (1:1)			[62]
	[Cu$_2$(bdc)$_{0.5}$(ina)$_2$(μ_3-OH)]$_n$ (**305**) (inaH = 4-pyridinecarboxylic(isonicotinic acid)	Cu^{II} (4)	2D	Hydrothermal (180 °C/48 h)	Not assigned		[185]
	[Cu$_2$(μ_3-OH)(1,3-bdc)$_{0.5}$(ison)$_2$]$_n$ (**306**) (ison = isonicotinate)	Cu^{II} (5)		Hydrothermal (160 °C/60 h)	–		[45]
	{[Zn$_2$(1,3-bdc)$_2$(ttbt)$_2$]·2(H$_2$O)}$_n$ (**90**) (10,11,12,13-tetrahydro-4,5,9,14-tetraaza-benzo[*b*] triphenylene)	Zn^{II} (6)	2D	Hydrothermal (140 °C/120 h)	–	1-μ-κO:κ^{2}O'',O''' 2-μ_4-κO,O':κO''', O'''	[96]
	[Zn(1,3-bdc)]$_n$ (**307**)	Zn^{II} (4)	3D	Solvothermal H$_2$O:benzene (5:3) (180 °C/72 h)	(1603–1539)$_{as}$; (1466–1408)$_s$ Δν = 134		[117]
	{[Zn$_5$(1,3-bdc)$_3$(Htea)$_2$(H$_2$O)]·2·.6H$_2$O}$_n$ (**280**) (H$_3$tea = triethanolamine)	Zn^{II} (4/5/ 6)	–	Solvothermal MeOH (110 °C/20 h)	Not assigned	1-μ_3-κO:κO':κO'' 2-μ_4-κO,O':κO''', O'''	[116]

(*continued on next page*)

Table 2 (*continued*)

Coordination mode	Formulae	Metal ion (CN)		Experimental approach	IR ν(COO$^-$) [cm^{-1}] Δν	Distinct coordination mode for 1,3-bdc in the compound	Ref.
	[Zn(1,3-bdc)(bmib)$_{0.5}$]$_n$ (**308**) (bmib = 1,4-bis(2-methyl-1H-imidazol-1-ylmethy) benzene)	Zn^{II} (5)	3D	Hydrothermal (160 °C/96 h)	Not assigned		[126]
	{[Zn$_3$Mn$_{1.5}$(1,3-bdc)$_4$(1,3-Hbdc)(bpe)]·bpe}$_n$ (**309**) (bpe = 1,2-bis(4-pyridyl)ethane)	Mn^{II} (6) Zn^{II} (4)	3D	Hydrothermal (180 °C/72 h)	–	1-μ$_4$-κO,O':κO''', O''' 2-κO:O'	[204]
	{[Zn$_3$(1,3-bdc)$_3$(py)$_2$](MeOH)}$_n$ (**197**) (py = pyridine)	Zn^{II} (6)		Slow evaporation MeOH:MeNO$_2$:py (10:5:6)	–	1-μ$_3$-κ^{2}O,O':κO'': κO''' 2-μ$_4$-κO,O':κO''', O'''	[189]
	{[Zn$_2$(1,3-bdc)$_4$(DMSO)$_2$(H$_2$O)]·3DMSO}$_n$ (**285**)	Z^{II} (6/4)	3D	Reaction (H$_2$O); Recryst. (DMF)		1-μ$_3$-κO:κO':κO'' 2-μ$_4$-κO,O':κO''', O'''	[198]
	{[M$_4$(μ4-O)(1,3-bdc)$_3$(bipy)]}$_n$ (**140**) (M$_4$ = Zn$_{2.36}$ Co$_{1.64}$) bipy = 4,4′-bipyridine	Zn^{II} Co^{II} (4/5)	2D	Hydrothermal (180 °C/60 h)	–	1-μ$_4$-κO,O':κO''', O''' 2-μ-κ^{2}O,O':κ^{2}O'', O'''	[132]
	[Mn$_2$(1,3-bdc)$_2$(ttbt)]$_n$ (**310**) (ttbt = 10,11,12,13-tetrahydro-4,5,9,14-tetraaza-benzo [*b*]triphenylene)	Mn^{II} (6)	2D	Hydrothermal (140 °C/120 h)	–	1-μ-κ^{2}O,O':κ^{2}O'', O''' 2-μ$_4$-κO,O':κO''', O'''	[96]
	{[Fe(1,3-bdc)$_3$O(H$_2$O)$_3$][Cl]·9(H$_2$O)}$_n$ (**311**)	Fe^{II} (6)	3D	Hydrothermal (130 °C/120 h)	Not assigned		[122]
	{[H$_2$N(CH$_3$)$_2$]$_2$[Co$_3$(1,3-bdc)$_4$]·(H$_2$O)}$_n$ (**312**)	Co^{II} (6)		Solvothermal DMF:MeOH (5:1) (160 °C/48 h)	Not assigned	1-μ$_4$-κO,O':κO''', O''' 2-μ$_5$-κO:κO':κO'': κO'':κO'''	[154]
	{Co$_6$(μ$_3$-OH)$_2$(1,3-bdc)$_5$(H$_2$O)$_5$]·8(H$_2$O)}$_n$ (**313**)	Co^{II} (4/5/6)	3D	Solvothermal MeOH (160 °C/72 h)	Not assigned	1-μ$_4$-κO,O':κO''', O''' 2-μ$_5$-κO:κO':κO'': κO'':κO'''	[30]
	{Co$_2$(1,3-bdc)$_2$(iPrOH)$_{0.5}$(H$_2$O)$_{0.5}$]·(iPrOH)$_{0.5}$(H$_2$O)}$_n$ (**314**) (iPrOH = 2-propanol)	Co^{II} (6)	3D	Solvothermal iPrOH (160 °C/72 h)	Not assigned	1-μ$_4$-κO,O':κO''', O''' 2-μ$_6$-κ^{2}O,O':κO: κO:κ^{2}O:κO'',O: κO'':κO'':κO''	[30]
	[In$_2$O(1,3-bdc)$_2$]$_n$ (**315**)	In^{III} (6)		Hydrothermal (220 °C/336 h)	Not assigned		[10]
	{[Cd$_6$(1,3-bdc)$_6$(H$_2$O)$_4$]·(H$_2$O)}$_n$ (**316**)	Cd^{II} (6/7)	2D	Hydrothermal (170 °C/72 h)	–		[155]
	[Cd(1,3-bdc)(H$_2$O)]$_n$ (**317**)	Cd^{II} (5)	3D	Solvothermal H$_2$O:DMF (2:1) (90 °C/72 h)	–		[280]
	[Cd$_3$(1,3-bdc)$_3$(Hdatrz)]$_n$ (**318**) (Hdatrz = 3,5-diamino-1,2,4-triazole)	Cd^{II} (5)	3D	Hydrothermal (110 °C/72 h)	Not assigned	1-μ$_4$-κO,O':κO''', O''' 2-μ$_3$-κ^{2}O,O':κO: κ^{2}O'',O''' 3-μ$_5$-κO:κO':κO'': κO'':κO'''	[187]
	[Ln$_2$(1,3-bdc)$_3$(H$_2$O)$_2$]$_n$ Ln = Nd (**319**) or Gd (**320**)	Nd^{III} Gd^{III} (7/8)	2D	Hydrothermal (170 °C/96 h)	Nd = 1545$_{as}$, 1452$_{as}$; 1389$_s$ Δν = 156; 63 Gd = 1531$_{as}$, 1456$_{as}$; 1390$_s$ Δν = 141; 66	1-μ$_4$-κO,O':κO''', O''' 2-μ$_4$-κ^{2}O,O':κO: κ^{2}O'',O''':κO''	[33]
	[Yb$_2$(1,3-bdc)$_3$(phen)$_{0.5}$]$_n$ (**321**) (phen = 1,10-phenanthroline)	Yb^{III} (6/7/8)	3D	Hydrothermal (150 °C/120 h)	Not assigned	1-μ$_4$-κO,O':κO''', O''' 2-μ$_4$-κ^{2}O,O':κO: κO'':κO'''	[63]
	[Yb$_2$(1,3-bdc)$_3$(mpip)]$_n$ (**289**) (mpip = 2-(3-methylphenyl)imidazo(4,5-f)(1,10)-phenanthroline)	Yb^{III} (6)	2D	Hydrothermal (180 °C/72 h)	Not assigned	1-μ$_4$-κO,O':κO''', O''' 2-μ$_3$-κO:κO':κO''	[195]
	{[Ln$_2$(1,3-bdc)$_3$(mpip)$_2$]·2H$_2$O}$_n$ Ln = Dy (**128**), Ho (**129**), or Er (**130**) (mpip = 2-(3-methylphenyl)imidazo(4,5-f)(1,10)-phenanthroline)	Dy^{III} Ho^{III} Er^{III} (8)	2D	Solvothermal CH$_3$CN:H$_2$O (3:2) (120 °C/72 h)	Not assigned	1-μ-κO:κ^{2}O'',O''' 2-μ$_3$-κ^{2}O,O':κO'': κO''' 3-μ$_4$-κO,O':κO''', O'''	[195]
	{[Ln$_2$(1,3-bdc)$_2$(mpip)$_2$(NO$_3$)$_2$]·3(H$_2$O)}$_n$ Ln = Tb (**269**) or Gd (**270**) (mpip = 2-(3-methylphenyl)imidazo(4,5-f)(1,10)-phenanthroline)	Tb^{III} Gd^{III} (8)	2D	Solvothermal CH$_3$CN:H$_2$O (5:1) (120 °C/72 h)	Not assigned	1-μ$_4$-κO,O':κO''', O''' 2-μ$_3$-κ^{2}O,O':κO'': κO'''	[195]
	{[Dy$_3$(1,3-bdc)$_4$(NO$_3$)(phen)$_3$]·2(H$_2$O)}$_n$ (**255**)	Dy^{III} (9)	3D	Solvothermal DMF:H$_2$O:EtOH (10:3:2) (85 °C/48 h)	1641$_{as}$; 1393$_s$	1-μ$_3$-κ^{2}O,O':κO'': κO''' 2-μ$_4$-κO,O':κO''', O'''	[25]
	[Dy$_2$(1,3-bdc)$_3$(H$_2$O)$_2$]·(H$_2$O)}$_n$ (**256**)	Dy^{III} (7/8)	2D	Hydrothermal (160 °C/96 h)	1602$_{as}$; 1372$_s$	1-μ$_3$-κ^{2}O,O':κO'': κO''' 2-μ$_4$-κO,O':κO''', O''' 3-μ$_4$-κ^{2}O,O':κO: κO'':κO'''	[25]
	{[Ln$_4$(1,3-bdc)$_6$(DMF)(H$_2$O)$_4$]·DMF·2(H$_2$O)}$_n$ Ln = Tb (**257**), Ho (**258**), or Er (**259**)	Tb^{III} Ho^{III} Er^{III} (7/9)	–	Solvothermal DMF:H$_2$O (5:2) (85 °C/72 h)	1612$_{as}$; 1534$_s$	1-μ$_3$-κ^{2}O,O':κO'': κO''' 2-μ$_4$-κO,O':κO''', O'''	[25]
	{[Ln$_2$(1,3-bdc)$_3$(phen)H$_2$O]·(H$_2$O)}$_n$ Ln = La (**322**), Pr (**323**), or Yb (**324**) (phen = 1,10-phenanthroline)	La^{III} Pr^{III} Yb^{III} (8)	2D	Hydrothermal (140 °C/96 h)	(1616–1546)$_{as}$; (1453–186)$_s$	1-μ-κ^{2}O,O':κ^{2}O'', O''' 2-μ$_4$-κ^{2}O,O':κO: κO'':κO'''	[165]
	{[Ln$_2$(1,3-bdc)$_3$(ptcp)$_2$]·(H$_2$O)}$_n$ (ptcp = 2-phenyl-1H-1,3,7,8-tetraazacyclopenta[*l*] phenanthrene) Ln = Pr (**167**), Sn (**168**), Eu (**169**), Tb (**170**), or Dy (**171**)	Pr^{III} Sn^{III} Eu^{III} Tb^{III} Dy^{III} (8)	1D	Hydrothermal (160 °C/72 h)	Pr = 1608 ;1479 Sm = 1603; 1456 Eu = 1637; 1451 Tb = 1629; 1449 Dy = 1646; 1408	1-μ$_4$-κO,O':κO''', O''' 2-μ-κ^{2}O,O':κ^{2}O'', O'''	[55]
	{K[Gd$_2$(1,3-bdc)$_3$(ox)(H$_2$O)$_3$]•(Hdma)•(H$_2$O)}$_n$ (**325**) (ox = oxalic acid)	Gd^{III} (9)	3D	Solvothermal DMF (150 °C/96 h)	Not assigned	1-μ$_4$-κO,O':κO''', O''' 2-μ$_4$-κ^{2}O,O':κO: κ^{2}O'',O''':κO''	[69]
	{[Eu(1,3-bdc)$_{1.5}$(mopip)]·0.5(H$_2$O)}$_n$ (**172**) (mopip = 2-(4-methoxyphenyl)-1H-imidazo[4,5-f][1,10] phenanthroline).	Eu^{III} (8)	1D	Hydrothermal (165 °C/120 h)	1640$_{as}$; 1485$_s$ Δν = 155	1-μ-κ^{2}O,O':κ^{2}O'', O''' 2-μ$_4$-κO,O':κO''', O'''	[138]

Table 2 (*continued*)

Coordination mode	Formulae	Metal ion (CN)		Experimental approach	IR ν(COO$^-$) [cm^{-1}] Δν	Distinct coordination mode for 1,3-bdc in the compound	Ref.
	{[Ln$_2$(1,3-bdc)$_3$(mopip)$_2$]·(H$_2$O)}$_n$ (**173**) (mopip = 2-(4-methoxyphenyl)-1H-imidazo[4,5-f][1,10] phenanthroline). Ln = Sm or Nd	Sm^{III}, Nd^{III} (8)	1D	Hydrothermal (160 °C/120 h)	Sm = 1615$_{as}$; 1451$_s$ Nd = 1614$_{as}$; 1450$_s$	1-μ-κ^{2}O,O':κ^{2}O'', O''' 2-μ_4-κO,O':κO''', O'''	[137]
	{[Gd$_2$(1,3-bdc)$_3$(mopip)$_2$]·(H$_2$O)}$_n$ (**174**) (mopip = 2-(4-methoxyphenyl)-1H-imidazo[4,5-f][1,10] phenanthroline)	Gd^{III} (8)	1D	Hydrothermal (165 °C/120 h)	Not assigned	1-μ-κ^{2}O,O':κ^{2}O'', O''' 2-μ_4-κO,O':κO''', O'''	[79]
	[Sm$_2$(1,3-bdc)$_3$(H$_2$O)$_2$]$_n$ (**326**)	Sm^{III} (7)	2D	Hydrothermal (180 °C/96 h)	(1613; 1546)$_{as}$; (1453; 1389)$_s$		[281]
	[Eu$_2$(1,3-bdc)$_3$(H$_2$O)$_2$]$_n$ (**327**)	Eu^{III} (7)	2D	Hydrothermal (180 °C/96 h)	(1614; 1548)$_{as}$; (1454; 1390)$_s$	1-μ_4-κO,O':κO''', O''' 2-μ_4-κ^{2}O,O':κO: κO'':κO'''	[281]
	{(NH$_4$)$_2$[Ga$_8$Ln$_2$(1,3-bdc)$_4$(shi)$_8$(DMF)$_2$(H$_2$O)$_2$]· xDMF·yH$_2$O} $_n$ Ln = Dy (**328**), Nd, Sm,, Eu, Gd, Tb, Pr, Ho, Er, Tm (x = 12; y = 0); Yb (x = 12 ; y = 1); Y (x = 8 ; y = 3) (The structure was only determined for Ln = Dy)	Dy^{III} (8) Ga^{III} (6)		Slow evaporation DMF	–		[219]
	[UO$_2$(1,3-bdc)]$_n$ (**329**)	U^{VI} (6)	3D	Hydrothermal (140 °C/24 h)	–		[282]
μ_4-κO:κO:κO'':κO''' 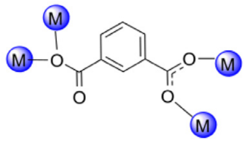	[Zn$_3$(1,3-bdc)$_2$(ppaa)$_2$]$_n$ (**330**) (ppaa$^-$ = 2-(3-(pyridin-2-yl)-1H-pyrazol-1-yl) acetate)	Zn^{II} (5/6)	2D	Hydrothermal (140 °C/72 h)	Not assigned		[162]
	{[Cd$_4$(1,3-bdc)$_2$(ppaa)$_4$]·2(H$_2$O)}$_n$ (**331**) (ppaa-= 2-(3-(pyridin-2-yl)-1H-pyrazol-1-yl) acetate)	Cd^{II} (6)	2D	Hydrothermal (140 °C/72 h)	Not assigned		[161]
	{[Pb$_5$(1,3-bdc)$_4$(tcpbc)$_2$]·3(H$_2$O)}$_n$ (**253**) (Htcpbc = 2′-(1H-1,3,7,8-tetraaza-cyclopenta [l] phenanthren-2-yl)biphenyl-2-carboxylic acid)	Pb^{II} (4/5/6)	2D	Hydrothermal (140 °C/72 h)	–	1-μ_3-κ^{2}O,O':κO'': κO''' 2-μ_4-κO:κO:κO'': κO'''	[70]
μ_4-κ^{2}O,O':κO: κO'':κO''' 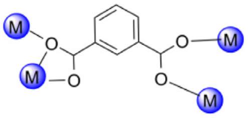	{[Cu$_5$(1,3-bdc)$_2$(μ3-OH)$_2$(ta)$_4$]·2(H$_2$O)}$_n$ (**291**) (ta = 1,2,3-triazolate)	Cu^{II} (4)	3D	Hydrothermal (160 °C/96 h)	Not assigned	1-μ_4-κ^{2}O,O':κO: κO'':κO''' 2-μ_3-κ^{2}O:κO''	[158]
	{[Cu$_4$(1,3-bdc)$_4$(bpa)$_2$(DMF)]·DMF}$_n$ (**185**) (bpa = 1,2-bis(4-pyridyl)ethane)	Cu^{II} (5/6)	3D	Microwave DMF (140 °C/1 h)	Not assigned	1-μ_3-κ^{2}O,O':κO'': κO''' 2-μ_4-κO,O':κO''', O''' 3-μ_4-κ^{2}O,O':κO: κO'':κO'''	[221]
	{[H$_2$N(CH$_3$)$_2$]$_2$[Co$_3$(1,3-bdc)$_4$]·(H$_2$O)}$_n$ (**312**)	Co^{II} (6)		Solvothermal DMF:MeOH (5:1) (160 °C/48 h)	Not assigned	1-μ_4-κO,O':κO''', O''' 2-μ_4-κ^{2}O,O':κO: κO'':κO'''	[154]
	[Cd$_3$(1,3-bdc)$_3$(Hdatrz)]$_n$ (**318**) (Hdatrz = 3,5-diamino-1,2,4-triazole)	Cd^{II} (5)	3D	Hydrothermal (110 °C/72 h)	Not assigned	1-μ_4-κO,O':κO''', O''' 2-μ_3-κ^{2}O,O':κO: κ^{2}O'',O''' 3-μ_5-κO:κO':κO'': κO'':κO'''	[187]
	{(Me$_2$NH$_2$)$_2$[Cd$_3$(1,3-bdc)$_4$]·(H$_2$O)·2(EtOH)}$_n$ (**233**)	Cd^{II} (6)	2D	Solvothermal DMF:EtOH (1:1) (130 °C/48 h)	1576; 1385	1-μ_3-κ^{2}O,O':κO'': κO''' 2-μ_4-κ^{2}O,O':κO: κO'':κO'''	[184]
	[Dy$_2$(1,3-bdc)$_3$(H$_2$O)$_2$]·(H$_2$O)}$_n$ (**256**)	Dy^{III} (7/8)	2D	Hydrothermal (160 °C/96 h)	1602$_{as}$; 1372$_s$	1-μ_3-κ^{2}O,O':κO'': κO''' 2-μ_4-κO,O':κO''', O''' 3-μ_4-κ^{2}O,O':κO: κO'':κO'''	[25]
	{[Eu$_2$(1,3-bdc)$_3$(DMF)$_2$]·(DMF)$_{1.7}$}$_n$ (**332**)	Eu^{III} (9)	3D	Solvothermal DMF:H$_2$O (2:1) (60 °C/96 h)	Not assigned		[11]
	[Eu$_2$(1,3-bdc)$_3$(H$_2$O)$_2$]$_n$ (**327**)	Eu^{III} (7)	2D	Hydrothermal (180 °C/96 h)	(1614; 1548)$_{as}$; (1454; 1390)$_s$	1-μ_4-κO,O':κO''', O''' 2-μ_4-κ^{2}O,O':κO: κO'':κO'''	[281]
	[Ln$_2$(1,3-bdc)$_3$(H$_2$O)$_2$]$_n$ Ln = Nd (**319**) or Gd (**320**)	Nd^{III} Gd^{III} (7/8)	2D	Hydrothermal (170 °C/96 h)	Nd = 1545$_{as}$, 1452$_{as}$; 1389$_s$ Δν = 156; 63 Gd = 1531$_{as}$, 1456$_{as}$; 1390$_s$ Δν = 141; 66	1-μ_4-κO,O':κO''', O''' 2-μ_4-κ^{2}O,O':κO: κ^{2}O'',O''':κO''	[33]
	[Yb$_2$(1,3-bdc)$_3$(phen)$_{0.5}$]$_n$ (**321**) (phen = 1,10-phenanthroline)	Yb^{III} (6/7/8)	3D	Hydrothermal (150 °C/120 h)	Not assigned	1-μ_4-κO,O':κO''', O''' 2-μ_4-κ^{2}O,O':κO: κO'':κO'''	[63]
	{[Ln$_2$(1,3-bdc)$_3$(phen)(H$_2$O)]·(H$_2$O)}$_n$ Ln = La (**322**), Pr (**323**), or Yb (**324**) (phen = 1,10-phenanthroline)	La^{III} Pr^{III} Yb^{III} (8)	2D	Hydrothermal (140 °C/96 h)	La 1618$_{as}$, 1546 $_{as}$, 1453$_s$;1400$_s$ Pr 1616$_{as}$, 1546$_{as}$, 1458$_s$; 1400$_s$ Yb 1616$_{as}$, 1546$_{as}$, 1443$_s$; 1386$_s$	1-μ-κ^{2}O,O':κ^{2}O'', O''' 2-μ_4-κ^{2}O,O':κO: κO'':κO'''	[165]
	{[Y$_2$Co(1,3-bdc)$_4$(tpa)(H$_2$O)]·2(H$_2$O)}$_n$ (**175**) {[Y$_2$Zn(1,3-bdc)$_4$(tpa)(H$_2$O)]·2(H$_2$O)}$_n$ (**176**) {[Er$_2$Co(1,3-bdc)$_4$(tpa)(H$_2$O)]·2(H$_2$O)}$_n$ (**177**) {[Er$_2$Zn(1,3-bdc)$_4$(tpa)(H$_2$O)]·2(H$_2$O)}$_n$ (**178**) {[Sm$_2$Co(1,3-bdc)$_4$(tpa)(H$_2$O)]·0.5(H$_2$O)}$_n$ (**179**) (tpa = tris(2-pyridylmethyl)amine)	Y^{III} Er^{III} Sm^{III} (8) Zn^{II} Co^{II} (5)	2D	Hydrothermal (140 °C/96 h)	Not assigned	1-μ-κ^{2}O,O':κ^{2}O'', O''' 2-μ_3-κO:κO':κO'' 3-μ_3-κ^{2}O,O':κO'': κO''' 4-μ_4-κ^{2}O,O':κO: κO'':κO'''	[168]
μ_4-κ^{2}O,O':κO:κ^{2}O'',O''':κO'' 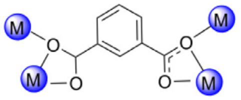	[Ca(1,3-bdc)$_2$(H$_2$O)$_2$]$_n$ (**333**)	Ca^{II} (8)		Hydrothermal (110 °C/96 h)	1535$_{as}$, 1448$_{as}$; 1396$_s$ Δν = 139; 52		[46]
	[Ca(1,3-bdc)(pyr)]$_n$ (**334**) (pyr = 2-pyrrolidinone)	Ca^{II} (8)	3D	Hydrothermal (190 °C/144 h)	–		[104]
	[Cd$_2$(1,3-bdc)$_2$(bib)$_{1.5}$]$_n$ (**229**) (bib = 1,4-bis(1-imidazol-yl)-2,5-dimethyl benzene)	Cd^{II} (6/7)	3D	Hydrothermal (160 °C/96 h)	Not assigned	1-μ_3-κ^{2}O,O':κO'': κO''' 2-μ_4-κ^{2}O,O':κO: κ^{2}O'',O''':κO''	[174]
	{K[Gd$_2$(1,3-bdc)$_3$(ox)(H$_2$O)$_3$]•(Hdma)•(H$_2$O)}$_n$ (**325**) (ox = oxalic acid)	Gd^{III} (9)	3D	Solvothermal DMF (150 °C/96 h)	Not assigned	1-μ_4-κO,O':κO''', O''' 2-μ_4-κ^{2}O,O':κO: κ^{2}O'',O''':κO''	[69]

(*continued on next page*)

Table 2 (*continued*)

Coordination mode	Formulae	Metal ion (CN)		Experimental approach	IR ν(COO⁻) [cm⁻¹] Δν	Distinct coordination mode for 1,3-bdc in the compound	Ref.
	$\{[La_2(1,3\text{-}bdc)_3(mpip)_2]\cdot 5(H_2O)\}_n$ (**271**) $\{[Nd_2(1,3\text{-}bdc)_3(mpip)_2]\cdot 7(H_2O)\}_n$ (**272**) (mpip = 2-(3-methylphenyl)imidazo(4,5-f)(1,10)-phenanthroline)	La^{III} Nd^{III} (9)	2D	Hydrothermal (180 °C/72 h)	Not assigned	1-μ_3-κ^2O,O':κO'':κO''' 2-μ_4-κ^2O,O':κO:κ^2O'',O''':κO''	[195]
	$[Ln_2(1,3\text{-}bdc)_2(ct)_2]_n$ (ct = 4′-(3-carboxyphenyl)-4,2′:6′,4′′-terpyridine) Ln = Nd (**335**), Sm (**336**), Eu (**337**), or Pr (**338**)	Pr^{III} Nd^{III} Sm^{III} Eu^{III} (8)	3D	Hydrothermal (160 °C/72 h)	Not assigned		[176]
	$\{[Zn_2Pr(1,3\text{-}bdc)_3(1,3\text{-}Hbdc)(bpe)]\cdot(H_2O)\}_n$ (**339**) (bpe = 1,2-bis(4-pyridyl)ethane)	Pr^{III} (8) Zn^{II} (4)	3D	Hydrothermal (180 °C/72 h)	–		[204]
μ_5-κO:κO':κ^2O'',O''':κO'':κO''' 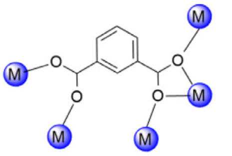	$\{[Ca_2(1,3\text{-}bdc)_2(nmp)]\cdot 0.5(H_2O)\}_n$ (**340**) (nmp = 1-methyl-2-pyrrolidinone)	Ca^{II} (6/8)	3D	Hydrothermal (150 °C/120 h)	–	1-μ_5-κO:κO':κ^2O'',O''':κO'':κO''' 2-μ_5-κ^2O,O':κO:κO':κ^2O'',O''':κO''	[104]
μ_5-κ^2O,O':κO:κO':κ^2O'',O''':κO'' 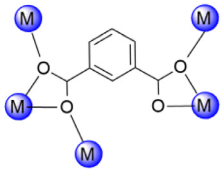	$\{[Ca_2(1,3\text{-}bdc)_2(nmp)]\cdot 0.5(H_2O)\}_n$ (**340**) (nmp = 1-methyl-2-pyrrolidinone)	Ca^{II} (6/8)	3D	Hydrothermal (150 °C/120 h)	–	1-μ_5-κO:κO':κ^2O'',O''':κO'':κO''' 2-μ_5-κ^2O,O':κO:κO':κ^2O'',O''':κO''	[104]
μ_5-κO:κO':κO'':κO'':κO''' 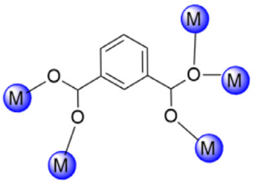	$\{Co_6(\mu_3\text{-}OH)_2(1,3\text{-}bdc)_5(H_2O)_5]\cdot 8(H_2O)\}_n$ (**313**)	Co^{II} (4/5/6)	3D	Solvothermal MeOH (160 °C/72 h)	Not assigned	1-μ_4-κO,O':κO''',O''' 2-μ_5-κO:κO':κO'':κO'':κO'''	[30]
	$[Cd_3(1,3\text{-}bdc)_3(Hdatrz)]_n$ (**318**) (Hdatrz = 3,5-diamino-1,2,4-triazole)	Cd^{II} (5)	3D	Hydrothermal (110 °C/72 h)	Not assigned	1-μ_3-κ^2O,O':κO:κ^2O'',O''' 2-μ_4-κO,O':κO''',O''' 3-μ_5-κO:κO':κO'':κO'':κO'''	[187]
	$[Cd_4Co_2(1,3\text{-}bdc)_6(Him)_4]_n$ (**341**) (Him = imidazole)	Cd^{II} (6) Co^{II} (5)	3D	Hydrothermal (180 °C/72 h)	–		[283]
μ_5-κ^2O,O':κO':κO':κO'',O''':κO''' 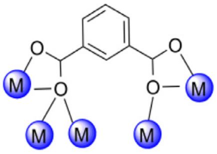	$[Pb_{13}Na(1,3\text{-}bdc)_{12}(\mu_3\text{-}O)(\mu_3\text{-}OH)]_n$ (**342**)	Pb^{II} (6/7)	3D	Hydrothermal (160 °C/72 h)	Not assigned	1-μ_5-^{2}O,O':κO':κO':κO'',O''':κO''' 2-μ_6-κ^2O,O':κO:κO':κO'':κO'':κO'''	[206]
μ_6-κ^2O,O':κO:κO':κO'':κO'':κO''' 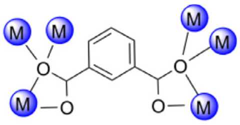	$[Pb_{13}Na(1,3\text{-}bdc)_{12}(\mu_3\text{-}O)(\mu_3\text{-}OH)]_n$ (**342**)	Pb^{II} (6/7)	3D	Hydrothermal (160 °C/72 h)	Not assigned	1-μ_5-κ^2O,O':κO':κO':κO'',O''':κO''' 2-μ_6-κ^2O,O':κO:κO':κO'':κO'':κO'''	[206]
μ_6-κ^2O,O':κO:κO:κ^2O:κO'',O:κO'':κO'':κO'' 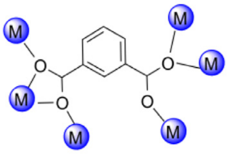	$\{[Co^2(1,3\text{-}bdc)^2(iPrOH)^{0.5}(H^2O)^{0.5}]\cdot(iPrOH)^{0.5}(H^2O)\}^n$ (**314**) (iPrOH = 2-propanol)	Co^{II} (6)	3D	Solvothermal iPrOH (160 °C/72 h)	Not assigned	1-μ^4-κO,O':κO''',O''' 2-μ^6-κ^2O,O':κO:κO:κ^2O:κO'',O:κO'':κO'':κO''	[30]

Table 2 (*continued*)

Coordination mode	Formulae	Metal ion (CN)		Experimental approach	IR $\nu(COO^-)$ [cm^{-1}] $\Delta\nu$	Distinct coordination mode for 1,3-bdc in the compound	Ref.
κ^2O,O' 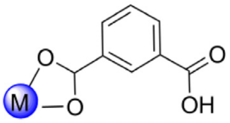	$\{[Cd(1,3\text{-}bdc)(cmb)(H_2O)_2][Cd(1,3\text{-}bdc)(1,3\text{-}Hbdc)(H_2O)]\}_n$ (**160**) (cmb = 1-(1-cyclohexylmethane)-4,4′-bipyridinium bromide)	Cd^{II} (7)		Slow evaporation H_2O:DMF:EtOH (5:1:1)	Not assigned	1-μ-κ^2O,O’:κ^2O”, O’” 2-κ^2O,O’	[136]
	$[Ag(1,3\text{-}Hbdc)(bdzh)]_n$ (**343**) (bdzh = 1,6-bis(5,6-dimethylben-zimidazol-1-yl) hexane)	Ag^{I} (3)	1D	Hydrothermal (140 °C/72 h)	Not assigned		[180]
κO 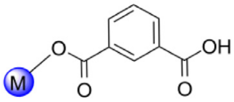	$\{[Cu(1,3\text{-}Hbdc)(phen)(H_2O)_2]ClO_4\cdot[Cu(1,3\text{-}bdc)(phen)(H_2O)_2]\cdot2(H_2O)\}$ (**1**) (phen = 1,10-phenanthroline)	Cu^{II} (5)		Hydrothermal (150 °C/36 h)	1568_{as}; 1387_s, 1370_s $\Delta\nu$ = 198; 181		The present work
	$[Cu(1,3\text{-}Hbdc)_2(bipyen)]_n$ (**344**) (bipyen = *trans*-1,2-bis(4-pyridyl)ethylene))	Cu^{II} (4)	1D	Hydrothermal (150 °C/48 h)	Not assigned		[205]
	$[Zn(1,3\text{-}Hbdc)(trz)]_n$ (**345**) (trz = 1,2,4-triazole)	Zn^{II} (4)	2D	Hydrothermal (150 °C/72 h)	Not assigned		[121]
	$[Ni(1,3\text{-}Hbdc)(tib)(H_2O)_2]\cdot0.5(H_2O)$ (**346**) (tib = 1,3,5-tris(1-imidazolyl)benzene)	Ni^{II} (6)	3D	Hydrothermal (170 °C/72 h)	Not assigned		[114]
	$[Mg(1,3\text{-}Hbdc)_2(phen)(H_2O)_2](phen)$ (**355**) (phen = 1,10-phenanthroline)	Mg^{II} (8)		Hydrothermal (70 °C/–)	Not assigned		[284]
κO 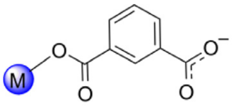	$\{[Cu(1,3\text{-}Hbdc)(phen)(H_2O)_2]ClO_4\cdot[Cu(1,3\text{-}bdc)(phen)(H_2O)_2]\cdot2(H_2O)\}$ (**1**) (phen = 1,10-phenanthroline)	Cu^{II} (5)		Hydrothermal (150 °C/36 h)	1568_{as}; 1387_s, 1370_s $\Delta\nu$ = 198; 181		The present work
	$\{[Cu(1,3\text{-}bdc)(phen)_2]\cdot5(H_2O)\cdot(EtOH)\cdot0.5(MeOH)$ (**355**) (phen = 1,10-phenanthroline)	Cu^{II} (5)		Slow evaporation EtOH	Not assigned		[285]
	$[Co(1,3\text{-}bdc)(mopip)_2\cdot2(H_2O)]_n$ (**347**) (mopip = 2-(4-Methoxyphenyl)-1H-imidazo[4,5-f][1,10]-phenanthroline)	Co^{II} (6)	0D	Hydrothermal (165 °C/120 h)	1608_{as}; 1484_s		[138]
κO 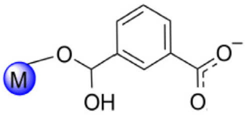	$[Ag(1,3\text{-}Hbdc)(bbbm)]_n$ (**348**) (bbbm = 1,1′-(1,4-butanediyl)bis-1H-benzimidazole)	Ag^{I} (3)	2D	Hydrothermal (140 °C/72 h)	1612_{as}; 1380_s $\Delta\nu$ = 232		[94]
$\kappa O:O'$ 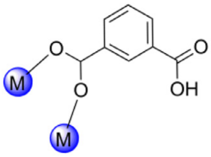	$\{[Zn_3Mn_{1.5}(1,3\text{-}bdc)_4(1,3\text{-}Hbdc)(bpe)]\cdot bpe\}_n$ (**309**) (bpe = 1,2-bis(4-pyridyl)ethane))	Mn^{II} (6) Zn^{II} (4)	3D	Hydrothermal (180 °C/72 h)	–	1-μ_4-κO,O’:κO’”, O’” 2-κO:O’	[204]
$\kappa O:O'$ 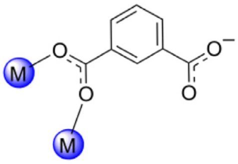	$[Cu_3(1,3\text{-}bdc)_4(dpq)_2]_n$ (**275**) (dpq = dipyrido[3,2-*d*:2′,3′-*f*]quinoxaline)	Cu^{II} (4/5)	1D	Hydrothermal (120 °C/96 h)	1624_{as}; 1570_s; 1380_s	1-μ_3-κO:κO’:κO” 2-κO:O’	[98]
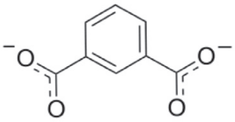	$[Co_2(H_2biim)_2(H_2O)_2]\cdot(1,3\text{-}bdc)\cdot4(H_2O)$ (**349**) (biim = 2,2′-biimidazole)	Co^{II} (6)	1D	Slow evaporation	Not assigned		[209]
	$\{[Ag_2(dpb)_2]\cdot(1,3\text{-}bdc)\cdot9(H_2O)\}_n$ (**350**) (dpb = 1,4-bis(pyrid-4-yl)benzene)	Ag^{I} (2)	1D	Ultrasonic conditions MeOH:H_2O (2:1)	Not assigned		[103]
	$\{[Ag(bpetan)_2]\cdot(1,3\text{-}bdc)\cdot8(H_2O)\}_n$ (**351**) (bpetan = 1,2-bis(4-pyridyl)ethane))	Ag^{I} (3)	2D	Ultrasonic conditions	–		[199]
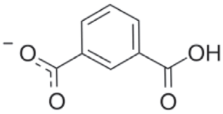	$\{[A_{g1.5}(biyb)]\cdot1.5(H_{0.5}bdc)\cdot4(H_2O)\}_n$ (**352**) (biyb = 1,4-bis(imidazol-1-ylmethyl)benzene)	Ag^{I} (2)	1D	Hydrothermal (140 °C/72 h)	1688		[210]
	$\{[Ag(bbi)](1,3\text{-}Hbdc)\}_n$ (**353**) (bbi = 1,1′-(1,4-butanediyl)bis(imidazole))	Ag^{I} (2)		Hydrothermal (100 °C/36 h)	Not assigned		[143]

DMA = N,*N*-dimethylacetamide; DMF = N,*N*-dimethylformamide; DMSO = dimethy sufoxide; MeOH = methanol; EtOH = ethanol; iPrOH = isopropyl alcohol; Me_2NH_2 =-dimethylamine cation

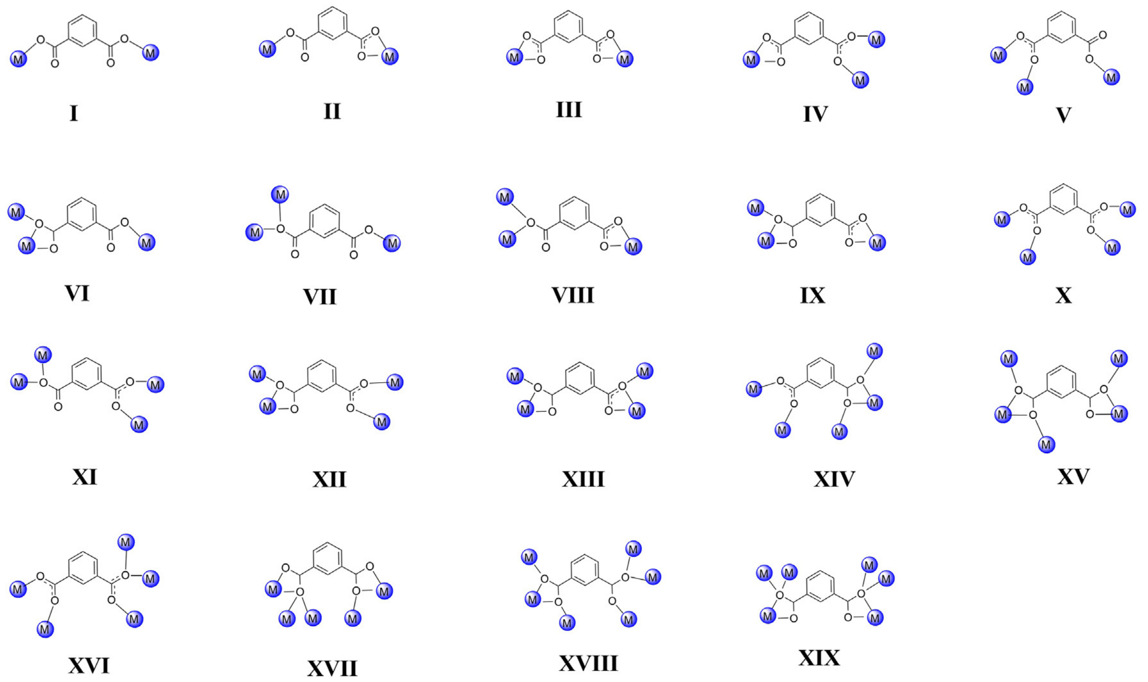

Fig. 6. Coordination modes of 1,3-bdc acting as a bridge between metal centers.

and μ_3-bis-chelating-monoatomic bridge (**IX**) modes are encountered more often for the structures of metal cations with larger ionic radii and coordination numbers. The strong influence of the type of metal ion and the coordination number on carboxylate coordination mode is unquestionable [215]; however, some studies indicate that the final network structure is a result of a combination of a variety of parameters. Several factors including the noncovalent interactions, the coordination number of the center, the type of ligand other than the 1,3-bdc, the total charge of the metal complex, and the presence of solvent molecules should be taken into account to determine the carboxylate binding mode [216,217].

Lanthanide ions exhibit flexible coordination environments owing to the large ionic radius and variable coordination number (CN varying from 6 to 12), so they can adopt many types of 1,3-bdc coordination modes, and, therefore, display a range of geometric configurations. Beyond the coordination modes **III**, **IV**, and **V**, in general, lanthanide ions also commonly adopt μ_4-bridging modes, **X**, **XII**, and **XIII** (Fig. 8). Concerning the diversiform of lanthanide's networks, several heteronuclear lanthanide-based frameworks bearing 1,3-bdc as ligand have been reported [168,194,204,218,219]. The possibility to obtain lanthanide-only heterometallic frameworks may result in fascinating physical properties, such as conductivity, magnetic ordering, or photoluminescent attributes [168,194,218].

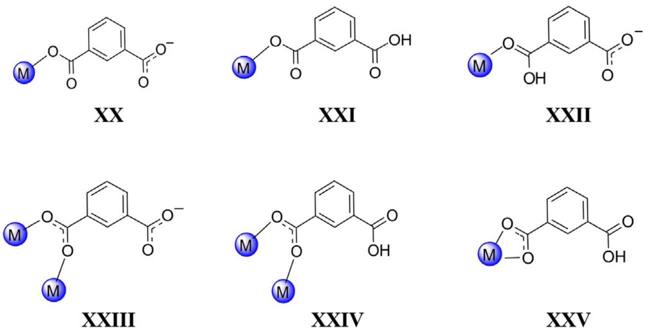

Fig. 7. Coordination modes of 1,3-Hbdc and 1,3-bdc acting as terminal ligands.

Regarding the less common metal centers present in 1,3-bdc-based coordination networks, Pb^{II} and Ca^{II} must be highlighted on account of the μ_5- and μ_6-bridging coordination modes (**XIV–XIX**). Indeed, these kind of coordination modes have been noticed only for these metal ions, besides Cd^{II} and Co^{II}. In general, carboxylate coordination bridging modes that connect more than four metal centers are relatively rare and are rather restricted to large metal cations, as in the case of Cd^{II}, Ca^{II} and Pb^{II} with ionic radii greater than 95 pm [214]. However, despite of the small ionic radius of Co^{II} (65 pm for NC = 6) [214], we found two cobalt(II)-based coordination networks with 1,3-bdc adopting μ_5- and μ_6-bridging coordination modes (compounds **313** and **314**, respectively) [30], showing that coordination modes of 1,3-bdc cannot be explained by simple ionic radius considerations. It is worth noting that one of these compounds (**313**) is a cluster composed of six cobalt atoms.

Furthermore, regarding the Ag^{I} ion, another less common metal center employed to build networks based on 1,3-bdc, we found ten examples. In four of them, the 1,3-bdc acts as a bis-monodentate bridging (**I**) ligand in its deprotonated (**76–78**) [113,152,169] and partially deprotonated (**81**) [208] forms. In the other two structures, both 1,3-Hbdc and 1,3-bdc act as monodentate terminal ligands (**348** and **343**) [94,180]. Finally, in the other four Ag^{I}-based structures, 1,3-bdc (**350** and **351**) [103,199] and 1,3-Hbdc (**352** and **353**) [143,210] act as counterions. The lability and coordination flexibility of Ag^{I} [220] may support its dynamic behavior within coordination networks with 1,3-bdc in its fully and partially deprotonated forms.

Another situation that should be examined happens when a network possesses more than one 1,3-bdc in its asymmetrical unit, strongly contributing to the structural diversity and complexity of the coordination modes. In numerous cases, each independent 1,3-bdc exhibits a distinct coordination mode within the single coordination network. Furthermore, certain coordination networks even presented three (**128–130**, **185**, **256**, and **318**) [25,187,195,221]

Table 3
Descriptions of coordination modes of 1,3-bdc, represented in Figs. 6 and 7, given in the kappa (κ) convention and the Harris notation.

Coordination mode	kappa (κ) convention 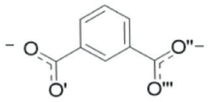	Harris notation
I	μ-κO:κO”	2.1001
II	μ-κO:κ^{2}O”,O’”	2.1011
III	μ-κ^{2}O,O’:κ^{2}O”,O’”	2.1111
IV	μ$_3$-κ^{2}O,O’:κO”:κO’”	3.1111
V	μ$_3$-κO:κO’:κO”	3.1110
VI	μ$_3$-κ^{2}O,O’:κO:κO”	3.2101
VII	μ$_3$-κ^{2}O:κO”	3.2001
VIII	μ$_3$-κO:κO:κO”,O’”	3.2011
IX	μ$_3$-κ^{2}O,O’:κO:κ^{2}O”,O’”	3.2111
X	μ$_4$-κO,O’:κO’”,O’”	4.1111
XI	μ$_4$-κO:κO:κO”:κO’”	4.2011
XII	μ$_4$-κ^{2}O,O’:κO: κO”:κO’”	4.2111
XIII	μ$_4$-κ^{2}O,O’:κO:κ^{2}O”,O’”:κO”	4.2112
XIV	μ$_5$-κO:κO’:κ^{2}O”,O’”:κO”:κO’”	5.1122
XV	μ$_5$-κ^{2}O,O’:κO:κO’:κ^{2}O”,O’”:κO”	5.2212
XVI	μ$_5$-κO:κO’:κO”:κO”:κO’”	5.1112
XVII	μ$_5$-κ^{2}O,O’:κO’:κO’:κO”,O’”:κO’”	5.1321
XVIII	μ$_6$-κ^{2}O,O’:κO:κO’:κO”:κO”:κO’”	6.2212
XIX	μ$_6$-κ^{2}O,O’:κO:κO:κ^{2}O:κO”,O:κO”: κO”:κO”	6.3113
XX–XXII	κO	1.1000
XXIII, **XXIV**	κO:κO’	2.1100
XXV	κ^{2}O,O’	1.1100

or four (**80**, **175–179**) [168] distinct coordination modes for 1,3-bdc.

4. Aspects that affect structural versatility of 1,3-bdc coordination networks

One major challenge faced in the development of coordination networks with specific chemical and physical properties is the rational design of structures. As such, the systematic investigation on the correlation between experimental conditions and final structures can provide a promising pathway to reasonable design; however, even so, it is difficult to control all the governing principles in the system and predict with reasonable certainty the resulting molecular architecture. The construction of coordination networks significantly depends on various factors, such as the metal center and the counteranion in the starting metal salt, the ligands (shape, functionality, flexibility, and symmetry), and the experimental approach (synthetic route, reactants ratio, temperature, reaction time, pH value, and solvent) [196,222].

For coordination networks based on 1,3-bdc, as we have previously discussed, the selection of metal ion is a critical consideration since the type of metal ion has a particular influence on the coordination configuration of the ligand, which, in turn, drastically interferes in the resulting final architecture. In general, the first-row *d*-block elements are a common choice for preparing coordination networks due to their availability and relatively predictable geometric parameters producing in most cases μ and μ$_3$-bridging coordination modes for 1,3-bdc, and preferably adopting monodentade modes instead of chelating ones (Fig. 8). Nevertheless, considerable attention has also been extended to second-row transition metal ions and the *f*-block elements. In coordination networks with these metal ions as nodes, 1,3-bdc adopts an assortment of coordination fashions especially the chelating modes and those that link many metal centers. For instance, Zhang *et al.* [31] related two coordination compounds utilizing 1,3-bdc, phen, and Cd^{II} (**236**) or Zn^{II} (**278**), prepared under the same hydrothermal conditions (160 °C for 120 h). The resulting CPs present the same compositional structures, [M^{II}(1,3-bdc)(phen)]$_n$ (M = Cd or Zn), but distinct coordination modes for 1,3-bdc: chelate-bidentate (**IV**) for Cd^{II} and monodentate-bidentate (**V**) for Zn^{II}. These distinct coordination environments may be attributed to the difference in the radius of the Cd^{II} and Zn^{II} ions [31]. As another example, a Pb^{II}-based CP with 1,3-bdc and phen, also prepared under hydrothermal conditions (160 °C for 48 h), [Pb(1,3-bdc)(phen)]$_n$ (**354**), exhibits the coordination mode **IX** for 1,3-bdc [223]. Furthermore, lanthanide-based CPs synthetized with the same building blocks and under hydrothermal conditions also display distinct coordination configurations for 1,3-bdc. The compounds {[Ln$_2^{III}$(1,3-bdc)$_3$(phen)](H$_2$O)}$_n$ (Ln = La, **322**; Pr, **323**; or Yb, **324**) (140 °C for 96 h) exhibit coordination modes **III** and **XII** [165], while [Yb$_2^{III}$(1,3-bdc)$_3$(phen)$_{0.5}$]$_n$ (**321**) (150 °C for 120 h) presents the coordination modes **III** and **X** [63].

Lanthanide ions often exhibit higher coordination numbers and flexible coordination geometry; therefore, remaining binding sites are frequently occupied by solvent molecules like water and DMF. Based on that, one can assume that is hard to construct Ln-based compounds with higher dimensionalities [11]. Even so, lanthanides are commonly used in coordination networks particularly on

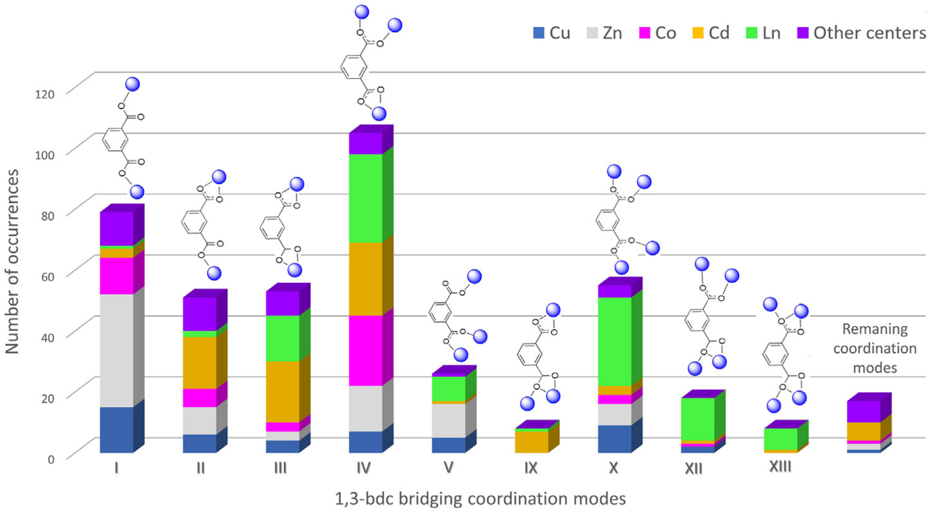

Fig. 8. The most frequent 1,3-bdc bridging coordination modes and the most common metal centers for each fashion.

account of their trend to form multinuclear structures with potential photoluminescent applications [224].

The starting metal salt can also impact on the resulting coordination network. To illustrate the effect of the counteranion from the starting metal salt, Su *et al.* [97] reported two distinct Zn^{II}-based coordination networks obtained under the same reaction conditions except that the starting metal salts are different: $ZnCl_2$ (**48**) and $Zn(NO_3)_2·6H_2O$ (**49**). The first CP, **48**, exhibits a neutral 2D rectangular grid network in which 1,3-bdc adopts the bis-monodentate mode (**I**); whereas **49** displays a 3D framework where 1,3-bdc adopts bis-monodentate (**I**) and chelate-monodentate (**II**) coordination modes. Interestingly, neither Cl^- nor NO_3^- appear in the CPs frameworks.

For coordination networks employing 1,3-bdc, the auxiliary ligand also makes a significant contribution to the final architecture and their change can strongly impact the packings of the CPs [179]. As such, added to the relevance of the metal ion choice, the judicious selection of the ligands is the foundation to build a wide variety of coordination networks. The multidentate *N*-donor organic building blocks have been the most employed molecules as auxiliary ligands since they facilitate the formation of single crystals [13,14]. Terminal *N*-donor ligands reduce the available metal ion binding sites and restrict the polymer growth in other directions, generating structures with lower dimensionalities [33]. In contrast, *exo*-bidentate ligands, for example, can cause a distinct spatial effect, thus resulting in unpredicted entangled architectures. As an illustration, Ma *et al.* [225] reported that replacing the pyridine with 4,4′-bipyridine in a CP containing Mn^{II} and 1,3-bdc results in structures from 1D double-chain to 2D double-layer architecture. Moreover, compared to rigid ligands, the flexible ones can assume many types of conformations that offer a possible way to achieve more robust polymeric structures [226].

The selection of the synthetic route and experimental parameters directly affect the structure of the resulting coordination network. As presented in Fig. 9, the most common synthetic strategies used to prepare 1,3-bdc-based networks are hydro- and solvothermal syntheses, as well as conventional methods (including slow diffusion of solutions or syntheses carried out at room temperature, under heating, or reflux conditions followed by slow evaporation of solvent). Syntheses employing microwave-assisted heating or sonochemical methods were rarely reported for these networks (Fig. 9). The hydro- and solvothermal techiniques are the most employed presumably because these methods frequently allow for growing single crystals suitable for X-ray diffraction experiment [222]. In addition, these configurations seem to allow a better control of the crystal growth of coordination networks, paving the way toward their reproducibility and scalability, what is generally more difficult to achieve by other synthetic routes. Moreover, another advantage over other typical synthetic approaches is that even insoluble reagents can be used under the hydro- and solvothermal conditions.

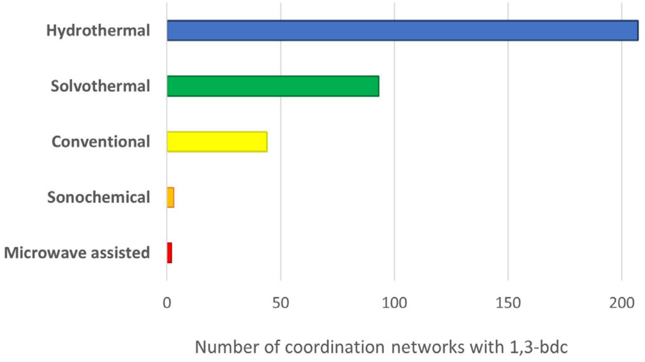

Fig. 9. The most common synthetic methods for preparing coordination networks based on 1,3-bdc.

Some aspects can help explain the reason why the hydrothermal method is vastly employed when compared to the solvothermal one. Besides being environmentally friendly, under hydrothermal conditions water has its viscosity reduced, contributing to a rapid diffusivity of reactants and playing an important role while participating in the assembly of supramolecular interactions by establishing hydrogen bonds, for instance.

Due to the coordinating flexibility of 1,3-bdc, the obtained structure is considerably sensitive to the solvent, temperature, reaction time, and heating/cooling rates. The solvent system also affects the resulting composition and structure; even a subtle difference in the solvent ratio can have a profound effect on the structural variation. Zhao *et al.* [124] reported two distinct Cu^{II} CPs (**133** and **184**) which were prepared with the same composition and experimental conditions but distinct solvent ratios ($H_2O:CH_3CN$ 2:3 and 1:1 for **133** and **184**, respectively). The coordination modes of 1,3-bdc are distinct for these CPs: **133** presents μ-bridging mode (**III**), whereas **184** exhibits μ_3-bridging mode (**IV**). Likewise, the temperature is another critical controlling factor which affects the resultant dimensionality of coordination complexes. Xu *et al.* [163] reported two Cd^{II} CPs prepared under the same hydrothermal conditions except for the temperature, 160 °C for **75** and 130 °C for **159**. The former present a 3D framework with 1,3-bdc adopting the μ-bis-monodentate coordination mode (**I**), while the latter displays a 2D grid-layer with 1,3-bdc in its bis-chelating mode (**III**). These results reveal that the temperature is yet another parameter that plays a significant role on the coordination modes of the ligands, with greater temperature favoring products with.

Concerning other experimental parameters which affect the final structures, it is noteworthy to mention the role of reagent ratios. Wang *et al.* [25] demonstrated that the alteration of the metal–ligand ratio in the initial reaction system yielded dysprosium(III) structures with different dimensionalities: a 3D network (**255**) and a 2D structure (**256**), in which the metal–ligand ratios were 1:1 and 1:3, respectively. These observations point out that the increase on metal content seems to provide structures with higher dimensionalities [25]. The metal–ligand ratio also impacts the bond between the carboxylate oxygen atoms and the metal ions; as such, **255** presents two distinct coordination modes for 1,3-bdc (**IV** and **X**), while **256** adopts three different fashions (**IV**, **X** and **XII**) [25].

Considering the variability of parameters that impact final architectures, the construction of coordination networks with the same reagents but different synthetic routes can be an interesting strategy to provide insights on the rational design of an aimed coordination network. With this in mind, we chose a system comprised of reagents vastly explored in the field of *Coordination Chemistry*, Cu^{II} and phen [227–229], beyond 1,3-bdc, for our study. Aiming at investigating this system further, we have prepared two novel compounds (**1** and **2**) applying different synthetic routes from the compounds previously related in the literature with the same combination of reactants (**3** and **4**) [17,18] (see Fig. 10). The detailed syntheses procedures of **1** and **2** are described in the SI.

Compound **1** consists of the neutral $[Cu(1,3\text{-bdc})(phen)(H_2O)_2]$ complex cocrystallized with the cationic $[Cu(1,3\text{-Hbdc})(phen)(H_2O)_2]^+$ as a perchlorate salt, due to presence of partially protonated 1,3-Hbdc (Fig. 11A). Both Cu^{II} centers are pentacoordinate, chelated by one phen molecule and one 1,3-bdc ligand in a terminal monodentate mode, besides two water molecules. The geometry of the Cu^{II} centers are mostly close to square pyramid on the analysis of the τ parameter [230], being equal to 0.10 for Cu1 and 0.09 for Cu2. Compound **2** (Fig. 11B) is a neutral 1D CP built

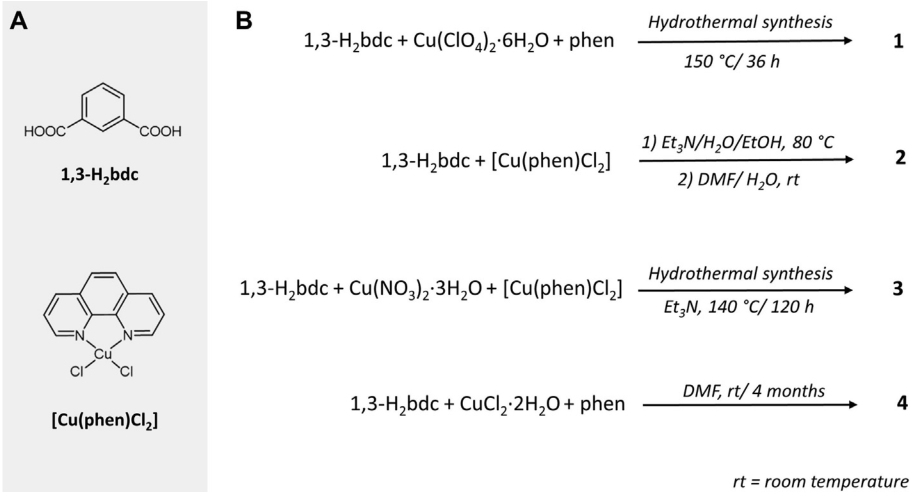

Fig. 10. (A) Structures of the building blocks 1,3-bdc and [Cu(phen)Cl$_2$] and (B) schematic representation of reactional conditions for the syntheses of **1** and **2**, and the CPs previously reported **3** and **4** [17,18].

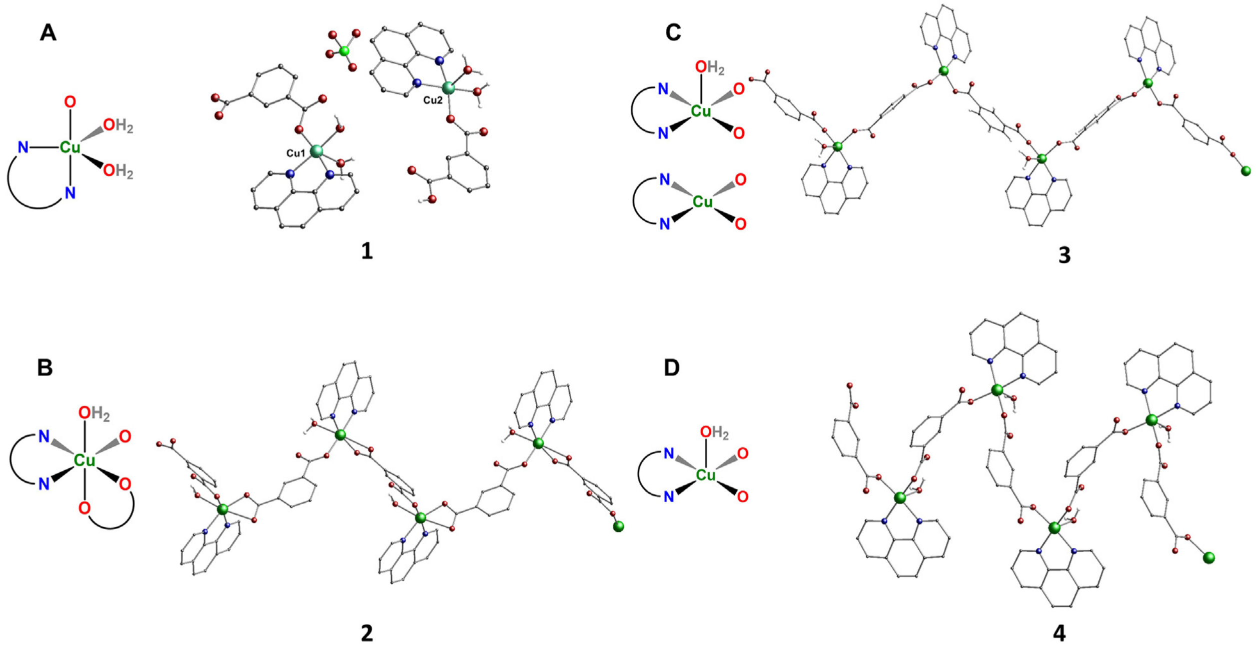

Fig. 11. Coordination spheres around the Cu^{II} in (A) **1**, (B) **2**, (C) **3**, and (D) **4**, featuring the asymmetric unit of **1** with the neutral and cationic complexes cocrystallized and zigzag 1D CP for **2**–**4**.

up by a Cu^{II} center coordinated by phen, one water molecule, and 1,3-bdc bridging the Cu^{II} ions; one DMF crystallization molecule per Cu^{II} center fills the voids in the structure. The Cu^{II} centers are in hexacoordinated environments, in which three oxygen atoms belong to two different 1,3-bdc ligands (see Fig. S3). The 1,3-bdc ligand in this structure exhibits the coordination mode μ-κO:κ^{2}O”,O”’ (**II**). The structure can be described as a zigzag CP with a bending angle of 106.47(1)° with the Cu^{II} centers in **2** being 10.0011(7) Å far from each other. See the SI for a detailed description of the structures of **1** and **2**.

Concerning the previously reported compounds, the first example, **3** [18] (Fig. 11C), has no solvates and the CP intercalates square pyramid and square planar geometries for the Cu^{II} ions. The coordination spheres are filled with a phen, a water molecule and two monodentate carboxylate groups for the square pyramid metal atom, one phen, and two monodentate carboxylate groups for the square planar metal center. Although there are two different copper atoms in **3**, all 1,3-bdc ligands adopt a μ-κO:κO” coordination mode (**I**). The second example, **4** [17] (Fig. 11D), is a DMF and water solvated CP, with Cu^{II} ions in square pyramid geometry, coordinated to one phen, one water molecule and two monodentate carboxylate groups. For **4**, we also found the μ-κO:κO” coordination mode (**I**) for the 1,3-bdc ligand. In **3** and **4** a coordinated water molecule is found filling the apical positions of the square pyramids.

Regarding the geometries and packings of the CPs **2**–**4**, on the one hand, we observed that **2** and **3** have a similar bending angle to that of the zigzag polymer (102.4° and 106.47° for **2** and **3**, respectively), and **4** has a considerably smaller bending angle (64.2°), causing a compression of **4** along the axis on which the polymer extends (Fig. 11). On the other hand, **2** and **4** present crystallization solvent molecules (one DMF for **2** and one DMF and one water for **4**), while **3** is not a solvate.

Compounds **1** and **3** were prepared using hydrothermal method but subjected to different experimental conditions (e.g., metal source, pH, temperature, and reaction time), which rendered completely distinct structures. Compound **1** was produced under milder conditions compared to **3**, with shorter reaction time and without any pH adjustment, which favored the presence of the monodeprotonated species, 1,3-Hbdc. Hydrothermal synthesis performed only for 36 h, as used for yielding **1**, is unusual for obtaining CPs as can be observed in Table 2, where most CPs were prepared in reaction times higher than 72 h. Therefore, reaction time can be one of the most relevant factors that influenced the formation of a discrete complex instead of the expected CP.

Comparing the CPs **2**–**4**, almost the same structure was obtained from the three distinct synthetic approaches. CPs **2** and **4** were obtained by conventional methods with a great difference in time (7 days and 4 months, respectively). While **2** was prepared by recrystallizing the previously obtained (H_2O/EtOH, 80 °C) solid in DMF, crystals of **4** were yielded after slow diffusion of the starting materials in DMF. CP **2** may refer to a kinetic product, whereas **4** can be the result of a thermodynamically favored self-assembly; therefore, the preliminary stage of heating the reagents could be a key factor in achieving the desired product quickly. Furthermore, although the conventional synthetic approach for obtaining CPs is currently less employed than hydro/solvothermal techniques, it remains an interesting option to synthesize CPs since it does not require long reaction times and high energy consumption.

5. Probing coordination M–O bonds of 1,3-bdc using Fourier-transform infrared spectroscopy (FTIR)

The coordination modes of carboxylate anions, and therefore 1,3-bdc, in a complex can be inferred by analyzing the absorption bands in the infrared spectrum related to the asymmetric and symmetric stretching of COO^- groups. This highlights the relevance of this powerful technique to probe the configuration of the carboxylate around a metal ion within a metal complex. The difference between $\nu_{as}(COO^-)$ and $\nu_s(COO^-)$, $\Delta\nu$ (cm^{-1}), in a coordination compound (compared to the corresponding values for the sodium or potassium salts of the fully deprotonated ligand) can be employed to determine the coordination mode of the carboxylate group around the metal center [231–233]. Therefore, this tool is relevant to support the characterization of amorphous or polycrystalline materials whose single crystal growth is not feasible. Additionally, once the coordination modes were unambiguously proved by X-ray diffraction experiments, this tool helps to cooroborate the presence of the same modes in the bulk sample. Moreover, this complementary characterization is helpful to easily monitor the purity of samples since it distinguishes between monodentate (κO), chelating (κ^2O,O'), bridging bidentate (κO:O'), and monoatomic bridging (κO:κO) coordination modes [234].

For all carboxylate groups, the energies of the stretching modes are dependent on the covalent contribution of the bond established between the metal ion and carboxylate oxygen atoms. Especially for monodentate interactions, in which M–$O_{carboxylate}$ distances are usually well defined [235,236], the covalency is higher than for bidentate carboxylate modes. Indeed, a wide range of M–$O_{carboxylate}$ distances can be observed for bidentate carboxylate due to different possibilities of coordination modes. Thus, a high Δν value would be expected for the monodentate mode [pseudo-ester configuration (R–COO–M)] for which there is no equivalence of the two oxygen atoms of the carboxylate. This non-equivalence of the two oxygen atoms of the carboxylate in the monodentate mode causes an increase in the asymmetric stretching $\nu_{as}(COO^-)$ and a decrease in the symmetric stretching $\nu_{as}(COO^-)$, which raise the separation (Δν) between the $\nu(COO^-)$ frequencies relative to values for the free carboxylate ion [237]. On the contrary, medium and low Δν values are anticipated for the bridging bidentate and chelate interactions, respectively [234], and the lower Δν values for chelating modes are presumably a result of the formation of an extra M–$O_{carboxylate}$ bond formed, which is less energetically favorable causing a weakening of the M–O bonds and, as a consequence, the elongation of the M–O bond [238,239].

In this respect, it is expected that the M–$O_{carboxylate}$ bond from a bidentate carboxylate will be slightly longer/weaker than that observed for a monodentate carboxylate [239]. For the monodentate mode, there is no equivalence of the two oxygen atoms of the carboxylate. Therefore, the C—O bonds are differently affected by the coordination to the metal center, causing an increase in the Δν value in comparison to the carboxylate ion in the sodium/potassium salt of the ligand [201]. For the chelate and bidentate bridging modes, there are no differences in the bond orders and, consequently, the separations are similar to the values found for the sodium salt [201]. Concerning the monoatomic bridging, a weaker bond is usually observed since the electronic density in the single oxygen atom is shared with two different metal centers, causing the greater Δν among the coordination modes presented in this section [232,240]. Finally, we summarize the correlation of Δν values to the coordination modes through the order shown in Fig. 12.

To corroborate the aforementioned observations, we analyzed the Cu–$O_{carboxylate}$ distances present in different Cu^{II} coordination compounds based on 1,3-bdc. Table S6 presents the Cu–$O_{carboxylate}$ distances of selected Cu^{II} complexes containing 1,3-bdc reported over the last 20 years. We limited the analysis to Cu^{II}-based compounds aiming at facilitating the analysis by avoiding the discrepancy in the bonding forces, which strongly depend on other factors including oxidation state, coordination number, axiality, and non-covalent interactions. Table S6 shows that in the monodentate coordination mode the Cu–$O_{carboxylate}$ distance is in the range 1.916–2.284 Å (Cu–$O_{average}$ = 1.972 Å) with an average bond distance shorter than those observed for bidentate chelating (Cu–$O_{average}$ = 2.236 Å) and bidentate bridging (Cu–$O_{average}$ = 2.007 Å) modes, which may be an indication that the monodentate coordination mode is the most stable for Cu^{II} complexes. This difference

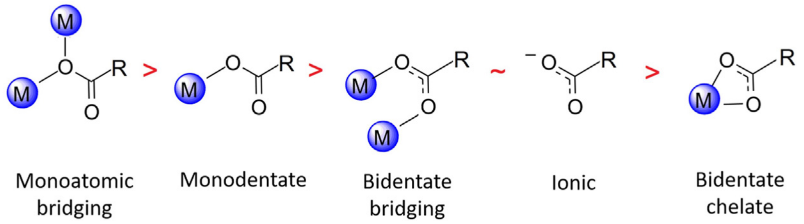

Fig. 12. Decreasing order of Δν values [$\Delta\nu = \nu_{as}(COO^-) - \nu_s(COO^-)$] for some coordination modes of the carboxylate group.

can be more evident in the cases where Cu–O bond is elongated in the axial position due to the Jahn-Teller effect arising from its $3d^9$ electron configuration [49,241]. The compression along the z axis for Cu^{II} complexes, although equally favorable in terms of energy, is much less reported [242]. As an example, for the polymer **2** described herein, a tetragonal distortion in the octahedral geometry was observed. In this case, the 1,3-bdc adopts the bidentate mode, showing the Jahn–Teller elongated distortion with the Cu–O_{axial} being 2.563(3) Å while the Cu–$O_{equatorial}$ distance is 1.997 (2) Å.

Focusing on FTIR analysis of the 1,3-bdc-based compounds, one can use the sodium 1,3-benzenedicarboxylate salt [Na_2(1,3-bdc)] as a reference, with the $\nu_{as}(COO^-)$ centered at 1567 cm^{-1} and $\nu_s(COO^-)$ at 1383 cm^{-1} ($\Delta\nu$ of 184 cm^{-1}). As an application of the considerations in this section – FTIR spectroscopy concerning the carboxylate group as the coordinating site – we carefully analyzed the spectra of the two novel compounds described in this study (**1** and **2**). The FTIR spectra of 1,3-bdc, Na_2(1,3-bdc), **1**, and **2** are shown in Fig. S5.

In the FTIR spectrum of **1**, an absorption band centered at 1662 cm^{-1} was observed indicating that one of the carboxylate groups is protonated [221]. It also showed one $\nu_{as}(COO^-)$ stretching mode at 1568 cm^{-1} and two $\nu_s(COO^-)$ stretching modes centered at 1370 and 1387 cm^{-1}. The resulting $\Delta\nu$ values of 198 and 181 cm^{-1} point out the presence of two different coordination modes of the carboxylate groups around the Cu^{II} centers in **1**: the $\Delta\nu$ = 198 cm^{-1} suggests a monodentate coordination mode, while $\Delta\nu$ = 181 cm^{-1} indicates a deprotonated carboxylate group. This result corroborates the crystallography data, that shows carboxylate groups adopting monodentate (R–COO–M), noncoordinated ionic ($RCOO^-$), and protonated (R–COOH) fashions. In summary, there are two types of 1,3-bdc ligands in the structure, one acting as monodentate/noncoordinated ionic and the other as monodentate/protonated.

The FTIR spectrum of **2** showed a band centered at 1554 cm^{-1} assigned to the asymmetric stretching vibration $\nu_{as}(COO^-)$ and bands centered at 1360 and 1382 cm^{-1} attributed to the symmetric stretching vibration modes $\nu_s(COO^-)$. The two distinct $\nu_s(COO^-)$ values resulted in two different $\Delta\nu$ values: 194 and 172 cm^{-1}. These values, when compared to the corresponding value for the salt Na_2(1,3-bdc) ($\Delta\nu$ = 184 cm^{-1}), are in a good agreement with the monodentate and bidentate coordination modes of the carboxylate groups, respectively. The coordination modes (monodentate and bidentate) of the 1,3-bdc carboxylate in **2** were also observed for complexes reported previously (see Table 2).

Regarding the other absorption bands observed in both spectra of **1** and **2**, we can highlight the $\nu(C{=}C/C{=}N)$ modes of phen; bands centered at 1611, 1512, 1502, 1485, 1425 (**1**) and 1603, 1519, 1491, and 1421 cm^{-1} (**2**) are in agreement with the coordination to Cu^{II} centers as chelate bidentate *via* the pyridyl-nitrogen atoms [243]. In **1**, the intense absorptions in the range 1088–1000 cm^{-1} with a strong band centered at 1058 cm^{-1} corroborates the presence of perchlorate anions [244]. In **2**, the band at 1674 cm^{-1} in the spectrum is assigned to the presence of DMF molecules [245]. Finally, broad absorption bands centered at 3334, 3231 cm^{-1} (**1**) and at 3299 cm^{-1} (**2**) are attributed to the presence of water molecules involved in hydrogen bonds.

6. Conclusion and outlook

Exploring benzenedicarboxylates as platforms in *Coordination Chemistry*, *Supramolecular Chemistry*, and *Materials Chemistry* is an incredibly effervescent approach to isolate fascinating molecular materials. Compounds based on this family of linkers have been proposed and synthesized at an impressive rate over the last two decades. It is related to the fact that self-assembled tailored materials, including CPs, have vast potential to be applied in different fields, rendering benzenedicarboxylates excellent building blocks for creating robust molecular-based materials. More interesting, the richness of chemical structures is governed by the diverse coordination modes adopted by the carboxylates when connecting metal-ions within metal–organic structures.

Understanding the nature and features of the metal-carboxylate bonds, the coordination modes present as well as the structural-spectroscopic correlation are keys for opening the doors for the design of new functional materials based on benzenedicarboxylates. In this study, we focused on exploring in detail several metal–organic crystal structures based on 1,3-benzenedicarboxylate, looking closely at the behavior of this ligand when coordinated to different transition metals and lanthanides. We succeeded in extracting and compiling useful information and behavioral tendencies that will pave the way for advancements in the field. For example, we were able to track the most employed synthetic methodologies to grow single crystals of the "desired" materials. The "quotes" signalize the unpredicted structures isolated in the playground and show that sometimes the rational approach fails, which is intriguing but at the same time motivating since it highlights the untapped potential of this research field.

Pursuing single crystals is, in many cases, a reflection of a stay in the "comfort zone", though. This study brought to light that in the past two decades at least, FTIR spectroscopic data for 1,3-bdc-based compounds are extremely underexplored. Definitely, it is not due to the lack of knowledge since advancements in the FTIR spectroscopic analysis of carboxylates have been reported since the early 1980s [237]. The structural analysis is commonly based solely on terms of single crystal structures, which is often treated by peers as a mandatory tool for proceeding with other characterizations and further applications of the isolated materials.

As a result, we detected the lack in exploring modern synthetic approaches including mechanosynthesis or Liquid-Assisted Resonant Acoustic Mixing (LA-RAM), for example, which are environmentally friendly approaches shedding lights for scale production of polycrystalline and amorphous metal–organic systems [246,247]. This technique is vastly faced as an alternative route for the preparation of "known" materials only, although it can also render new crystalline phases. Moreover, a better exploration of the spectroscopy data could build a cheap and reachable platform for characterizing mechanosynthesized solids and those countless materials which have failed in all attempts to crystallize using varied methods. This "limitation" seems to be preventing the field of solid-state metal–organic materials to evolve. In fact, these polycrystalline and amorphous materials represent the large extent of the "iceberg", while the reported crystal structures are only its "tip".

Although tackling the issue of characterizing coordination modes of benzenedicarboxylates within metal–organic structures using FTIR spectroscopy sounds like an alluring possibility, we recognize there is one major obstacle. Probing carboxylate groups in polycrystalline and amorphous materials is an exceedingly hard task due to their versatility and unexpected behavior in several cases. In this sense, the structural-spectroscopic correlation is extremely welcome to support the creation of libraries to provide researchers in the field with a stronger database.

Other point to highlight from this systematic study is that there is a lack of standardization in data interpretation and structure description, which made difficult a more accurate analysis of the data compiled.

Finally, we believe that the development of metal–organic structures especially using 1,3-bdc is a promising field of research, with many corners still unexplored. The combination of multiple functionalities in its derivatives will undoubtedly expand the richness of these structures and open new avenues in the field. We are optimistic that the data compiled in this systematic study will pave the way for the development and implementation of the next generation of benzenedicarboxylates-based metal–organic structures as well as support a more accurate description of the FTIR spectroscopy data in the future publications in this field.

Crystallographic data for the structures reported in this paper have been deposited with the Cambridge Crystallographic Data Centre as supplementary publication CCDC numbers 2035305 (**1**) and 2035306 (**2**). Copies of the data can be obtained free of charge from www.ccdc.cam.ac.uk/conts/retrieving.html.

CRediT authorship contribution statement

Isabelle K.V. Gonçalves: Investigation, Methodology, Formal analysis, Data curation. **Willian X.C. Oliveira:** Methodology, Formal analysis, Data curation, Writing - original draft. **Filipe B. de Almeida:** Methodology, Formal analysis, Data curation. **Maria Vanda Marinho:** Formal analysis, Data curation, Writing - original draft. **Walace D. do Pim:** Conceptualization, Data curation, Supervision, Project administration, Writing - original draft, Writing - review & editing. **Priscila P. Silva-Caldeira:** Conceptualization, Data curation, Supervision, Project administration, Writing - original draft, Writing - review & editing.

Declaration of Competing Interest

The authors declare that they have no known competing financial interests or personal relationships that could have appeared to influence the work reported in this paper.

Acknowledgements

We acknowledge the Brazilian agencies: Fundação de Amparo à Pesquisa do Estado de Minas Gerais (FAPEMIG), Conselho Nacional de Desenvolviemento Científico e Tecnológico (CNPq), and Coordenação de Aperfeiçoamento de Pessoal de Nível Superior (CAPES) as well as Rede Mineira de Química (RQ-MG) and Centro Federal de Educação Tecnoló W.D.d.P. thanks CNPq (204774/2018-7) for a granted PDF scholarship.

Appendix A. Supplementary data

Supplementary data to this article can be found online at https://doi.org/10.1016/j.poly.2021.115068.

References

[1] T. Bala, B.L.V. Prasad, M. Sastry, M.U. Kahaly, U.V. Waghmare, Interaction of different metal ions with carboxylic acid group: a quantitative study, J. Phys. Chem. A 111 (2007) 6183–6190, https://doi.org/10.1021/jp067906x.
[2] P.-C. Cheng, P.-T. Kuo, Y.-H. Liao, M.-Y. Xie, W. Hsu, J.-D. Chen, Ligand-isomerism controlled structural diversity of Zn(II) and Cd(II) coordination polymers from mixed dipyridyladipoamide and benzenedicarboxylate ligands, Cryst. Growth Des. 13 (2) (2013) 623–632, https://doi.org/10.1021/cg301311m.
[3] I. Hisaki, Hydrogen-bonded porous frameworks constructed by rigid π-conjugated molecules with carboxy groups, J. Inclusion Phenom. Macrocyclic Chem. 96 (3-4) (2020) 215–231, https://doi.org/10.1007/s10847-019-00972-0.
[4] C. Chen, K. Zhang, Y. Sun, S. Xiang, Y. Geng, K. Liu, L. Wang, Supramolecular structural motifs in compounds of acetoguanamine and various carboxylic acids: N-H$\cdots$O heterosynthons and N-H$\cdots$N homosynthons, J. Mol. Struct. 1170 (2018) 60–69, https://doi.org/10.1016/j.molstruc.2018.05.079.
[5] O. Ivasenko, D.F. Perepichka, Mastering fundamentals of supramolecular design with carboxylic acids. Common lessons from X-ray crystallography and scanning tunneling microscopy, Chem. Soc. Rev. 40 (1) (2011) 191–206, https://doi.org/10.1039/C0CS00022A.
[6] C. Liu, J. Wang, J. Wan, Y. Cheng, R. Huang, C. Zhang, W. Hu, G. Wei, C. Yu, Amorphous metal-organic framework-dominated nanocomposites with both compositional and structural heterogeneity for oxygen evolution, Angew. Chemie – Int. Ed. 59 (9) (2020) 3630–3637, https://doi.org/10.1002/anie.201914587.
[7] C. Orellana-Tavra, E.F. Baxter, T. Tian, T.D. Bennett, N.K.H. Slater, A.K. Cheetham, D. Fairen-Jimenez, Amorphous metal-organic frameworks for drug delivery, Chem. Commun. 51 (73) (2015) 13878–13881, https://doi.org/10.1039/c5cc05237h.
[8] T.D. Bennett, A.K. Cheetham, Amorphous metal-organic frameworks, Acc. Chem. Res. 47 (5) (2014) 1555–1562, https://doi.org/10.1021/ar5000314.
[9] H. Li, M. Eddaoudi, M. O'Keeffe, O.M. Yaghi, Design and synthesis of an exceptionally stable and highly porous metal-organic framework, Nature 402 (6759) (1999) 276–279, https://doi.org/10.1038/46248.
[10] M. Vougo-Zanda, X. Wang, A.J. Jacobson, Influence of ligand geometry on the formation of In—O Chains in metal-oxide organic frameworks (MOOFs), Inorg. Chem. 46 (21) (2007) 8819–8824, https://doi.org/10.1021/ic701126t.
[11] G. Wang, T. Song, Y. Fan, J. Xu, M. Wang, L. Wang, L. Zhang, L.i. Wang, A porous lanthanide metal–organic framework with luminescent property, nitrogen gas adsorption and high thermal stability, Inorg. Chem. Commun. 13 (1) (2010) 95–97, https://doi.org/10.1016/j.inoche.2009.10.026.
[12] D. Feng, K. Wang, Z. Wei, Y.-P. Chen, C.M. Simon, R.K. Arvapally, R.L. Martin, M. Bosch, T.-F. Liu, S. Fordham, D. Yuan, M.A. Omary, M. Haranczyk, B. Smit, H.-C. Zhou, Kinetically tuned dimensional augmentation as a versatile synthetic route towards robust metal–organic frameworks, Nat. Commun. 5 (2014) 5723, https://doi.org/10.1038/ncomms6723.
[13] L. Liu, J. Ding, M. Li, X. Lv, J. Wu, H. Hou, Y. Fan, Structural variability, topological analysis and photocatalytic properties of neoteric Cd(ii) coordination polymers based on semirigid bis(thiazolylbenzimidazole) and different types of carboxylic acid linkers, Dalton Trans. 43 (2014) 12790–12799, https://doi.org/10.1039/c4dt01080a.
[14] X.-Z. Song, S.-Y. Song, C. Qin, S.-Q. Su, S.-N. Zhao, M. Zhu, Z.-M. Hao, H.-J. Zhang, Syntheses, structures, and photoluminescent properties of coordination polymers based on 1,4-bis(imidazol-l-yl-methyl)benzene and various aromatic dicarboxylic acids, Cryst. Growth Des. 12 (1) (2012) 253–263, https://doi.org/10.1021/cg201025u.
[15] J. Zhou, T. Yan, Y.-F. Qiao, Y.-D. Zhao, X. Wang, L. Du, M.-J. Xie, J. Xu, Q.-H. Zhao, Three unique MOFs constructed by 1,4-bis(4-pyridyl)-2,3-diaza-1,3-butadiene and dicarboxylates: from rhombic tetrameric zinc(II) 2D layer to 2D+2D→3D polycatenated frameworks, Inorg. Chem. Commun. 73 (2016) 161–165, https://doi.org/10.1016/j.inoche.2016.10.021.
[16] A.U. Czaja, N. Trukhan, U. Müller, Industrial applications of metal–organic frameworks, Chem. Soc. Rev. 38 (5) (2009) 1284, https://doi.org/10.1039/b804680h.
[17] H.-P. Xiao, X.-H. Li, M.-L. Hu, catena-Poly[[[aqua(1,10-phenanthroline)copper (II)]-μ-isophthalato] N, N-dimethylformamide solvate monohydrate], Acta Crystallogr. Sect. E Struct. Rep. Online 60 (4) (2004) m468–m470, https://doi.org/10.1107/S1600536804006592.
[18] X.M. Chen, G.F. Liu, Double-stranded helices and molecular zippers assembled from single-stranded coordination polymers directed by supramolecular interactions, Chem. - Eur. J. 8 (2002) 4811–4817, https://doi.org/10.1002/1521-3765(20021018)8:20<4811::AID-CHEM4811>3.0.CO;2-R.
[19] X. Zhu, Q. Chen, Z. Yang, B.-L. Li, H. Li, Tuning zinc(II) coordination polymers based on bis(1,2,4-triazol-1-yl)ethane and 5-substituted 1,3-benzenedicarboxylates: syntheses, structures and properties, CrystEngComm 15 (2013) 471–481, https://doi.org/10.1039/C2CE26515J.
[20] J.J. Perry, G.J. McManus, M.J. Zaworotko, Sextuplet phenyl embrace in a metal-organic Kagomé lattice, Chem. Commun. (22) (2004) 2534–2535, https://doi.org/10.1039/b408973a.
[21] H.-J. Cheng, H.-X. Li, Z.-G. Ren, C.-N. Lü, J. Shi, J.-P. Lang, Substituted groups-directed assembly of Cd(II) coordination polymers based on 5-R-1,3-benzenedicarboxylate and 4,4'-bis(1-imidazolyl)bibenzene: syntheses, structures and photoluminescent properties, CrystEngComm 14 (18) (2012) 6064, https://doi.org/10.1039/c2ce25677k.
[22] Y. Ge, N.Y. Li, X.Y. Ji, J.F. Wang, D. Liu, X.Y. Tang, Assembly of a series of zinc coordination polymers based on 1,4-bis[2-(4-pyridyl)ethenyl]-2,3,5,6-tetramethylbenzene and 1,3-benzenedicarboxylate derivatives, CrystEngComm 16 (2014) 6621–6629, https://doi.org/10.1039/c4ce00696h.
[23] Y. Liu, H. Zhang, C. Tian, P. Lin, S. Du, Interweaving of two enantiomorphic 3D Cd(II)/K(I) coordination polymers with homochiral unequal triple concentric helical chains, CrystEngComm 15 (26) (2013) 5201, https://doi.org/10.1039/c3ce40397a.
[24] X. Wang, J. Luan, H. Lin, C. Xu, G. Liu, J. Zhang, A. Tian, The design and construction of a series of metal–organic coordination polymers based on two isomeric semi-rigid bis-pyridyl-bis-amide ligands and three aromatic polycarboxylates, CrystEngComm 15 (46) (2013) 9995, https://doi.org/10.1039/c3ce41498a.
[25] P. Wang, R. Fan, Y. Yang, X. Liu, W. Cao, B. Yang, Synthesis, crystal structures and properties of lanthanide-organic frameworks based benzene carboxylates with two/three-dimensional structure, J. Solid State Chem. 196 (2012) 441–450, https://doi.org/10.1016/j.jssc.2012.07.018.
[26] G. Wang, T. Song, Y. Fan, J. Xu, M. Wang, H. Zhang, L. Wang, L. Huang, L. Wang, Y2(H2O)(BDC)3(DMF)]·(DMF)3: a rare 2-D (42.6)(45.6)2(48.62)(49.65.8) net with multi-helical-array and opened windows, Inorg. Chem. Commun. 13 (2010) 502–505, https://doi.org/10.1016/j.inoche.2010.01.021.
[27] J. Xu, X. Sun, C. Ju, L. Yang, C. Bi, M.i. Sun, Hydrothermal synthesis, crystal structures, and photoluminescent properties of two cadmium(II) coordination polymers derived from dicarboxylates and N-donor ligands, J.

Coord. Chem. 66 (15) (2013) 2693–2701, https://doi.org/10.1080/00958972.2013.813493.

[28] J.G. Lin, Y.Y. Xu, L. Qiu, S.Q. Zang, C.S. Lu, C.Y. Duan, Y.Z. Li, S. Gao, Q.J. Meng, Ligand-to-metal ratio controlled assembly of nanoporous metal-organic frameworks, Chem. Commun. (2008) 2659–2661, https://doi.org/10.1039/b802992j.

[29] K.-T. Chen, J.-H. Hu, X.-K. Yang, J.-D. Chen, Impact of isomeric dicarboxylate ligands on the formation of one-dimensional coordination polymers and metallocycles: a novel cis→trans isomerization, Polymers 12 (2020) 1281, https://doi.org/10.3390/polym12061281.

[30] X.-N. Cheng, W. Xue, X.-M. Chen, Synthesis, structures, and magnetic properties of two Cobalt(II) isophthalate coordination polymers, Eur. J. Inorg. Chem. 2010 (2010) 3850–3855, https://doi.org/10.1002/ejic.201000146.

[31] L.-Y. Zhang, G.-F. Liu, S.-L. Zheng, B.-H. Ye, X.-M. Zhang, X.-M. Chen, Helical ribbons of cadmium(II) and zinc(II) dicarboxylates with bipyridyl-like chelates – syntheses, crystal structures and photoluminescence, Eur. J. Inorg. Chem. 2003 (16) (2003) 2965–2971, https://doi.org/10.1002/ejic.200300061.

[32] Y.u. Hou, E. Shen, S. Wang, E. Wang, D. Xiao, Y. Li, L. Xu, C. Hu, Hydrothermal synthesis and crystal structure of a metal-organic coordination polymer with double-helical structure: [Fe(phen)(ipt)]n (ipt = isophthalate, phen = 1,10-phenanthroline), Inorg. Chem. Commun. 6 (10) (2003) 1347–1349, https://doi.org/10.1016/j.inoche.2003.08.015.

[33] Y.-F. Zhou, F.-L. Jiang, Y. Xu, R. Cao, M.-C. Hong, Two-dimensional lanthanide-isophthalate coordination polymers containing right- and left-handed helical chains, J. Mol. Struct. 691 (1-3) (2004) 191–195, https://doi.org/10.1016/j.molstruc.2003.12.018.

[34] H.H. Li, Y.Q. Zhao, G.Y. Li, G.H. Cui, Crystal structure and fluorescence of a 2D cadmium(II) coordination polymer based on flexible bis(2-methylbenzimidazole) and benzenedicarboxylate co-ligands, J. Struct. Chem. 56 (8) (2015) 1577–1580, https://doi.org/10.1134/S0022476615080181.

[35] X.-L. Wan, L. Dong, J.-Z. Wang, H.-T. Shi, L.-B. Yang, Synthesis, structure and in vitro anti-gastric cancer activity of two new mixed-ligand Cu(II) and Cd(II)-coordination polymers, J. Inorg. Organomet. Polym. Mater. 29 (4) (2019) 1184–1191, https://doi.org/10.1007/s10904-019-01081-8.

[36] T. Nakano, Y. Okamoto, Synthetic helical polymers: conformation and function, Chem. Rev. 101 (2001) 4013–4038, https://doi.org/10.1021/cr0000978.

[37] X.-D. Zheng, T.-B. Lu, Constructions of helical coordination compounds, CrystEngComm 12 (2) (2010) 324–336, https://doi.org/10.1039/b911991d.

[38] D. Zhao, Y.u. Xiu, X.-L. Zhou, X.-R. Meng, Syntheses, structures, and fluorescent properties of two new d 10-metal coordination polymers containing 1-((benzotriazol-1-yl)methyl)-1-H-1,2,4-triazole ligand, J. Coord. Chem. 65 (1) (2012) 112–121, https://doi.org/10.1080/00958972.2011.642301.

[39] Z. Zhang, M. Pi, T. Wang, C.-M. Jin, Synthesis, structure and photoluminescence of two cadmium coordination polymers with 1,3-benzenedicarboxylate and two flexible bis-imidazole ligands, J. Mol. Struct. 992 (1-3) (2011) 111–116, https://doi.org/10.1016/j.molstruc.2011.02.056.

[40] X.-L. Wang, B. Mu, H.-Y. Lin, G.-C. Liu, Three new two-dimensional metal-organic coordination polymers derived from bis(pyridinecarboxamide)-1,4-benzene ligands and 1,3-benzenedicarboxylate: syntheses and electrochemical property, J. Organomet. Chem. 696 (11-12) (2011) 2313–2321, https://doi.org/10.1016/j.jorganchem.2010.12.009.

[41] H.-Y. Bai, J.-F. Ma, J. Yang, B.o. Liu, L.-P. Zhang, J.-C. Ma, Y.-Y. Liu, Syntheses, structures and properties of a series of ZnII Complexes Constructed from a Tetrakis(imidazole) Ligand and Various Anions, Eur. J. Inorg. Chem. 2010 (36) (2010) 5709–5717, https://doi.org/10.1002/ejic.201000766.

[42] Y.Y. Liu, J.F. Ma, J. Yang, J.C. Ma, G.J. Ping, Structures of metal-organic networks based on flexible 1,1′-(1,4-butanediyl)bis(imidazole-2-phenyl) ligand, CrystEngComm 10 (2008) 565–572, https://doi.org/10.1039/b714399k.

[43] X.L. Wang, Y.F. Bi, G.C. Liu, H.Y. Lin, T.L. Hu, X.H. Bu, Zn(ii) coordination architectures with mixed ligands of dipyrido[3,2-d : 2′22′2,3-f]quinoxaline/2,3-di-2-pyridylquinoxaline and benzenedicarboxylate: syntheses, crystal structures, and photoluminescence properties, CrystEngComm 10 (2008) 349–356, https://doi.org/10.1039/b706071h.

[44] M. Padmanabhan, K.C. Joseph, A. Thirumurugan, X. Huang, T.J. Emge, J. Li, One-dimensional zig-zag type coordination polymers of Ni(II) and Cu(II) containing 1,3-benzenedicarboxylate and 1,3-diaminopropane: structural, spectral and thermal studies, Inorg. Chim. Acta 360 (8) (2007) 2583–2588, https://doi.org/10.1016/j.ica.2006.12.048.

[45] J. Zhang, Y. Kang, J. Zhang, Z.-J. Li, Y.-Y. Qin, Y.-G. Yao, Syntheses, structures and characterisation of two CuII polymers with 8-connected topologies based on highly connected SBUs, Eur. J. Inorg. Chem. 2006 (11) (2006) 2253–2258, https://doi.org/10.1002/ejic.200500904.

[46] L.-C. Yu, Z.-F. Chen, H. Liang, C.-S. Zhou, Y. Li, A triple helical calcium-based coordination polymer with strong blue fluorescent emission, J. Mol. Struct. 750 (1-3) (2005) 35–38, https://doi.org/10.1016/j.molstruc.2005.04.017.

[47] P. Cheng, S.-P. Yan, C.-Z. Xie, B. Zhao, X.-Y. Chen, X.-W. Liu, C.-H. Li, D.-Z. Liao, Z.-H. Jiang, G.-L. Wang, Ferromagnetic and antiferromagnetic polymeric complexes with the macrocyclic ligand 1,4,7-triazacyclononane, Eur. J. Inorg. Chem. 2004 (11) (2004) 2369–2378, https://doi.org/10.1002/ejic.200300791.

[48] L.u. Gao, B. Zhao, G. Li, Z. Shi, S. Feng, Mixed solvothermal synthesis and X-ray characterization of a layered copper coordination polymer, Cu(H2O)(1,3-BDC)·H2O (BDC = benzenedicarboxylate), Inorg. Chem. Commun. 6 (9) (2003) 1249–1251, https://doi.org/10.1016/S1387-7003(03)00242-9.

[49] S. Pérez-Yáñez, G. Beobide, O. Castillo, J. Cepeda, A. Luque, P. Román, Structural Diversity in a Copper(II)/Isophthalato/9-Methyladenine System. From One- to Three-Dimensional Metal-Biomolecule Frameworks, Cryst. Growth Des. 13 (7) (2013) 3057–3067, https://doi.org/10.1021/cg400458a.

[50] M.H. Wang, J.G. Wu, G.Y. Luan, Catena-Poly[[(1,10-phenanthroline-2 N, N′)copper(II)]-5-hydroxy-isophthalato-2 O 1: O 3], Acta Crystallogr. Sect. E: Struct. Rep. Online 63 (2007) 1039–1041, https://doi.org/10.1107/S1600536807010999.

[51] X.X. Wang, Y.G. Liu, Y.H. Li, G.H. Cui, One- and two-dimensional cobalt(II) coordination polymers derived from flexible bis(benzimidazole) and aromatic carboxylate co-ligands, Transition Met. Chem. 39 (4) (2014) 461–467, https://doi.org/10.1007/s11243-014-9820-2.

[52] L.-L. Zhai, Y. Zhao, L. Luo, P. Wang, Q. Liu, K. Chen, W.-Y. Sun, Synthesis, structure and property of Ni(II) coordination polymers with mixed dicarboxylate and benzoimidazol-containing ligands, Microporous Mesoporous Mater. 187 (2014) 86–93, https://doi.org/10.1016/j.micromeso.2013.12.019.

[53] D.-X. Li, M. Chen, F. Li, Z. Ren, B. Wu, J. Lang, Substituent groups-driven construction of two different Cd(II) coordination polymers from CdSO4, tetrakis(4-pyridyl)cyclobutane and 5-R-1,3-benzenedicarboxylates, Inorg. Chem. Commun. 35 (2013) 302–306, https://doi.org/10.1016/j.inoche.2013.07.014.

[54] L. Liu, X. Li, C. Xu, G. Han, Y. Zhao, H. Hou, Y. Fan, Construction of six coordination networks based on a flexible bis(methylbenzimidazole) ligand and isomeric benzenedicarboxylates, Inorg. Chim. Acta 391 (2012) 66–74, https://doi.org/10.1016/j.ica.2012.04.043.

[55] G. Che, X. Wang, C. Liu, J. Chen, S. Wang, X. Li, Hydrothermal syntheses, structural characterization, and photoluminescent properties of five lanthanide coordination polymers, J. Coord. Chem. 65 (23) (2012) 4185–4193, https://doi.org/10.1080/00958972.2012.736970.

[56] H.-Y. Ju, G. Zhang, M. Yang, D.-Z. Liu, Y.-S. Yang, Y.-B. Zhang, Synthesis, Crystal Structures and Luminescence Properties of Three New Cadmium 3D Coordination Polymers, Molecules 25 (2020) 2465, https://doi.org/10.3390/molecules25112465.

[57] X.-J. Zheng, T.-T. Zheng, L.-P. Jin, Self-assembly of lanthanide mixed-carboxylates coordination polymers, J. Mol. Struct. 740 (1-3) (2005) 31–35, https://doi.org/10.1016/j.molstruc.2005.01.012.

[58] P. Zhang, D.-S. Li, J. Zhao, Y.-P. Wu, C. Li, K. Zou, J.Y. Lu, Four Zn(II)/Cd(II) coordination polymers derived from isomeric benzenedicarboxylates and 1,6-bis(triazol)hexane ligand: synthesis, crystal structure, and luminescent properties, J. Coord. Chem. 64 (13) (2011) 2329–2341, https://doi.org/10.1080/00958972.2011.597052.

[59] X. Gu, D. Xue, Selected Controlled Synthesis of Three-Dimensional 4d–4f Heterometallic Coordination Frameworks by Lanthanide Carboxylate Subunits and Silver Centers, Cryst. Growth Des. 6 (11) (2006) 2551–2557, https://doi.org/10.1021/cg060485o.

[60] J. Liu, J. Li, W. Lu, Chromism of three coordination polymers based on 1-(2-carboxyethyl)-4,4′-bipyridinium ligand, Dyes Pigm. 172 (2020) 107792, https://doi.org/10.1016/j.dyepig.2019.107792.

[61] X.-l. Wang, F.-F. Sui, H.-Y. Lin, J.-W. Zhang, G.-C. Liu, Multifunctional cobalt(II) coordination polymers tuned by flexible bis(pyridylamide) ligands with different spacers and polycarboxylates, Cryst. Growth Des. 14 (7) (2014) 3438–3452, https://doi.org/10.1021/cg500371n.

[62] D.-X. Xue, Y.-Y. Lin, X.-N. Cheng, X.-M. Chen, A Tetracarboxylate-Bridged Dicopper(II) Paddle-Wheel-Based 2-D Porous Coordination Polymer with Gas Sorption Properties, Cryst. Growth Des. 7 (7) (2007) 1332–1336.

[63] Q.-F. Yang, Y. Yu, T.-Y. Song, J.-H. Yu, X. Zhang, J.-Q. Xu, T.-G. Wang, 2D and 3D networks of lanthanide with mixed dicarboxylate ligands: syntheses, crystal structures and photoluminescent properties, CrystEngComm 11 (8) (2009) 1642, https://doi.org/10.1039/b900522f.

[64] Y.-Q. Gong, J.-T. Chen, D.-Q. Yuan, M.-Y. Wu, Y.-G. Huang, F.-L. Jiang, M.-C. Hong, Syntheses, crystal structures and photoluminescences of two (4,4) topological coordination networks derived from the flexible bipyridyl ligands, Inorg. Chim. Acta 360 (7) (2007) 2207–2214, https://doi.org/10.1016/j.ica.2006.10.044.

[65] H. Ju, I.-H. Park, E. Lee, S. Kim, J.H. Jung, M. Ikeda, Y. Habata, S.S. Lee, Guest-triggered assembly of zinc(II) supramolecular isomers with accompanying dimensional change and reversible single-crystal-to-single-crystal transformation, CrystEngComm 18 (2016) 1600–1608, https://doi.org/10.1039/C5CE02194D.

[66] X.-L. Wang, F.-F. Sui, H.-Y. Lin, J. Luan, G.-C. Liu, Aromatic Polycarboxylate-Tuned Assembly of Three New 2D Copper(II) Complexes Derived from a Flexible Bis(pyridylamide) Ligand, Aust. J. Chem. 66 (1) (2013) 67, https://doi.org/10.1071/CH12357.

[67] Q.-F. Jiang, Y.-T. Ao, Z.-F. Zhang, W. Yue, D.-N. Fu, Two mixed-ligand coordination polymers: structural insights and treatment effect on atherosclerosis by regulating the miRNA-9 mediated NF-κB signaling pathway, Inorg. Nano-Met. Chem. 50 (11) (2020) 1123–1129, https://doi.org/10.1080/24701556.2020.1735429.

[68] H.-Y. Liu, H. Wu, J.-F. Ma, Y.-Y. Liu, B.o. Liu, J. Yang, Syntheses, Structures, and Photoluminescence of Zinc(II) Coordination Polymers Based on Carboxylates

and Flexible Bis-[(pyridyl)-benzimidazole] Ligands, Cryst. Growth Des. 10 (11) (2010) 4795–4805, https://doi.org/10.1021/cg100688z.

[69] F. Krichen, S. Walha, J. Lhoste, F. Goutenoire, A. Kabadou, Design of lanthanide metal organic frameworks incorporating dicarboxylate ligands, J. Porous Mater. 26 (6) (2019) 1679–1689, https://doi.org/10.1007/s10934-019-00768-0.

[70] C. Liu, S. Wang, G. Che, H. Zhao, W.-W. Li, X. Li, Z. Xu, Hydrothermal syntheses and crystal structures of PbII coordination polymers based on a N, O-donor ligand, Inorg. Chem. Commun. 27 (2013) 69–75, https://doi.org/10.1016/j.inoche.2012.10.007.

[71] L. Xu, G.-C. Guo, B. Liu, M.-S. Wang, J.-S. Huang, 2-D open frameworks and blue fluorescence of two new zinc coordination polymers with mixed ligands, Inorg. Chem. Commun. 7 (10) (2004) 1145–1149, https://doi.org/10.1016/j.inoche.2004.08.016.

[72] G.C. Liu, Y. Li, J. Chi, N.a. Xu, X.L. Wang, H.Y. Lin, Y.Q. Chen, Multi-functional fluorescent responses of cobalt complexes derived from functionalized amide-bridged ligand, Dyes Pigm. 174 (2020) 108064, https://doi.org/10.1016/j.dyepig.2019.108064.

[73] R.-X. Yang, H.-M. Lan, P.-Y. Zhu, L.-Z. Yang, Y.-M. Yu, L.-L. Wang, D.-Z. Wang, Synthesis, structures, magnetic and electric properties of four new coordination polymers constructed with heterocyclic nitrogen ligands and multidentate organic acid, Inorg. Chim. Acta 506 (2020) 119410, https://doi.org/10.1016/j.ica.2019.119410.

[74] H. Zhu, Y.-H. Li, Q.-Q. Xiao, G.-H. Cui, Three luminescent Cd(II) coordination polymers containing aromatic dicarboxylate and flexible bis(benzimidazole) ligands as highly sensitive and selective sensors for detection of Cr2O72– oxoanions in water, Polyhedron 187 (2020) 114648, https://doi.org/10.1016/j.poly.2020.114648.

[75] T. Fan, L.i. Ye, H. Jiang, H. Wang, D. He, J. Zhang, C. Liu, Two mixed-ligand Cu (II) coordination polymers: treatment on neonatal septic infections by reducing the serum procalcitonin production, Inorg. Nano-Met. Chem. 51 (3) (2021) 434–441, https://doi.org/10.1080/24701556.2020.1793356.

[76] H. Lin, Y.u. Liu, M. Ji, J. Zhao, G. Liu, Two Zn(II) coordination polymers based on two isomeric flexible bis(pyridyl-tetrazolyl) ligands: synthesis, structures and properties, Inorg. Chem. Commun. 112 (2020) 107734, https://doi.org/10.1016/j.inoche.2019.107734.

[77] X.-L. Wang, X.-M. Wu, G.-C. Liu, H.-Y. Lin, X. Wang, A series of pyridyl-amide-based Zn II/Cd II coordination polymers and their polypyrrole-functionalized composite materials for tuning their photocatalytic properties, RSC Adv. 6 (88) (2016) 85030–85040, https://doi.org/10.1039/C6RA18428F.

[78] L.-L. Liu, C.-X. Yu, J.-M. Du, S.-M. Liu, J.-S. Cao, L.-F. Ma, Construction of five Zn (II)/Cd(II) coordination polymers derived from a new linear carboxylate/pyridyl ligand: design, synthesis, and photocatalytic properties, Dalton Trans. 45 (2016) 12352–12361, https://doi.org/10.1039/C6DT02312F.

[79] Lei Wang, WEN.-XUAN. Li, XIAO.-MIN. Gu, WEN.-LI. Zhang, LIANG Ni, Structure variation from one-dimensional chain to three-dimensional architecture: effect of ligand on construction of lanthanide coordination polymers, J. Chem. Sci. 129 (2) (2017) 271–280, https://doi.org/10.1007/s12039-017-1225-2.

[80] X.L. Wang, J. Zhao, H.Y. Lin, G.C. Liu, X. Wang, Three new coordination polymers based on a flexible bis(pyridyl-tetrazole): synthesis, fluorescent and photocatalytic properties, Polyhedron 145 (2018) 101–107, https://doi.org/10.1016/j.poly.2018.02.004.

[81] X. Wang, J. Zhao, H. Lin, M. Le, G. Liu, X. Wang, Flexible bis(pyridyl-tetrazole) ligand-induced ring-containing metal–organic coordination polymers: synthesis, structures, and properties, J. Coord. Chem. 71 (8) (2018) 1114–1126, https://doi.org/10.1080/00958972.2018.1444757.

[82] X. Zhang, Y. Wang, Ligand isomerism-controlled structural diversity of three new Cd(II) coordination polymers constructed by mixed dipyridyl-containing and benzenedicarboxylate ligands: syntheses, crystal structures, and photoluminescent properties, Inorg. Nano-Met. Chem. 47 (7) (2017) 978–983, https://doi.org/10.1080/15533174.2016.1228669.

[83] Z.-G. Kong, S.-N. Guo, B. Sun, S.W. Ng, A 3D mixed-valence Cu(I)/Cu(II) coordination polymer constructed by 2-(2-fluorophenyl)-1H-imidazo[4,5-f][1,10]phenanthroline and 1,3-benzenedicarboxylate, Z. Naturforsch. B 70 (2015) 857–861, https://doi.org/10.1515/znb-2015-0095.

[84] Y. Ran, J. Xie, Y. Mu, L. Zhang, B. Han, A series of 2D Cd(II) coordination polymers constructed from dicarboxylate acids and a flexible imidazole-based ligand, Inorg. Chim. Acta 425 (2015) 17–27, https://doi.org/10.1016/j.ica.2014.09.025.

[85] H. Lin, J. Luan, X. Wang, G. Liu, A. Tian, J. Zhang, Assembly and properties of four new metal-organic coordination polymers with flexible bis-pyridyl-bis-amide ligands: effect of aromatic dicarboxylates and central metal ions on the structures, J. Coord. Chem. 68 (1) (2015) 71–87, https://doi.org/10.1080/00958972.2014.983492.

[86] L.L. Liu, C.X. Yu, F.J. Ma, Y.R. Li, J.J. Han, L. Lin, L.F. Ma, Structural diversity and photocatalytic properties of Cd(ii) coordination polymers constructed by a flexible V-shaped bipyridyl benzene ligand and dicarboxylate derivatives, Dalton Trans. 44 (2015) 1636–1645, https://doi.org/10.1039/c4dt03271c.

[87] H.-Y. Lin, M. Le, F.-F. Sui, G.-C. Liu, Two New 3D ZN(II)/CU(II) coordination polymers based on N, N-DI(3-pyridyl)succinamide and two different aromatic dicarboxylates: syntheses, crystal structures and properties, J. Chem. Crystallogr. 45 (2) (2015) 94–102, https://doi.org/10.1007/s10870-015-0570-6.

[88] Y.J. Mu, X.L. Ma, B. Han, G.F. Qin, Y.Y. Niu, H.X. Lü, A series of Zn(II) coordination polymers derived from dicarboxylate acids and flexible imidazole-based ligands: syntheses, crystal structures and photoluminescent properties, Polyhedron 67 (2014) 44–50, https://doi.org/10.1016/j.poly.2013.08.054.

[89] S. Zhang, D. Liu, An unprecedented 5-connected self-penetrated cadmium(II) coordination polymer: synthesis, crystal structure, and luminescent property, Z. Anorg. Allg. Chem. 640 (7) (2014) 1374–1377, https://doi.org/10.1002/zaac.201300682.

[90] W. Yan, R. He, M. Dai, Z. Ren, H. Li, J. Lang, Assembly of 1D and 2D zinc(II) coordination polymers from flexible polyimidazolyl-based ligands, Inorg. Chem. Commun. 36 (2013) 51–55, https://doi.org/10.1016/j.inoche.2013.08.002.

[91] X. Wang, J. Luan, Q. Lu, H. Lin, C. Xu, G. Liu, Four new metal e organic complexes by tuning the spacer length of fl exible bis-pyridyl e bis-amide ligands : assembly, structures and properties, J. Organomet. Chem. 740 (2013) 17–25, https://doi.org/10.1016/j.jorganchem.2013.04.040.

[92] X.-L. Wang, F.-F. Sui, H.-Y. Lin, C. Xu, G.-C. Liu, J.-W. Zhang, A.-X. Tian, Role of aromatic dicarboxylates in the structural diversity of cobalt(ii) and copper(ii) coordination polymers containing a flexible N, N′-di(3-pyridyl) octanediamide ligand, CrystEngComm 15 (36) (2013) 7274, https://doi.org/10.1039/c3ce40825f.

[93] Z.-G. Kong, X.-R. Sun, L. Li, H.-X. Wang, X.-Y. Wang, S.W. Ng, Syntheses, structures, and luminescent properties of two cadmium(II) and manganese (II) coordination polymers based on the 11-fluoro-dipyrido[3,2-a:2′,3′-c]-phenazine ligand, Transition Met. Chem. 38 (4) (2013) 449–453, https://doi.org/10.1007/s11243-013-9710-z.

[94] C. He, J. Hao, S. Xiao, G.H. Cui, Synthesis, structures, and catalytic properties of two silver(I) coordination polymers constructed from 1,4-bis (benzimidazolyl)butane, Z. Naturforsch. B 68 (2013) 1207–1213, https://doi.org/10.5560/znb.2013-3115.

[95] S.-S. Chen, J. Fan, T.-A. Okamura, M.-S. Chen, Z. Su, W.-Y. Sun, N. Ueyama, Synthesis, crystal structure, and photoluminescence of a series of zinc(II) coordination polymers with 1,4-Di(1H-imidazol-4-yl)benzene and varied carboxylate ligands, Cryst. Growth Des. 10 (2) (2010) 812–822, https://doi.org/10.1021/cg9011857.

[96] G. Che, J. Wang, C. Liu, X. Li, B.o. Liu, J. Sun, Y. Liu, L.u. Lu, Syntheses, structures and photoluminescence properties of a series of metal–organic complexes with 1,3-benzenedicarboxylate and 10,11,12,13-tetrahydro-4,5,9,14-tetraaza-benzo[b]triphenylene ligands, Inorg. Chim. Acta 362 (8) (2009) 2756–2761, https://doi.org/10.1016/j.ica.2008.12.011.

[97] Z. Su, J. Xu, J. Fan, D.-J. Liu, Q. Chu, M.-S. Chen, S.-S. Chen, G.-X. Liu, X.-F. Wang, W.-Y. Sun, Synthesis, crystal structure, and photoluminescence of coordination polymers with mixed ligands and diverse topologies, Cryst. Growth Des. 9 (6) (2009) 2801–2811, https://doi.org/10.1021/cg900059m.

[98] X.-L. Wang, H.-Y. Lin, G.-C. Liu, H.-Y. Zhao, B.-K. Chen, Synthesis, structures, electrochemistry and electrocatalysis of two novel copper(II) complexes constructed with aromatic polycarboxylates and dipyrido[3,2-d:2′,3′-f] quinoxaline, J. Organomet. Chem. 693 (16) (2008) 2767–2774, https://doi.org/10.1016/j.jorganchem.2008.05.031.

[99] X. Shi, G. Zhu, X. Wang, G. Li, Q. Fang, X. Zhao, G. Wu, G. Tian, M. Xue, R. Wang, S. Qiu, Polymeric frameworks constructed from a metal-organic coordination compound, in 1-D and 2-D systems: synthesis, crystal structures, and fluorescent properties, Cryst. Growth Des. 5 (2005) 341–346, https://doi.org/10.1021/cg049884e.

[100] D.-F. Cai, Y.-S. Lu, Z.-H. Xing, H.-Y. Chen, X.-R. Liu, D.-L. Ma, Two Co(II) coordination polymers exhibit picric acid sensing property and treatment activity in nonalcoholic fatty liver disease by reducing intestinal Escherichia coli counts, J. Mol. Struct. 1221 (2020) 128832, https://doi.org/10.1016/j.molstruc.2020.128832.

[101] I. Mihalcea, N. Henry, T. Loiseau, Crystal chemistry of uranyl carboxylate coordination networks obtained in the presence of organic amine molecules, Eur. J. Inorg. Chem. 2014 (8) (2014) 1322–1332, https://doi.org/10.1002/ejic.201301575.

[102] J. Zhou, L. Du, Y.-F. Qiao, Y. Hu, B. Li, L. Li, X.-Y. Wang, J. Yang, M.-J. Xie, Q.-H. Zhao, Intriguing architectures generated from 1,4-Bis(3- or 4-pyridyl)-2,3-diaza- 1,3-butadiene with aromatic dicarboxylates: syntheses, crystal structures, and properties, Cryst. Growth Des. 14 (3) (2014) 1175–1183, https://doi.org/10.1021/cg401692e.

[103] L.L. Han, T.P. Hu, J.S. Chen, Z.H. Li, X.P. Wang, Y.Q. Zhao, X.Y. Li, D. Sun, Simultaneous encapsulation of an infinite T4(0)A(0)6(0) water tape and discrete water hexamers in a hydrogen-bonded Ag(i) supramolecular framework, Dalton Trans. 43 (2014) 8774–8780, https://doi.org/10.1039/c4dt00494a.

[104] M. Kang, D. Luo, Y. Deng, R. Li, Z. Lin, Solvothermal synthesis and characterization of new calcium carboxylates based on cluster- and rod-like building blocks, Inorg. Chem. Commun. 47 (2014) 52–55, https://doi.org/10.1016/j.inoche.2014.07.015.

[105] J.M. Hao, H. Zhang, G.Y. Li, G.H. Cui, Two 1-D zinc(II) coordination polymers based on flexible bis(2-methylbenzimidazole) and rigid dicarboxylate co-ligands, J. Coord. Chem. 67 (11) (2014) 1992–2003, https://doi.org/10.1080/00958972.2014.928288.

[106] Y. Gong, Z. Hao, J.L. Sun, H.-F. Shi, P.-G. Jiang, J.-H. Lin, Metal(ii) complexes based on 1,4-bis(3-pyridylaminomethyl)benzene: structures, photoluminescence and photocatalytic properties, Dalton Trans. 42 (36) (2013) 13241, https://doi.org/10.1039/c3dt51188j.

[107] F. Xie, D. Zhang, X. Zhang, Poly[(μ3benzene-1,3-dicarboxylato-k4O 1:O1′:O3, O3′) bis(pyridine-kN)cobalt(II)], Acta Crystallogr. Sect. E: Struct. Rep. Online 68 (2012), https://doi.org/10.1107/S1600536812020028.

[108] X.-L. Wang, Y.-Q. Chen, J.-X. Zhang, G.-C. Liu, H.-Y. Lin, A.-X. Tian, One- and two-dimensional Pb II complexes constructed from N-donor chelating ligands with extended π-system and organic dicarboxylates, Z. Anorg. Allg. Chem. 636 (5) (2010) 830–834, https://doi.org/10.1002/zaac.200900354.

[109] X.L. Wang, J.X. Zhang, G.C. Liu, H.Y. Lin, Z.H. Kang, Two manganese(II) complexes constructed from 2-(3-pyridyl)-imidazo[4,5-f] 1,10-phenanthroline and organic dicarboxylates: syntheses, crystal structures, and luminescence, J. Coord. Chem. 63 (2010) 3933–3943, https://doi.org/10.1080/00958972.2010.522235.

[110] X.L. Wang, X.M. Wu, G.C. Liu, N.L. Chen, H.Y. Lin, X. Wang, structural diversity and properties of Six ZnII/CdII coordination polymers based on an O-bridged semi-rigid bis-pyridyl-bis-amide and different dicarboxylates, Aust. J. Chem. 69 (2016) 846–855, https://doi.org/10.1071/CH15728.

[111] G.C. Liu, H.X. Yu, H.Y. Lin, X.L. Wang, X.W. Li, Spacers-induced structural diversity of cobalt coordination polymers based on "V"-type dipyridylamide and dicarboxylic ligands: fluorescent, magnetic and photocatalytic properties, Polyhedron 126 (2017) 205–213, https://doi.org/10.1016/j.poly.2017.01.022.

[112] J.-M. Hu, R. Guo, Y.-G. Liu, G.-H. Cui, Four Co(II) coordination polymers based on 4,4′-bis(benzimidazol-1-ylmethyl)biphenyl and aromatic carboxylic acids co-ligands: synthesis, structures, and photocatalytic properties, Inorg. Chim. Acta 450 (2016) 418–425, https://doi.org/10.1016/j.ica.2016.06.042.

[113] S.-B. Miao, Z.-H. Li, C.-Y. Xu, B.-M. Ji, Syntheses, characterization, and luminescence properties of three novel Ag(I) coordination polymers based on polycarboxylic acid ligands and 1,3-di-(1,2,4-triazole-4-yl)benzene, CrystEngComm 18 (2016) 4636–4642, https://doi.org/10.1039/C6CE00625F.

[114] Y.u. Chen, J. Yang, X.-C. Wang, Y.-C. Xu, H.-L. Xu, X.-S. Zeng, D.-R. Xiao, Syntheses, structures and properties of five entangled coordination polymers constructed with trigonal N-donor ligands, RSC Adv. 6 (7) (2016) 5729–5738, https://doi.org/10.1039/C5RA19086J.

[115] X. Wang, N. Chen, G. Liu, A.T.X. Sha, K. Ma, A series of CdII/ZnII coordination polymers containing helical chains constructed from a "V"-like bis-pyridyl-bis-amide and various dicarboxylates: assembly, structures, photoluminescent and selective photocatalysis, Inorg. Chim. Acta 432 (2015) 128–135, https://doi.org/10.1016/j.ica.2015.03.043.

[116] C. Paraschiv, A. Cucos, S. Shova, A.M. Madalan, C. Maxim, D. Visinescu, B. Cojocaru, V.I. Parvulescu, M. Andruh, New Zn(II) coordination polymers constructed from amino-alcohols and aromatic dicarboxylic acids: synthesis, structure, photocatalytic properties, and solid-state conversion to ZnO, Cryst. Growth Des. 15 (2) (2015) 799–811, https://doi.org/10.1021/cg501604c.

[117] J. Kulesza, B. Silva Barros, S. Alves Júnior, C.A. Fernandes de Oliveira, D.M. de Araújo Melo, J. Chojnacki, Benzene-induced hydro(solvo)thermal synthesis of Cu2+ and Zn2+ coordination polymers based on 1,3-benzenedicarboxylate, Mater. Chem. Phys. 143 (3) (2014) 1522–1527, https://doi.org/10.1016/j.matchemphys.2013.12.014.

[118] H.-Y. Lin, J. Luan, X.-L. Wang, G.-C. Liu, J.-W. Zhang, Three transition metal(II) coordination polymers constructed by a semi-rigid bis-pyridyl-bis-amide and dicarboxylates mixed ligands: assembly, structures and properties, Z. Anorg. Allg. Chem. 640 (10) (2014) 2041–2048, https://doi.org/10.1002/zaac.201400111.

[119] X.-L. Wang, P. Liu, J. Luan, H.-Y. Lin, C. Xu, The role of the coordination modes of a flexible bis(pyridylamide) ligand in the topology of 2D copper(II) complexes, Z. Naturforsch. B 67 (2012) 877–886, https://doi.org/10.5560/znb.2012-0179.

[120] Z. Ming, Y. Miao, S. Si, {Na2[Nd4(OX)(BDC)6(H2O) 6]}n: a 3-D coordination polymer with hybrid dicarboxylates, J. Coord. Chem. 62 (2009) 833–839, https://doi.org/10.1080/00958970802314977.

[121] Z. Song, H. Gao, G. Li, Y. Yu, Z. Shi, S. Feng, Influence of noncovalent intermolecular interactions on crystal packing: syntheses and crystal structures of three layered Zn(ii)/1,2,4-triazole/carboxylate coordination polymers, CrystEngComm 11 (2009) 1579–1584, https://doi.org/10.1039/b901445d.

[122] B. Li, S.-T. Zheng, G.-Y. Yang, Synthesis and description of a novel metal-organic framework based on trigonal prismatic building blocks, Z. Anorg. Allg. Chem. 635 (9-10) (2009) 1345–1347, https://doi.org/10.1002/zaac.200801363.

[123] C.-H. Lin, T.-H. Tsao, Solvothermal syntheses and magnetic properties of two new coordination polymers with mixed ligands, Z. Anorg. Allg. Chem. 634 (10) (2008) 1759–1764, https://doi.org/10.1002/zaac.200800143.

[124] J. Zhao, H.-Y. Lin, G.-C. Liu, X. Wang, X.-L. Wang, Two Cu(II) coordination polymers based on a flexible bis(pyridyl-tetrazole): solvent-ratio induced various structures and distinct adsorption performance for organic dyes, Inorg. Chim. Acta 464 (2017) 114–118, https://doi.org/10.1016/j.ica.2017.05.008.

[125] I. Voda, G. Makhloufi, V. Lozan, S. Shova, C. Heering, C. Janiak, Mixed-ligand cobalt, nickel and zinc coordination polymers based on flexible 1,4-bis((1H-imidazol-1-yl)methyl)benzene and rigid carboxylate linkers, Inorg. Chim. Acta 455 (2017) 118–131, https://doi.org/10.1016/j.ica.2016.10.007.

[126] J. Cui, W. Zhang, A new Zn(II) coordination polymers with two-fold pcu topological net: synthesis, crystal structure, and luminescent property, Synth. React. Inorg., Metal-Org. Nano-Met. Chem. 44 (8) (2014) 1154–1157, https://doi.org/10.1080/15533174.2013.799203.

[127] Q.L. Lu, J. Luan, X.L. Wang, H.Y. Lin, M. Le, G.C. Liu, A series of two-dimensional coordination polymer crystal materials based on two flexible bis-pyridyl-bis-amide ligands with fluorescent sensing activities and photocatalytic properties, Polyhedron 83 (2014) 108–115, https://doi.org/10.1016/j.poly.2014.05.024.

[128] R.B. Simonetti, Hydrothermal synthesis and crystal structure of Co(II) coordination polymer, Asian J. Chem. 26 (2014) 6097–6100, https://doi.org/10.14233/ajchem.2014.17410.

[129] G. Zhou, J. Han, Y. Yang, R. Fan, J. Li, L. Fu, Y. Zhang, Solvothermal syntheses, crystal structures and luminescent properties of two new aromatic dicarboxylate indium coordination polymers, Inorg. Chem. Commun. 40 (2014) 124–128, https://doi.org/10.1016/j.inoche.2013.11.039.

[130] P.-K. Chen, Y. Qi, Y.-X. Che, J.-M. Zheng, Network topology and property studies for two binodal self-penetrated coordination polymers, CrystEngComm 12 (3) (2010) 720–724, https://doi.org/10.1039/b919676p.

[131] G.-H. Wei, J. Yang, Y.-Y. Liu, J.-F. Ma, J.-C. Ma, A novel Zn(II) framework with 3-fold interpenetrating α-polonium topology, Inorg. Chem. Commun. 12 (5) (2009) 371–374, https://doi.org/10.1016/j.inoche.2009.02.019.

[132] P.-K. Chen, Y.-X. Che, S.R. Batten, J.-M. Zheng, An inclined interpenetrating heteropolynuclear polymer with unusual propagation of metal carboxylate secondary building units by both carboxylate and pyridyl bridging ligands, Inorg. Chem. Commun. 10 (4) (2007) 415–418, https://doi.org/10.1016/j.inoche.2006.11.018.

[133] G.B. Che, C.B. Liu, L. Wang, Y.C. Cui, Solvothermal syntheses, structures, and luminescence of two heterometallic metal-organic frameworks constructed from m-BDC (m-BDC = 1,3-benzene-dicarboxylate), J. Coord. Chem. 60 (2007) 1997–2007, https://doi.org/10.1080/00958970701220390.

[134] J.-J. Liu, Photochromism and decolorization controlled by auxiliary ligands of complexes derived from 1-methyl-4,4′-bipyridinium cation, Appl. Organomet. Chem. 33 (1) (2019) e4578, https://doi.org/10.1002/aoc.4578.

[135] X.-D. Yang, C. Chen, Y.-J. Zhang, L.-X. Cai, J. Zhang, The effects of molecular configuration on the photochromism and decolorization of two bipyridinium-based coordination polymers, Inorg. Chem. Commun. 60 (2015) 122–125, https://doi.org/10.1016/j.inoche.2015.07.022.

[136] J. Liu, Y. Lu, J. Li, W. Lu, UV and X-ray dual photochromic properties of three CPs based on a new viologen ligand, Dyes Pigm. 177 (2020) 108276, https://doi.org/10.1016/j.dyepig.2020.108276.

[137] L. Wang, L. Ni, Synthesis, structures, and fluorescence properties of two lanthanide [Ln=Sm(III), Nd(III)] coordination polymers, J. Coord. Chem. 65 (2012) 1475–1483, https://doi.org/10.1080/00958972.2012.675433.

[138] L. Wang, Z. Jun, L. Ni, J. Yao, Synthesis, structures, fluorescence properties, and natural bond orbital (NBO) analysis of two metal [Eu III, Co II] coordination polymers containing 1, 3-benzenedicarboxylate and 2-(4-methoxyphenyl)-1H- imidazo[4,5-f][1,10]phenanthroline ligands, Z. Anorg. Allg. Chem. 638 (1) (2012) 224–230, https://doi.org/10.1002/zaac.201100345.

[139] Y.-H. Xu, Y.-Q. Lan, K.-Z. Shao, Z.-M. Su, Y.i. Liao, Auxiliary aromatic-acid effect on the structures of a series of ZnII coordination polymers: syntheses, crystal structures, and photoluminescence properties, J. Solid State Chem. 183 (4) (2010) 849–857, https://doi.org/10.1016/j.jssc.2010.01.027.

[140] W.Q. Kan, J. Yang, Y.Y. Liu, J.F. Ma, A series of coordination polymers based on a multidentate N-donor ligand and different polycarboxylate anions: syntheses, structures and photoluminescent properties, CrystEngComm 14 (2012) 6271–6281, https://doi.org/10.1039/c2ce25388g.

[141] W.-Q. Kan, J. Yang, Y.-Y. Liu, J.-F. Ma, Effect of organic anions on the self-assembly of Zn(II)-containing coordination polymers based on trigonal N-donor ligands, CrystEngComm 14 (20) (2012) 6934, https://doi.org/10.1039/c2ce25907a.

[142] C. Xu, Q. Guo, X. Wang, H. Hou, Y. Fan, A case study of Zn II-bmb meso-helical coordination polymers upon the spacer angles and lengths of dicarboxylate coligands, Cryst. Growth Des. 11 (5) (2011) 1869–1879, https://doi.org/10.1021/cg200052t.

[143] Y.-Y. Liu, J.-C. Ma, L.-P. Zhang, J.-F. Ma, Four silver-containing coordination polymers based on bis(imidazole) ligands, J. Coord. Chem. 61 (22) (2008) 3583–3593, https://doi.org/10.1080/00958970802087078.

[144] W.-Q. Kan, Z.-C. Zhang, Y.-C. He, S.-Z. Wen, P.-S. Zhao, Syntheses, crystal structures, characterization, optical band gaps and photoluminescence of two Zn(II) coordination polymers, J. Chem. Crystallogr. (2020), https://doi.org/10.1007/s10870-020-00830-9.

[145] J. Pan, D. Zhang, Z.-Z. Xue, L. Wei, S.-D. Han, G.-M. Wang, Three d 10 coordination polymers assembled from 3,5-bis(imidazole-1-yl)pyridine and different polycarboxylates: syntheses, structures and luminescence properties, Solid State Sci. 73 (2017) 13–18, https://doi.org/10.1016/j.solidstatesciences.2017.09.003.

[146] W.-Q. Kan, S.-Z. Wen, H.-Y. Hu, Y.-H. Kan, Cd(II) and Cu(II) coordination polymers based on a multidentate N-donor ligand: syntheses, crystal structures, optical band gaps, and photoluminescence, J. Coord. Chem. 68 (14) (2015) 2492–2506, https://doi.org/10.1080/00958972.2015.1052805.

[147] Z.-Q. Shi, Z.-J. Guo, H.-G. Zheng, Syntheses, crystal structures, and optical properties of five metal complexes constructed from a V-shaped thiophene-containing ligand and different dicarboxylate ligands, Dalton Trans. 43 (35) (2014) 13250–13258, https://doi.org/10.1039/C4DT01400F.

[148] H.-Y. Liu, J.-F. Ma, Y.-Y. Liu, J. Yang, A series of Zn(II) and Cd(II) coordination polymers based on flexible bis-[(pyridyl)-benzimidazole] ligand and different carboxylates: syntheses, structures, and photoluminescent properties, CrystEngComm 15 (14) (2013) 2699, https://doi.org/10.1039/c3ce00009e.

[149] H. Zhang, B. Zhao, W. Yuan, W. Tang, F. Xiong, L. Jing, D. Qin, Syntheses and characterizations of two-dimensional polymers based on tetraimidazole tetraphenylethylene ligand with aggregation-induced emission property,

Inorg. Chem. Commun. 35 (2013) 208–212, https://doi.org/10.1016/j.inoche.2013.06.035.

[150] Y.-Y. Liu, H.-Y. Liu, J.-F. Ma, Y. Yang, J. Yang, Syntheses, structures and photoluminescent properties of Zn(ii) and Cd(ii) coordination polymers with flexible tripodal triazole-containing ligands, CrystEngComm 15 (10) (2013) 1897, https://doi.org/10.1039/c2ce26958a.

[151] X.-J. Wei, D. Liu, Y.-H. Li, G.-H. Cui, Construction of a series of Zn(II) and Cd(II) coordination polymers bearing 1,3-bis(benzimidazol-1-yl)-2-propanol ligands: syntheses, crystal structures, and sensing properties, J. Solid State Chem. 284 (2020) 121218, https://doi.org/10.1016/j.jssc.2020.121218.

[152] C.-P. Li, J. Chen, Q. Yu, M. Du, Structural Modulation and Properties of Silver(I) Coordination Frameworks with Benzenedicarboxyl Tectons and trans-1-(2-Pyridyl)-2-(4-pyridyl)ethylene Spacer, Cryst. Growth Des. 10 (4) (2010) 1623–1632, https://doi.org/10.1021/cg901188g.

[153] H.A. Habib, A. Hoffmann, H.A. Höppe, C. Janiak, Crystal structures and solid-state CPMAS 13C NMR correlations in luminescent zinc(II) and cadmium(II) mixed-ligand coordination polymers constructed from 1,2-bis(1,2,4-triazol-4-yl)ethane and benzenedicarboxylate, J. Chem. Soc. Dalton Trans. (2009) 1742–1751, https://doi.org/10.1039/b812670d.

[154] F. Luo, Y.-X. Che, J.-M. Zheng, Trinuclear cobalt based porous coordination polymers showing unique topological and magnetic variety upon different dicarboxylate-like ligands, Cryst. Growth Des. 9 (2) (2009) 1066–1071, https://doi.org/10.1021/cg800895g.

[155] F. Luo, Y.-X. Che, J.-M. Zheng, Employing Cd–O–C rod-shaped secondary building units to construct 2D metal-organic frameworks (MOFs): hydrothermal synthesis, structures, and luminescent properties, J. Coord. Chem. 61 (13) (2008) 2097–2104, https://doi.org/10.1080/00958970701870186.

[156] H.-K. Zhao, H.-W. Yang, X.-G. Wang, B.o. Ding, Z.-Y. Liu, X.-J. Zhao, E.-C. Yang, An unusual 2D polymeric Co(II) complex with 2,6-diaminopurine: synthesis, crystal structure, and magnetic behavior, Inorg. Chem. Commun. 107 (2019) 107483, https://doi.org/10.1016/j.inoche.2019.107483.

[157] X.-L. Wang, X.-M. Wu, G.-C. Liu, H.-Y. Lin, X. Wang, The assembly of thiophene-based bis-pyridyl-bis-amide CoII coordination polymers and their polypyrrole-functionalized hybrid materials for boosting their photocatalytic performances, Dalton Trans. 45 (48) (2016) 19341–19350, https://doi.org/10.1039/C6DT03430F.

[158] Y.-Y. Zhang, H. Zhao, E.-C. Yang, Z.-Y. Liu, Q. Shang, X.-J. Zhao, Triazolate-based 3D frameworks and a 2D layer with centrosymmetric CuII7, CuII5, CuII4 clusters and tunable interlayer/interchain compactness: hydrothermal syntheses, crystal structures and magnetic properties, Dalton Trans. 44 (12) (2015) 5826–5836, https://doi.org/10.1039/C4DT04013A.

[159] S.-L. Xiao, L.i. Liu, P.-J. Ma, G.-H. Cui, Assembly and catalytic properties of cobalt(II) and copper(II) coordination polymers based on bis(imidazole) and carboxylic acid mixed ligands, Z. Anorg. Allg. Chem. 640 (7) (2014) 1484–1489, https://doi.org/10.1002/zaac.201300478.

[160] S. Freslon, Y. Luo, G. Calvez, C. Daiguebonne, O. Guillou, K. Bernot, V. Michel, X. Fan, Influence of photoinduced electron transfer on lanthanide-based coordination polymer luminescence: a comparison between two pseudoisoreticular molecular networks, Inorg. Chem. 53 (2) (2014) 1217–1228, https://doi.org/10.1021/ic402841d.

[161] H. Cai, Y. Guo, J. Li, Hydrothermal syntheses and characterization of a series of mixed-ligand luminescent CdII frameworks with novel 2-(3-(pyridin-2-yl)-1H-pyrazol-1-yl) acetate ligand and benzenedicarboxylate isomers, Inorg. Chem. Commun. 34 (2013) 37–41, https://doi.org/10.1016/j.inoche.2013.05.003.

[162] H. Cai, Y. Guo, J. Li, Two novel coordination polymers with Zn(II): synthesis, structural characterization, thermal analysis and fluorescent properties, Inorg. Chem. Commun. 37 (2013) 178–181, https://doi.org/10.1016/j.inoche.2013.09.055.

[163] C. Xu, L. Li, Q. Guo, H. Hou, Y. Fan, Temperature-controlled dimensionality variety from 3D to 2D and 1D based on Cd(II)/ip/bmb polymers, Inorg. Chem. Commun. 14 (8) (2011) 1204–1208, https://doi.org/10.1016/j.inoche.2011.04.018.

[164] Y. Wen, D. Shi, Z. Duan, Two copper (II) complexes based on different copper salts, 1,3-benzenedicarboxylic acid and 1,4-di(imidazolidin-1-yl) benzene and their fluorescence recognition to nitrobenzene derivatives, J. Solid State Chem. 287 (2020) 121334, https://doi.org/10.1016/j.jssc.2020.121334.

[165] C. Wang, Z. Wang, F. Gu, G. Guo, Three novel lanthanide MOFs constructed from 1,3-benzenedicarboxylic acid and 1,10-phenanthroline: hydrothermal synthesis, crystal structure and thermal properties, J. Mol. Struct. 1004 (1-3) (2011) 39–44, https://doi.org/10.1016/j.molstruc.2011.07.014.

[166] Q. Huang, W. Tang, C. Liu, X. Su, X. Meng, Syntheses, structures, and properties of two 2-D Cd(II) complexes based on 2-(1 H-imidazol-1-methyl)-1 H-benzimidazole and polycarboxylate ligands, J. Coord. Chem. 67 (1) (2014) 149–161, https://doi.org/10.1080/00958972.2013.879574.

[167] D.i. Sun, Z.-H. Yan, V.A. Blatov, L. Wang, D.-F. Sun, Syntheses, topological structures, and photoluminescences of six new Zn(II) coordination polymers based on mixed tripodal imidazole ligand and varied polycarboxylates, Cryst. Growth Des. 13 (3) (2013) 1277–1289, https://doi.org/10.1021/cg3017358.

[168] J.-C. Ma, Y.-Y. Liu, J. Yang, Y.-Y. Liu, J.-F. Ma, A series of lanthanide-transition metal coordination polymers with mixed ligands: syntheses, structures, photoluminescence and magnetic properties, CrystEngComm 13 (10) (2011) 3498, https://doi.org/10.1039/c0ce00724b.

[169] D.i. Sun, Q.-J. Xu, C.-Y. Ma, N.a. Zhang, R.-B. Huang, L.-S. Zheng, Self-assembly, thermal stability and photoluminescence of two mixed-ligand silver(i) networks via 2D → 2D and 2D → 3D parallel interpenetration of (4,4) nets, CrystEngComm 12 (12) (2010) 4161, https://doi.org/10.1039/c0ce00017e.

[170] R.-H. Cui, Y.-H. Xu, Z.-H. Jiang, Syntheses, structures, and photoluminescence of two Cd(II) coordination polymers constructed from analogue (pyridyl) imidazole derivative and polycarboxylate acid, Inorg. Chem. Commun. 12 (9) (2009) 933–936, https://doi.org/10.1016/j.inoche.2009.07.013.

[171] L. Wang, W. Xu, W.-Y. Li, M. Xie, Y.-Q. Zheng, A water-stable uranyl organic framework as a highly selective and sensitive bifunctional luminescent probe for Fe3+ and tetracycline hydrochloride, Chem. - Asian J. 14 (23) (2019) 4246–4254, https://doi.org/10.1002/asia.201901124.

[172] W. He, Q. Yuan, H. Zeng, Crystal structure and protective effect in osteoarthritis of Co(II)-mediated pyridinium-bearing coordination polymer, J. Coord. Chem. 72 (22-24) (2019) 3471–3480, https://doi.org/10.1080/00958972.2019.1700234.

[173] L.u. Lu, J. Wang, F. Chen, L.-T. Wei, L.-M. Lin, B.-H. Li, A. Singh, A. Kumar, Structures and photocatalytic performance of two d10 metal-based coordination polymers containing mixed building units, Transition Met. Chem. 44 (2) (2019) 107–114, https://doi.org/10.1007/s11243-018-0274-9.

[174] G. Xu, F. Guo, Construction of two new cadmium(II) coordination polymers based on dicarboxylate and 4,4-bis(1-imidazol-yl)-2,5-dimethyl benzene ligands, Inorg. Chem. Commun. 27 (2013) 146–148, https://doi.org/10.1016/j.inoche.2012.10.025.

[175] Y. Mu, Y. Ran, B. Zhang, J. Du, C. Jiang, J. Du, Dicarboxylate ligands modulated structural diversity in the construction of Cd(II) coordination polymers built from N-heterocyclic ligand: synthesis, structures, and luminescent sensing, Cryst. Growth Des. 20 (9) (2020) 6030–6043, https://doi.org/10.1021/acs.cgd.0c00739.

[176] B. Xu, L. Yan, H.-M. Hu, C. Bai, L.-L. Xue, S. He, Construction of lanthanide coordination polymers based on mixed terpyridyl and dicarboxylate ligands: syntheses, structures and luminescent properties, J. Solid State Chem. 288 (2020) 121424, https://doi.org/10.1016/j.jssc.2020.121424.

[177] Y. Chen, X.-C. Wang, Y.-C. Xu, H.-L. Xu, H. Yuan, J.-T. Tong, D.-R. Xiao, Syntheses, structures and magnetism of four Ni(II)/Co(II) interpenetrating coordination polymers based on 1,4-bis(4-(imidazole-1-yl)benzyl) piperazine, Inorg. Chim. Acta 451 (2016) 1–7, https://doi.org/10.1016/j.ica.2016.07.001.

[178] J.F. Lu, L.J. Qiao, L.Q. Li, Z.H. Liu, Syntheses, structures and luminescent properties of four novel Cd/Zn(II) complexes constructed from dicarboxylate and bis(imidazole) co-ligands, J. Mol. Struct. 1081 (2015) 79–84, https://doi.org/10.1016/j.molstruc.2014.09.085.

[179] S.A. Bourne, A. Mondal, M.J. Zaworotko, 1-D coordination polymers containing benzenedicarboxylate, Cryst. Eng. 4 (1) (2001) 25–36, https://doi.org/10.1016/S1463-0184(01)00007-7.

[180] A. Li, Z. Hao, C. Han, G. Cui, Cobalt(II) and silver(I) coordination polymers containing flexible bis (benzimidazol-1-yl)hexane ligands: synthesis, crystal structures, sensing and photocatalytic properties, Appl. Organomet. Chem. 34 (2020) 1–12, https://doi.org/10.1002/aoc.5313.

[181] J.-X. Li, D. Liu, Z.-B. Qin, G.-Y. Dong, Sonochemical synthesis of two nano-sized nickel(II) coordination polymers derived from flexible bis (benzimidazole) and isophthalic acid ligands, Polyhedron 160 (2019) 92–100, https://doi.org/10.1016/j.poly.2018.12.029.

[182] C.S. Hawes, S.E. Hamilton, J. Hicks, G.P. Knowles, A.L. Chaffee, D.R. Turner, S.R. Batten, Coordination Chemistry and Structural Dynamics of a Long and Flexible Piperazine-Derived Ligand, Inorg. Chem. 55 (13) (2016) 6692–6702, https://doi.org/10.1021/acs.inorgchem.6b00933.

[183] S.-D. Liu, B.-C. Kuo, Y.-W. Liu, J.-Y. Lee, K.Y. Wong, H.M. Lee, Tuning of net architectures of Ni(II) and Zn(II) coordination polymers using isomeric organic linkers, CrystEngComm 16 (2014) 8874–8884, https://doi.org/10.1039/C4CE01072H.

[184] X.-F. Wang, Y. Sun, S. Wang, Ligand-tuned metal coordination polymers constructed by the linear Cd3(COO)6/8 clusters: preparations, structures, topologies and gas adsorptive properties, Microporous Mesoporous Mater. 181 (2013) 262–269, https://doi.org/10.1016/j.micromeso.2013.07.022.

[185] H.S. Huh, S.W. Lee, Copper coordination polymers containing pyridinecarboxylate and multicarboxylate: [Cu1.5(ina)(btcH)]·H2O, [Cu2 (ina)2(bdc)0.5(μ3-OH)], and [Cu(ina)(na)] (inaH = 4-pyridinecarboxylic acid, btcH3 = 1,3,5-benzenetricarboxylic acid, bdcH2 = 1,3-benzenedicarbox, J. Mol. Struct. 829 (2007) 44–50, https://doi.org/10.1016/j.molstruc.2006.06.005.

[186] A.D. Burrows, S. Chan, W.J. Gee, M.F. Mahon, C. Richardson, V.M. Sebestyen, D. Turski, M.R. Warren, The impact of N, N′-ditopic ligand length and geometry on the structures of zinc-based mixed-linker metal–organic frameworks, CrystEngComm 19 (37) (2017) 5549–5557, https://doi.org/10.1039/C7CE01447C.

[187] Z.-W. Wei, X. Mu, Organic carboxylate ligands tuned structural variations of three new Cd(II) coordination polymers with guanazole as co-ligand, J. Inorg. Organomet. Polym. Mater. 25 (6) (2015) 1425–1433, https://doi.org/10.1007/s10904-015-0255-9.

[188] Z.-H. Chen, Y. Zhao, S. Chen, P. Wang, W. Sun, Synthesis and characterization of d10 metal complexes with mixed 1,3-di(1H-imidazol-4-yl)benzene and multicarboxylate ligands, J. Solid State Chem. 202 (2013) 215–226, https://doi.org/10.1016/j.jssc.2013.03.042.

[189] B.S. Luisi, Z. Ma, B. Moulton, Tri-metal secondary building units: toward the design of thermally robust crystalline coordination polymers, J. Chem. Crystallogr. 37 (11) (2007) 743–747, https://doi.org/10.1007/s10870-007-9244-3.

[190] H.K. Lee, D. Min, B.Y. Cho, S.W. Lee, Two-dimensional copper coordination polymers based on paddle-wheel type secondary building units of Cu2(CO2R) 4: [Cu(1,3-BDC)(H2O)]·2H2O and [Cu2(OBC) 2(H2O)2]·H2 (1,3-BDC = 1,3-benzenedicarboxylate; OBC = 4,4′-oxybis(benzoate)), Bull. Korean Chem. Soc. 25 (2004) 1955–1958, https://doi.org/10.5012/bkcs.2004.25.12.1955.

[191] S.W. Lee, H.J. Kim, Y.K. Lee, K. Park, J.H. Son, Y.U. Kwon, Triply interpenetrating coordination polymers based on paddle-wheel type secondary-building units, Inorg. Chim. Acta 353 (2003) 151–158, https://doi.org/10.1016/S0020-1693(03)00246-9.

[192] S. Hu, J. Zhang, Y. He, Z. Chen, Z. Fu, A N-aromatic-substituted viologen-based coordination polymer with layered assembly of hydrogen-bonded networks showing exceptional photochromic behaviors, Cryst. Growth Des. 19 (2) (2019) 543–546, https://doi.org/10.1021/acs.cgd.8b01614.

[193] O.J. Silva Junior, A.F.F. Monteiro, J.B.L. Oliveira, A.M.U. Araújo, D.G. Silva, J. Kulesza, B.S. Barros, Coordination polymer-derived CuO catalysts for oxidative degradation of methylene blue, Mater. Chem. Phys. 235 (2019) 121737, https://doi.org/10.1016/j.matchemphys.2019.121737.

[194] R.-L. Chen, X.-Y. Chen, S.-R. Zheng, J. Fan, W.-G. Zhang, Construction of Ag(I)–Ln(III) Heterometallic Coordination Polymers Based on Binuclear Ag 2 (DSPT) 2 (H 2 DSPT = 4′-(2,4-Disulfophenyl)-2,2′:6′2″-terpyridine) Rings and Ln(III) Dimeric Molecular Building Blocks, Cryst. Growth Des. 13 (10) (2013) 4428–4434, https://doi.org/10.1021/cg400926q.

[195] Y.Y. Liang, L.L. Xue, H.M. Hu, L.N. Zheng, X. Wang, G. Xue, Syntheses, structures, fluorescence sensing properties and white-light emission of lanthanide coordination polymers assembled from imidazophenanthroline derivative and isophthalate ligands, J. Solid State Chem. 276 (2019) 6–18, https://doi.org/10.1016/j.jssc.2019.04.021.

[196] F.-P. Huang, J.-L. Tian, G.-J. Chen, D.-D. Li, W. Gu, X. Liu, S.-P. Yan, D.-Z. Liao, P. Cheng, A case study of the ZnII-BDC/bpt mixed-ligand system: positional isomeric effect, structural diversification and luminescent properties, CrystEngComm 12 (4) (2010) 1269–1279, https://doi.org/10.1039/B915506F.

[197] T.-T. Li, Y. Zheng, Q.-Y. Chen, S.-R. Zheng, Structures and luminescent properties of four compounds based on binuclear metal-terpyridine building blocks, J. Coord. Chem. 69 (6) (2016) 966–975, https://doi.org/10.1080/00958972.2016.1143935.

[198] M.V. Nora, T. de Souza, R.A. Vasconcelos, Recent methodologies mediated by sodium borohydride in the reduction of different classes of compounds, Appl. Organomet. Chem. 20 (2006) 798–810, https://doi.org/10.1002/aoc.

[199] S. Kulovi, A. Pradhan, S. Maiti (Choudhury), H. Puschmann, E. Zangrando, S. Dalai, Polymorphism in [Ag(bpetan)] n coordination polymers with nitrate and isophthalate anions: photocatalytic and antibacterial activity, hemolysis assay and study of cytotoxicity, ChemistrySelect 5 (11) (2020) 3337–3346, https://doi.org/10.1002/slct.202000291.

[200] X.-F. Li, D.i. Cheng, X.-R. Meng, H.-X. Yang, Effects of two benzenedicarboxylic acids on the construction of Cd II coordination polymers incorporating a flexible N-donor ligand, Acta Crystallogr. Sect. C Struct. Chem. 75 (6) (2019) 643–649, https://doi.org/10.1107/S2053229619005758.

[201] B. Bhattacharya, D.K. Maity, R. Mondal, E. Colacio, D. Ghoshal, Two series of isostructural coordination polymers with isomeric benzenedicarboxylates and different azine based N, N′-donor ligands: syntheses, characterization and magnetic properties, Cryst. Growth Des. 15 (9) (2015) 4427–4437, https://doi.org/10.1021/acs.cgd.5b00741.

[202] L. Yan, C. Li, Y. Wang, Syntheses, characterizations and photoluminescent properties of two novel coordination polymers constructed by poly-carboxylate and N-heterocyclic ligands, J. Mol. Struct. 1035 (2013) 455–461, https://doi.org/10.1016/j.molstruc.2012.11.066.

[203] Z. Su, Y. Zhao, M. Chen, W.Y. Sun, Anion- and auxiliary ligand-directed synthesis of cadmium(ii) complexes with 3,5-di(1H-imidazol-1-yl)benzoate, CrystEngComm 13 (2011) 1539–1549, https://doi.org/10.1039/c0ce00527d.

[204] P. Ren, W. Shi, P. Cheng, Synthesis and characterization of three-dimensional 3d–3d and 3d–4f heterometallic coordination polymers with high thermal stability, Cryst. Growth Des. 8 (4) (2008) 1097–1099, https://doi.org/10.1021/cg700740m.

[205] Y.K. Lee, S.W. Lee, Preparation and structure of one-dimensional copper(II) coordination polymer: [Cu(bdcH)2 (bipyen)] (bdc=1,3-benzenedicarboxylate; bipyen=trans-1,2-bis(4-pyridyl)ethylene), J. Korean Chem. Soc. 46 (2002) 484–488.

[206] J. Shi, X. Liu, Y. Yan, Y. Dong, J. Li, F. Wang, X. Gu, Y. Jiang, D. Xu, H. Chen, Synthesis and structure of Pb13Na(μ3-O)(μ3-OH)(BDC)12: a holodirected/hemidirected mixed Pb–Na heterometal coordination polymer with Pb12O20 cage, Inorg. Chem. Commun. 36 (2013) 216–219, https://doi.org/10.1016/j.inoche.2013.08.013.

[207] S. Durot, C. Policar, G. Pelosi, F. Bisceglie, T. Mallah, J.P. Mahyt, Structural and magnetic properties of carboxylato-bridged manganese(II) complexes involving tetradentate ligands: discrete complex and 1D polymers. dependence of J on the Nature of the carboxylato bridge, Inorg. Chem. 42 (2003) 8072–8080, https://doi.org/10.1021/ic026130l.

[208] C.-K. Xia, C.-Z. Lu, X.-Y. Wu, Q.-Z. Zhang, J.-J. Zhang, D.-M. Wu, Syntheses and crystal structures of four silver(I) complexes based on 2-(4-pyridyl) benzimidazole, Polyhedron 26 (4) (2007) 941–947, https://doi.org/10.1016/j.poly.2006.09.102.

[209] R. Atencio, M. Chacón, T. González, A. Briceño, G. Agrifoglio, A. Sierraalta, Robust hydrogen-bonded self-assemblies from biimidazole complexes. Synthesis and structural characterization of [M(biimidazole)2(OH2)2]2+ (M = Co2+, Ni2+) complexes and carboxylate modules, J. Chem. Soc. Dalton Trans. 4 (2004) 505–513, https://doi.org/10.1039/b312541f.

[210] C.L. Ming, Y.H. Li, G.Y. Li, G.H. Cui, Synthesis, crystal structures, luminescence and catalytic properties of three silver(I) coordination polymers with bis (imidazole) and benzenedicarboxylic acid ligands, Transition Met. Chem. 39 (4) (2014) 477–485, https://doi.org/10.1007/s11243-014-9822-0.

[211] IUPAC, Nomenclature of Inorganic Chemistry IUPAC Recommendations, Royal Society of Chemistry, Cambridge, 2005.

[212] S.G. Harris, Crystallographic and modelling studies of organic ligands on metal surfaces Ph.D. Thesis, The University of Edinburgh, 1999.

[213] R.A. Coxall, S.G. Harris, D.K. Henderson, S. Parsons, P.A. Tasker, R.E.P. Winpenny, Inter-ligand reactions: in situ formation of new polydentate ligands, J. Chem. Soc., Dalton Trans. (2000) 2349–2356, https://doi.org/10.1039/b001404o.

[214] J.E. Huheey, E.A. Keiter, R.L. Keiter, Inorganic Chemistry: Principle of Structure and Reactivity, fourth ed., Prentice Hall, 1997.

[215] R. Janicki, A. Mondry, P. Starynowicz, Carboxylates of rare earth elements, Coord. Chem. Rev. 340 (2017) 98–133, https://doi.org/10.1016/j.ccr.2016.12.001.

[216] T. Dudev, C. Lim, Monodentate versus bidentate carboxylate binding in magnesium and calcium proteins: what are the basic principles?, J. Phys. Chem. B 108 (2004) 4546–4557, https://doi.org/10.1021/jp0310347.

[217] U. Ryde, Carboxylate binding modes in zinc proteins: a theoretical study, Biophys. J. 77 (5) (1999) 2777–2787, https://doi.org/10.1016/S0006-3495(99)77110-9.

[218] S.-T. Yue, Z.-Q. Wei, N. Wang, W.-J. Liu, X. Zhao, L.-M. Chang, Y.-L. Liu, H.-H. Mo, Y.-P. Cai, Three novel microporous 3D heterometallic 3d–4f coordination polymers: synthesis, crystal structures and photoluminescence properties, Inorg. Chem. Commun. 14 (9) (2011) 1396–1399, https://doi.org/10.1016/j.inoche.2011.05.031.

[219] T.N. Nguyen, C.Y. Chow, S.V. Eliseeva, E.R. Trivedi, J.W. Kampf, I. Martinić, S. Petoud, V.L. Pecoraro, One-step assembly of visible and near-infrared emitting metallacrown dimers using a bifunctional linker, Chem. - Eur. J. 24 (5) (2018) 1031–1035, https://doi.org/10.1002/chem.201703911.

[220] A.N. Khlobystov, A.J. Blake, N.R. Champness, D.A. Lemenovskii, A.G. Majouga, N.V. Zyk, M. Schröder, Supramolecular design of one-dimensional coordination polymers based on silver(I) complexes of aromatic nitrogen-donor ligands, Coord. Chem. Rev. 222 (1) (2001) 155–192, https://doi.org/10.1016/S0010-8545(01)00370-8.

[221] L. Bravo-García, G. Barandika, A. Fidalgo-Marijuan, B. Bazan, M.K. Urtiaga, L. Lezama, M.I. Arriortua, Thermal and magnetic diversity in the behaviour of the cuii-bdc-bpa system: 1D, 2D and interpenetrated 3D frameworks, Eur. J. Inorg. Chem. 2016 (29) (2016) 4783–4791, https://doi.org/10.1002/ejic.201600683.

[222] J. Gu, M. Wen, X. Liang, Z. Shi, M. Kirillova, A. Kirillov, Multifunctional aromatic carboxylic acids as versatile building blocks for hydrothermal design of coordination polymers, Crystals 8 (2) (2018) 83, https://doi.org/10.3390/cryst8020083.

[223] H.-D. Wang, H.-Y. He, Y.-J. Wang, L.-G. Zhu, S.W. Ng, Poly[[(1,10-phenanthroline)lead(II)]-μ 5–1,3-benzenedicarboxylato], Acta Crystallogr. Sect. E: Struct. Rep. Online 61 (3) (2005) m531–m532, https://doi.org/10.1107/S1600536805004599.

[224] J. Rocha, L.D. Carlos, F.A.A. Paz, D. Ananias, Luminescent multifunctional lanthanides-based metal–organic frameworks, Chem. Soc. Rev. 40 (2) (2011) 926–940, https://doi.org/10.1039/c0cs00130a.

[225] C. Ma, C. Chen, Q. Liu, D. Liao, L. Li, L. Sun, Structural transformation mediated by o-, m-, and p-phthalates from two to three dimensions for manganese/phthalate/4,4′-bpy complexes (4,4′-bpy = 4,4′-bipyridine), New J. Chem. 27 (2003) 890–894, https://doi.org/10.1039/b301076g.

[226] J.-X. Yang, Y.-Y. Qin, J.-K. Cheng, X. Zhang, Y.-G. Yao, Construction of a series of Zn(II) compounds with different entangle motifs by varying flexible aliphatic dicarboxylic acids, Cryst. Growth Des. 15 (5) (2015) 2223–2234, https://doi.org/10.1021/cg501879w.

[227] P. Silva, W. Guerra, J.N. Silveira, A.M. da C. Ferreira, T. Bortolotto, F.L. Fischer, A. Neves, E.C. Pereira-maia, Two new ternary complexes of copper (II) with tetracycline or doxycycline and 1, 10-phenanthroline and their potential as antitumoral: cytotoxicity and DNA cleavage, Inorg. Chem. (2011) 6414–6424, https://doi.org/10.1021/ic101791r.

[228] P.P. Silva, W. Guerra, G.C. Dos Santos, N.G. Fernandes, J.N. Silveira, A.M. Da Costa Ferreira, T. Bortolotto, H. Terenzi, A.J. Bortoluzzi, A. Neves, E.C. Pereira-Maia, Correlation between DNA interactions and cytotoxic activity of four new ternary compounds of copper(II) with N-donor heterocyclic ligands, J. Inorg. Biochem. 132 (2014) 67–76, https://doi.org/10.1016/j.jinorgbio.2013.09.014.

[229] Í.P. de Souza, B. de P. Machado, A.B. de Carvalho, I. Binatti, K. Krambrock, Z. Molphy, A. Kellett, E.C. Pereira-Maia, P.P. Silva-Caldeira, Exploring the DNA binding, oxidative cleavage, and cytotoxic properties of new ternary copper (II) compounds containing 4-aminoantipyrine and N, N-heterocyclic co-ligands, J. Mol. Struct. 1178 (2019) 18–28, https://doi.org/10.1016/j.molstruc.2018.10.004.

[230] A.W. Addison, T.N. Rao, J. Reedijk, J. van Rijn, G.C. Verschoor, Synthesis, structure, and spectroscopic properties of copper(II) compounds containing nitrogen–sulphur donor ligands; the crystal and molecular structure of aqua [1,7-bis(N-methylbenzimidazol-2′-yl)-2,6-dithiaheptane]copper(II) perchlorate, J. Chem. Soc., Dalton Trans. (1984) 1349–1356, https://doi.org/10.1039/DT9840001349.

[231] M.A. Silva, N.R. de Campos, L.A. Ferreira, L.S. Flores, J.C.A. Júnior, G.L. dos Santos, C.C. Corrêa, T.C. dos Santos, C.M. Ronconi, M.V. Colaço, T.R.G. Simões,

L.F. Marques, M.V. Marinho, A new photoluminescent terbium(III) coordination network constructed from 1,2,4,5-benzenetetracarboxylic acid: synthesis, structural characterization and application as a potential marker for gunshot residues, Inorg. Chim. Acta 495 (2019) 118967, https://doi.org/10.1016/j.ica.2019.118967.

[232] M.V. Marinho, M.I. Yoshida, K.J. Guedes, K. Krambrock, A.J. Bortoluzzi, M. Hörner, F.C. Machado, W.M. Teles, Synthesis, crystal structure, and spectroscopic characterization of trans-Bis[(μ-1,3-bis(4-pyridyl)propane)(μ-(3-thiopheneacetate-O))(3-thiopheneacetate-O)]dicopper(II), [Cu 2 (O 2 CCH 2 C 4 H 3 S) 4 μ-(BPP) 2] n: from a dinuclear Paddle-Wheel Co, Inorg. Chem. 43 (2004) 1539–1544, https://doi.org/10.1021/ic035251y.

[233] N.R. De Campos, M.A. Ribeiro, W.X.C. Oliveira, D.O. Reis, H.O. Stumpf, A.C. Doriguetto, F.C. Machado, C.B. Pinheiro, F. Lloret, M. Julve, J. Cano, M.V. Marinho, Magneto-structural versatility of copper(ii)-3-phenylpropionate coordination polymers with N-donor coligands, Dalton Trans. 45 (2015) 172–189, https://doi.org/10.1039/c5dt03401a.

[234] V. Robert, G. Lemercier, A combined experimental and theoretical study of carboxylate coordination modes: a structural probe, J. Am. Chem. Soc. 128 (4) (2006) 1183–1187, https://doi.org/10.1021/ja055121j.

[235] M.M. Harding, Small revisions to predicted distances around metal sites in proteins, Acta Crystallogr. Sect. D: Biol. Crystall. 62 (6) (2006) 678–682, https://doi.org/10.1107/S090744490601459410.1107/S0907444906014594/be5055sup1.pdf.

[236] R.L. Rardin, W.B. Tolman, S.J. Lippard, Monodentate carboxylate complexes and the carboxylate shift: implications for polymetalloprotein structure and function, New J. Chem. 15 (1991) 417–430.

[237] G.B. Deacon, R.J. Phillips, Relationships between the carbon-oxigen stretching frequencies of carboxylato complexes and the type of carboxylate coordination, Coord. Chem. Rev. 33 (1980) 227–250.

[238] B. Farkaš, U. Terranova, N.H. de Leeuw, Binding modes of carboxylic acids on cobalt nanoparticles, Phys. Chem. Chem. Phys. 22 (3) (2020) 985–996, https://doi.org/10.1039/C9CP04485J.

[239] M.M. Harding, Geometry of metal–ligand interactions in proteins, Acta Crystall. Sect. D Biol. Crystallogr. 57 (3) (2001) 401–411, https://doi.org/10.1107/S090744490001916810.1107/S0907444900019168/ad0141sup1.pdf.

[240] Yong-Hong Zhou, Yu-Peng Tian, Syntheses and crystal structure of two 1D coordination polymers bridged by 1,4-bis(imidazol-1-yl)-butane, J. Chem. Crystallogr. 43 (1) (2013) 31–35, https://doi.org/10.1007/s10870-012-0381-y.

[241] X.S. Gao, H.J. Dai, Y. Tang, M.J. Ding, W.B. Pei, X.M. Ren, Crystal structures, photoluminescence, and magnetism of two novel transition-metal complex cocrystals with three-dimensional H-bonding organic framework or alternating noncovalent anionic and cationic layers, ACS Omega 4 (7) (2019) 12230–12237, https://doi.org/10.1021/acsomega.9b01584.

[242] Malcolm A. Halcrow, Jahn-Teller distortions in transition metal compounds, and their importance in functional molecular and inorganic materials, Chem. Soc. Rev. 42 (4) (2013) 1784–1795, https://doi.org/10.1039/C2CS35253B.

[243] T.P. Gerasimova, S.A. Katsyuba, Bipyridine and phenanthroline IR-spectral bands as indicators of metal spin state in hexacoordinated complexes of Fe (ii), Ni(ii) and Co(ii), Dalton Trans. 42 (2013) 1787–1797, https://doi.org/10.1039/c2dt31922e.

[244] E.O. Ribeiro, N.R. De Campos, A.C. Doriguetto, W.P. Barros, M.A. Ribeiro, E.E.B. De Paula, H.O. Stumpf, F. Lloret, M. Julve, M.V. Marinho, Study of the complex formation between the [Cu(bpca)]+ secondary building unit and the aromatic N donors 2,3,5,6-tetra(2-pyridyl)pyrazine (tppz) and 1,3-bis(4-pyridyl) propane (bpp), CrystEngComm 19 (36) (2017) 5460–5472, https://doi.org/10.1039/C7CE01230F.

[245] L.D.S. Mariano, I.M.L. Rosa, N.R. De Campos, A.C. Doriguetto, D.F. Dias, W.D. Do Pim, A.K.S.M. Valdo, F.T. Martins, M.A. Ribeiro, E.E.B. De Paula, E.F. Pedroso, H.O. Stumpf, J. Cano, F. Lloret, M. Julve, M.V. Marinho, Polymorphic derivatives of niii and coii mesocates with 3D Networks and 'brick and mortar' structures: preparation, structural characterization, and cryomagnetic investigation of new single-molecule magnets, Cryst. Growth Des. 20 (4) (2020) 2462–2476, https://doi.org/10.1021/acs.cgd.9b01638.

[246] H.M. Titi, J.L. Do, A.J. Howarth, K. Nagapudi, T. Friščić, Simple, scalable mechanosynthesis of metal-organic frameworks using liquid-assisted resonant acoustic mixing (LA-RAM), Chem. Sci. 11 (29) (2020) 7578–7584, https://doi.org/10.1039/D0SC00333F.

[247] T. Stolar, L. Batzdorf, S. Lukin, D. Žilić, C. Motillo, T. Friščić, F. Emmerling, I. Halasz, K. Užarević, In situ monitoring of the mechanosynthesis of the archetypal metal-organic framework HKUST-1: effect of liquid additives on the milling reactivity, Inorg. Chem. 56 (11) (2017) 6599–6608, https://doi.org/10.1021/acs.inorgchem.7b00707.

[248] L. Qin, Y. Gu, G.Y. Li, S.L. Xiao, G.H. Cui, Preparation and crystal structure of a triple parallel interpenetrated copper coordination polymer based on a flexible bis(imidazole) ligand, Transition Met. Chem. 38 (4) (2013) 407–412, https://doi.org/10.1007/s11243-013-9705-9.

[249] S. Tripathi, S.K. Sachan, G. Anantharaman, Crystal engineering of zinc and cadmium coordination polymers via a mixed-ligand strategy regulated by aromatic rigid/flexible dicarboxylate ancillary ligands and metal ionic radii: tuning structure, dimension and photoluminescence properties, Polyhedron 119 (2016) 55–70, https://doi.org/10.1016/j.poly.2016.08.009.

[250] Y. Peng, K. Li, S. Zhao, S. Han, B. Li, H.-Y. Li, Tuning zinc coordination architectures by benzenedicarboxylate position isomers and bis(triazole), Spectrochim. Acta Part A: Mol. Biomol. Spectrosc. 147 (2015) 20–25, https://doi.org/10.1016/j.saa.2015.03.087.

[251] Y. Mu, G. Han, Z. Li, X. Liu, H. Hou, Y. Fan, Effect of organic polycarboxylate ligands on the structures of a series of zinc(II) coordination polymers based on a conformational bis-triazole ligand, Cryst. Growth Des. 12 (3) (2012) 1193–1200, https://doi.org/10.1021/cg201180u.

[252] Y. Gong, R. Wang, D. Yuan, W. Su, Y. Huang, C. Yue, F. Jiang, M. Hong, Chains, Chains, ladders and sheets of d10 metal-organic polymers generated from the flexible bipyridyl ligands, Polyhedron 26 (18) (2007) 5309–5316, https://doi.org/10.1016/j.poly.2007.07.048.

[253] Y.-Q. Jiang, Z.-X. Xie, S.W. Ng, A two-dimensional coordination polymer, μ-1,3-benzenedicarboxylato-μ-ethylenediaminezinc(II) trihydrate, Acta Crystallogr. Sect. E Struct. Rep. Online 59 (10) (2003) m947–m949, https://doi.org/10.1107/S1600536803020579.

[254] L.P. Zhang, J.F. Ma, J. Yang, Y.Y. Liu, G.H. Wei, 1D, 2D, and 3D Metal-organic frameworks based on bis(imidazole) ligands and polycarboxylates: syntheses, structures, and photoluminescent poperties, Cryst. Growth Des. 9 (2009) 4660–4673, https://doi.org/10.1021/cg900460k.

[255] L.L. Johnston, D.P. Martin, R.M. Supkowski, R.L. LaDuca, One- and two-dimensional copper benzenedicarboxylate coordination polymers incorporating the flexible tethering diimine N, N′-bis(3-pyridylmethyl) piperazine: synthesis, structure, and thermal properties, Inorg. Chim. Acta 361 (9-10) (2008) 2887–2894, https://doi.org/10.1016/j.ica.2008.02.040.

[256] T.-L. Hu, R.-Q. Zou, J.-R. Li, X.-H. Bu, d10 Metal complexes assembled from isomeric benzenedicarboxylates and 3-(2-pyridyl)pyrazole showing 1D chain structures: syntheses, structures and luminescent properties, Dalton Trans. (2008) 1302, https://doi.org/10.1039/b716398c.

[257] M. Li, Q. Ling, Z. Yang, B.-L. Li, H. Li, Seven structural versatile coordination polymers based on a flexible bis(triazole) and polycarboxylate co-ligands: syntheses, structures and properties, CrystEngComm 15 (18) (2013) 3630, https://doi.org/10.1039/c3ce00057e.

[258] J.-X. Chen, X. Zhu, S. Zhao, B.-L. Li, Z. Yong, Syntheses, structures, and luminescence of three manganese coordination polymers with flexible bistriazole and rigid benzenedicarboxylate ligands, synthesis and reactivity in inorganic, metal-organic, and nano-metal, Chemistry 46 (11) (2016) 1656–1663, https://doi.org/10.1080/15533174.2015.1137044.

[259] Y. Gong, Y. Zhou, J. Li, R. Cao, J. Qin, J. Li, Reversible color changes of metal(ii)-N1, N3-di(pyridin-4-yl)isophthalamide complexes via desolvation and solvation, Dalton Trans. 39 (2010) 9923–9928, https://doi.org/10.1039/c0dt00326c.

[260] G.-D. Feng, L.J. Xiao-Lin Luo, M.-J. Wang, Assembly of 1D cadmium(II) coordination polymer With Bis(2-Benzimidazole) and 1,3-benzenedicarboxylic acid mixed ligands, Asian J. Chem. 25 (6) (2013) 3434–3436, https://doi.org/10.14233/ajchem10.14233/ajchem.2013.13918.

[261] Y.-J. Hu, J. Yang, Y.-Y. Liu, S. Song, J.-F. Ma, A Family of capsule-based coordination polymers constructed from a new tetrakis(1,2,4-triazol-ylmethyl)resorcin[4]arene cavitand and varied dicarboxylates for selective metal-ion exchange and luminescent properties, Cryst. Growth Des. 15 (8) (2015) 3822–3831, https://doi.org/10.1021/acs.cgd.5b00469.

[262] G.B. Che, J. Wang, B. Liu, X.Y. Li, C.B. Liu, Synthesis, structure and characterization of two Cd(II) coordination polymers with helical structures, J. Coord. Chem. 62 (2) (2009) 302–310, https://doi.org/10.1080/00958970802238523.

[263] L. Bin Wang, X.M. Li, Q.W. Wang, B. Liu, Catena-Poly[[aqua-(1H-imidazole-kN 3)cadmium(II)]-μ-benzene-1,3-dicarboxyl-ato-k3 O,O′:O″], Acta Crystallogr. Sect. E: Struct. Rep. Online 63 (2007) 715–716, https://doi.org/10.1107/S160053680700637X.

[264] J. Rogan, D. Poleti, L. Karanović, Z. Jagličić, Synthesis, magnetic, thermal and structural properties of Co(II), Ni(II) and Cu(II) complexes containing isophthalato ligands, J. Mol. Struct. 985 (2-3) (2011) 371–379, https://doi.org/10.1016/j.molstruc.2010.11.024.

[265] X. Wang, S.W. Yan, J. Yang, D.R. Xiao, H.Y. Zhang, J.L. Zhang, X.L. Chi, E.B. Wang, Three interdigitated metal-quinolone complexes from self-assembly of mixed ligands and cadmium salts, Inorg. Chim. Acta 409 (2014) 208–215, https://doi.org/10.1016/j.ica.2013.09.031.

[266] J.-G. Ding, C. Yin, S.-S. Han, L.-Y. Zheng, B.-L. Li, B. Wu, Four cadmium coordination polymers based on a flexible bis(triazole) ligand and benzenedicarboxylate isomers, Polyhedron 83 (2014) 228–235, https://doi.org/10.1016/j.poly.2014.07.042.

[267] W. Zhang, W. Zhao, G. Cui, S. Dong, A coordination polymer of Cd II with benzene-1,3-dicarboxylate and 1,4-bis[1-(2-pyridylmethyl)benzimidazol-2-yl]butane, Acta Crystallogr. Sect. E Struct. Rep. Online 65 (2009) m1460, https://doi.org/10.1107/S1600536809043360.

[268] A. Dey, S.K. Konavarapu, H.S. Sasmal, K. Biradha, Porous coordination polymers containing pyridine-3,5-Bis(5-azabenzimidazole): exploration of water sorption, selective dye adsorption, and luminescent properties, Cryst. Growth Des. 16 (10) (2016) 5976–5984, https://doi.org/10.1021/acs.cgd.6b01028.

[269] K. Nath, A. Husain, P. Dastidar, Metallogels and silver nanoparticles generated from a series of transition metal-based coordination polymers derived from a new bis-pyridyl-bis-amide ligand and various carboxylates, Cryst. Growth Des. 15 (9) (2015) 4635–4645, https://doi.org/10.1021/acs.cgd.5b00911.

[270] F.-P. Huang, J.-L. Tian, W. Gu, X. Liu, S.-P. Yan, D.-Z. Liao, P. Cheng, Co(II) coordination polymers: positional isomeric effect, structural and magnetic diversification, Cryst. Growth Des. 10 (3) (2010) 1145–1154, https://doi.org/10.1021/cg901014r.

[271] K.M. Blake, M.A. Braverman, J.H. Nettleman, L.K. Sposato, R.L. Laduca, Pendant arm length control of dimensionality in cobalt dipyridylamine coordination polymers containing meta-benzenedicarboxylate ligands, Inorg. Chim. Acta 363 (14) (2010) 3966–3972, https://doi.org/10.1016/j.ica.2010.07.070.

[272] H. Wu, X.L. Lü, C.L. Yang, C.X. Dong, M.S. Wu, Diverse topologies of seven d10 coordination polymers constructed from a long ligand and different carboxylates, CrystEngComm 16 (6) (2014) 992–1000, https://doi.org/10.1039/C3CE41974F.

[273] G. Tian, G. Zhu, Q. Fang, X. Guo, M. Xue, J. Sun, S. Qiu, Design, synthesis and fluorescence of two-dimensional pillared layers by connecting infinite one-dimensional chains via 4,4′-bipyridine, J. Mol. Struct. 787 (1-3) (2006) 45–49, https://doi.org/10.1016/j.molstruc.2005.10.036.

[274] Y. Liu, J. Zhang, F. Xu, L. Sun, T. Zhang, W. You, Lithium-Based 3D Coordination Polymer with Hydrophilic & DESIGN 2008, Cryst. Growth Des. 8 (2008) 8–10.

[275] X. Lu, Y.Y. Chen, P.Z. Li, Y.G. Bi, C. Yu, X.D. Shi, Z.X. Chi, Self-assembly of three 1-D zinc-benzenedicarboxylate coordination polymers with 1,10-phenanthroline, J. Coord. Chem. 63 (22) (2010) 3923–3932, https://doi.org/10.1080/00958972.2010.523826.

[276] C.H. Lee, J.Y. Wu, G.H. Lee, S.M. Peng, J.C. Jiang, K.L. Lu, Amide-containing zinc (II) metal-organic layered networks: a structure-CO2 capture relationship, Inorg. Chem. Front. 2 (2015) 477–484, https://doi.org/10.1039/c4qi00241e.

[277] F.Y. Ge, X. Ma, D.D. Guo, L.N. Zhu, Z.P. Deng, L.H. Huo, S. Gao, Syntheses, structural evolutions, and properties of Cd(II) coordination polymers induced by bis(pyridyl) ligand with chelated or protonated spacer and diverse counteranions, Cryst. Growth Des. 17 (5) (2017) 2667–2681, https://doi.org/10.1021/acs.cgd.7b00174.

[278] Zhang, D.-S. Li, J. Zhao, F. Fu, Y.-Y. Chen, N. Wang, A novel Cd(II) coordination polymer constructed from benzenedicarboxylic Acid and 1,2-bis(triazol) ethane: synthesis, crystal structure, and luminescent properties, Synth. React. Inorg., Met. –Org., Nano-Met. Chem. 41 (7) (2011) 877–882, https://doi.org/10.1080/15533174.2011.591318.

[279] H.Y. Bai, J.F. Ma, J. Yang, Y.Y. Liu, J.C.Ma Hua-Wu, Effect of anions on the self-assembly of Cd(II)-containing coordination polymers based on a novel flexible tetrakis(imidazole) ligand, Cryst. Growth Des. 10 (2) (2010) 995–1016, https://doi.org/10.1021/cg901332m.

[280] F. Zhang, F.L. Bei, J.M. Cao, Sovolthermal synthesis and crystal structure of two CdII coordination polymers of benzenedicarboxylic, J. Chem. Crystallogr. 38 (7) (2008) 561–565, https://doi.org/10.1007/s10870-008-9336-8.

[281] Y. Qu, Y. Ke, S. Lu, R. Fan, G. Pan, J. Li, Hydrothermal synthesis, structures and spectroscopy of 2D lanthanide coordination polymers built from helical chains: [Ln2(BDC) 3(H2O)2]n (Ln=Sm, 1; Ln=Eu, 2; BDC=1,3-benzenedicarboxylate), J. Mol. Struct. 734 (1-3) (2005) 7–13, https://doi.org/10.1016/j.molstruc.2004.03.035.

[282] I. Mihalcea, N. Henry, T. Bousquet, C. Volkringer, T. Loiseau, Six-fold coordinated uranyl cations in extended coordination polymers, Cryst. Growth Des. 12 (9) (2012) 4641–4648, https://doi.org/10.1021/cg300853f.

[283] P.K. Chen, Y.X. Che, J.M. Zheng, A 3D heteropolynuclear network with 4,6-connected (44·62)(48·66·8) topology: synthesis, structure, thermal and magnetic properties, Inorg. Chem. Commun. 10 (2) (2007) 187–190, https://doi.org/10.1016/j.inoche.2006.10.015.

[284] A.X. Chen, G. Liu, H. Li, J. De Wang, F. Yue, Synthesis, crystal structure and luminescence property of a chiral magnesium (II) mixed-ligand complex [Mg (H2O)2(phen)(HBDC) 2](phen), J. Chem. Crystallogr. 41 (2) (2011) 143–146, https://doi.org/10.1007/s10870-010-9853-0.

[285] A. Kellett, M. O'Connor, M. McCann, M. McNamara, P. Lynch, G. Rosair, V. McKee, B. Creaven, M. Walsh, S. McClean, A. Foltyn, D. O'Shea, O. Howe, M. Devereux, Bis-phenanthroline copper(ii) phthalate complexes are potent in vitro antitumour agents with 'self-activating' metallo-nuclease and DNA binding properties, Dalton Trans. 40 (5) (2011) 1024–1027, https://doi.org/10.1039/C0DT01607A.